

GEMS & GEMOLOGY

VOLUME XXIX

SUMMER 1993



THE QUARTERLY JOURNAL OF THE GEMOLOGICAL INSTITUTE OF AMERICA

GEMS & GEMOLOGY

SUMMER 1993

Volume 29 No. 2

T A B L E O F C O N T E N T S



p. 91



p. 101



p. 117



p. 122

EDITORIAL

79 Stability Disclosure: Are We Going Far Enough?

Alice S. Keller and Richard T. Liddicoat

80 Letters

FEATURE ARTICLES

81 Flux-Grown Synthetic Red and Blue Spinel from Russia

Sam Muhlmeister, John I. Koivula, Robert C. Kammerling, Christopher P. Smith, Emmanuel Fritsch, and James E. Shigley

100 Emeralds and Green Beryls of Upper Egypt

Robert H. Jennings, Robert C. Kammerling, André Kovaltchouk, Gustave P. Calderon, Mohamed K. El Baz, and John I. Koivula

NOTES AND NEW TECHNIQUES

116 Reactor-Irradiated Green Topaz

Charles E. Ashbaugh III and James E. Shigley

REGULAR FEATURES

122 Gem Trade Lab Notes

129 Thank You, Donors

130 Gem News

142 Gemological Abstracts

ABOUT THE COVER: One of the most beautiful of gem materials, red spinel rivals—and has often been mistaken for—fine ruby. Recently, Russian laboratories have developed new flux-grown synthetic red and blue spinels, some of which can be identified only by sophisticated techniques. The lead article in this issue discusses these commercially available flux synthetic spinels and means of separating them from their natural counterparts. The three pieces in this photo represent historic and contemporary uses of fine spinel in jewelry. The Victorian-era bracelet contains approximately 9 ct of spinels, while the nine strands of faceted spinel beads weigh approximately 3.40 ct. Both are courtesy of Gary R. Hansen, Precious Gemstones, St. Louis, Missouri. The contemporary ring is highlighted by a 6.27-ct red spinel, 2.20 ct of yellow diamonds, and 2.54 ct. of tsavorite garnets. It is courtesy of R. Esmerian, Inc., New York.

Photo © Harold & Erica Van Pelt—Photographers, Los Angeles, CA.

Typesetting for *Gems & Gemology* is by Graphix Express, Santa Monica, CA. Color separations are by Effective Graphics, Compton, CA. Printing is by Waverly Press, Easton, MD.

© 1993 Gemological Institute of America All rights reserved ISSN 0016-626X

GEMS & GEMOLOGY

EDITORIAL STAFF**Editor-in-Chief**
Richard T. Liddicoat**Associate Editors**
William E. Boyajian
D. Vincent Manson
John Sinkankas**Technical Editor**
Carol M. Stockton**Assistant Editor**
Irv Dierdorff**Editorial Assistant**
Denise Heyl**Editor**
Alice S. Keller
1660 Stewart St.
Santa Monica, CA 90404
Telephone: (800) 421-7250 x251**Subscriptions**
Gail Young
Jin Lim
Telephone: (800) 421-7250 x201
FAX: (310) 453-4478**Contributing Editor**
John I. Koivula**Editor, Gem Trade Lab Notes**
C. W. Fryer**Editor, Gemological Abstracts**
C. W. Fryer**Editor, Book Reviews**
Susan B. Johnson**Editors, Gem News**
John I. Koivula
Robert C. Kammerling
Emmanuel Fritsch

PRODUCTION STAFF**Art Director**
Lisa Joko**Production Artist**
Carol Silver**Word Processor**
Ruth Patchick

EDITORIAL REVIEW BOARDRobert Crowningshield
*New York, NY*Alan T. Collins
*London, United Kingdom*Dennis Foltz
*Santa Monica, CA*Emmanuel Fritsch
*Santa Monica, CA*C. W. Fryer
*Santa Monica, CA*Henry Hänni
*Zürich, Switzerland*C. S. Hurlbut, Jr.
*Cambridge, MA*Robert C. Kammerling
*Santa Monica, CA*Anthony R. Kampf
*Los Angeles, CA*Robert E. Kane
*Lake Tahoe, NV*John I. Koivula
*Santa Monica, CA*Henry O. A. Meyer
*West Lafayette, IN*Kurt Nassau
*P.O. Lebanon, NJ*Ray Page
*Santa Monica, CA*George Rossman
*Pasadena, CA*Kenneth Scarratt
*New York, NY*Karl Schmetzer
*Petershausen, Germany*James E. Shigley
Santa Monica, CA

SUBSCRIPTIONS

Subscriptions in the U.S.A. are priced as follows: \$54.95 for one year (4 issues), \$134.95 for three years (12 issues). Subscriptions sent elsewhere are \$65.00 for one year, \$165.00 for three years.

Special annual subscription rates are available for all students actively involved in a GIA program: \$44.95 U.S.A., \$55.00 elsewhere. Your student number *must* be listed at the time your subscription is entered.

Single issues may be purchased for \$14.00 in the U.S.A., \$17.00 elsewhere. Discounts are given for bulk orders of 10 or more of any one issue. A limited number of back issues of G&G are also available for purchase.

Please address all inquiries regarding subscriptions and the purchase of single copies or back issues to the Subscriptions Department.

To obtain a Japanese translation of *Gems & Gemology*, contact the Association of Japan Gem Trust, Okachimachi Cy Bldg., 5-15-14 Ueno, Taito-ku, Tokyo 110, Japan. Our Canadian goods and service registration number is R126142892.

MANUSCRIPT SUBMISSIONS*Gems & Gemology* welcomes the submission of articles on all aspects of the field. Please see the suggestions for authors in the Spring 1993 issue of the journal, or contact the editor for a copy. Letters on articles published in *Gems & Gemology* and other relevant matters are also welcome.

COPYRIGHT AND REPRINT PERMISSIONS

Abstracting is permitted with credit to the source. Libraries are permitted to photocopy beyond the limits of U.S. copyright law for private use of patrons. Instructors are permitted to photocopy isolated articles for noncommercial classroom use without fee. Copying of the photographs by any means other than traditional photocopying techniques (Xerox, etc.) is prohibited without the express permission of the photographer (where listed) or author of the article in which the photo appears (where no photographer is listed). For other copying, reprint, or republication permission, please contact the editor.

Gems & Gemology is published quarterly by the Gemological Institute of America, a nonprofit educational organization for the jewelry industry, 1660 Stewart St., Santa Monica, CA 90404.Postmaster: Return undeliverable copies of *Gems & Gemology* to 1660 Stewart St., Santa Monica, CA 90404.

Any opinions expressed in signed articles are understood to be the views of the authors and not of the publishers.

STABILITY DISCLOSURE: ARE WE GOING FAR ENOUGH?

A few weeks ago, a jeweler called asking for information on "Ocean green" topaz, since he had recently sold several of these stones. We told him about the article in this issue, and that one of the key discoveries was that the Ocean-green topaz tested faded in less than a day of exposure to sunlight, but did not fade under artificial light. His next question: "What is my responsibility to my customers? I already told them that the material was irradiated—do I now have to tell them that the color isn't stable?" Our reply: *Yes*. Disclosure that "artificial coloring . . . is not permanent" is covered by U.S. Federal Trade Commission guidelines.

Yet, what about our colleague who, while in her early 20s, purchased a lovely dark amethyst pendant, wore it proudly to the beach every summer, and by the time she was 30 was sporting a pale purple stone? It is highly probable that the color of this stone was natural, so no treatment disclosure was required. But here, too, didn't the jeweler have a responsibility to warn her of the potential damage that prolonged exposure to bright sunlight could cause?

Much has been written about disclosure in gemology, but principally about disclosing that a stone has been treated or is a synthetic. Disclosure related to stability of color or durability of other aspects of an unenhanced gem is a gray area that industry rules and guidelines seldom address in depth.

The problem is potentially serious, and amethyst is only one example. Some kunzite fades to almost colorless on relatively short exposure to sunlight or heat, as does some brown topaz. As renowned gemologist Bob Crowningshield asks in a current Lab Note: How much do jewelers really tell their customers about pearl care? It is not uncommon for someone to wear a stud earring day and night—so the pearl damage he reports should not come as a surprise, if no care instructions were given. Similarly, whereas virtually any gem is subject to breakage, those like moonstone and topaz which have excellent cleavage, and those like opal which is very brittle and sensitive to heat, merit caveats regarding how they are worn (*not* while gardening or playing tennis, *not* while tanning in the hot Texas sun).

We at *Gems & Gemology* feel that disclosing the potential consequences of treatment is as important as disclosing the treatment itself. Therefore, we routinely ask our authors to test a new enhancement for its stability to normal light, heat, cleaning, and jewelry repair procedures. We also feel that the seller—the retailer in particular—has a responsibility to provide the appropriate cautions and care instructions, whether or not an enhancement is involved.

Many stones are *not* forever (and even diamonds can be scratched if stored with other diamonds or chipped during hard wear). By teaching the customer how to prolong the beauty of the stone, you instill confidence and avoid dissatisfaction—a good prescription for a long, prosperous relationship.

Alice S. Keller, Editor

Richard T. Liddicoat, Editor-in-Chief

LETTERS

RADIOACTIVITY REVISITED

In recent years, there has been much ado about radioactivity in gemstones, and a significant segment of the public has been unduly alarmed. The article "Gamma-Ray Spectroscopy to Measure Radioactivity in Gemstones," by C. E. Ashbaugh III (Vol. 28, No. 2, 1992, pp. 104–111), is a most lucid and interesting exposition of this problem. Unfortunately, few readers of this article are familiar with the earlier one that he wrote concerning radioactivity regulations (Vol. 24, No. 4, 1988, pp. 196–213). Consequently, they may be in danger of viewing this entire matter out of context.

Government regulations often arise at the prodding of "opportunists" and the media, followed by public demand. Subsequently, a regulatory agency is created and regulatory limits are set so low that safety and health are no longer relevant factors.

Often the net result of this regulatory activity is that industrial activity is moved offshore. Thus, this nation is left with fewer productive jobs, but more government and service jobs. Also, because later generations come to believe that any noncompliance with a regulatory limit is tantamount to the deliberate and callous creation of a serious health hazard, the continued prosperity of the regulatory agency is assured.

How, you might ask, does all this relate to radioactivity testing in gemstones? Let us consider common sense and some points that Mr. Ashbaugh made in his first paper.

It is generally recognized that "the dose makes the poison." This simply means that since there is a little bit of everything everywhere, the important factor is not so much "what" you are exposed to, but "how much." Dose is calculated by multiplying the concentration by the quantity of the substance ingested.

The U.S. Nuclear Regulatory Commission (NRC) recognized that radiation was already everywhere, and their goal was to stop humanity from making things worse. However, they completely ignored the concept of dose (how much one's body absorbs) and couched their regulations in terms of *release limits* (concentrations only) and release dates. This "legal release date," as described by Ashbaugh in his second article, is derived by means of a calculation based on concentrations of various nuclides determined to be present in the sample.

Ashbaugh's calculated release date for the diamond described in that article was June 30, 5071: This date marks the point in time at which the release of the gem to the public becomes a legal activity. Unfortunately, the public has the mistaken notion that, on this date, the handling of this gemstone passes from being an unsafe act to a safe one.

It is logical to assume that release values are well below the normal background radiation levels to which we are constantly exposed—and they are. As Ashbaugh stated, "The legal definition of 'radioactive material' means any material having a specific activity greater than 0.002 microcuries per gram" (i.e., greater than 2 nCi/g). He also wrote, "With respect to the small quantities of radioactivity found in gemstones and the resultant radiation doses people may receive, 2 nCi of any radioactive nuclide per gram of material can be judged to be harmless and safe, and a very small fraction of background radiation." He was saying that, in general, radioactivity in gemstones is not a serious problem for the individual.

This value of 2 nCi/g is accepted virtually worldwide—except in the United States. Our federal release limit has been set at 1 nCi/g, or less, for most radionuclides found in gemstones; although, to be "really safe," the NRC prefers a value of 0.4 nCi/g.

Consider the results on the yellowish green diamond reported by Ashbaugh and which, by the regulations, cannot be released to the public for 3,000 years. The determined activity was only 0.125 nCi/g, but the nuclide creating the radioactivity is americium (Am-241), for which the NRC has established a limit of 0.0009 nCi/g.

Americium, not a natural element, is a decay product of neutron-bombarded plutonium (think atom bombs). In their hearts, the NRC would like to set the allowable limit at zero, but they cannot set a limit that is below the limit of detection of the method used to demonstrate compliance. However, the fact is that, if anyone can detect americium in your product, you have an awful lot of explaining to do to the NRC.

Yet these regulatory values apply not only to gemstones but also to drinking water. Assume that, each day, you drink three liters of water containing this "allowable" level of americium. This means that you will ingest a total activity of 2.7 nCi of this nuclide each day. According to the NRC, this is legal and acceptable, although this quantity is greater than the dose you would get if you ground up 40 diamonds, similar to the aforementioned yellow-green diamond, and mixed the powder with your Jell-O.

Thus it appears that, according to U.S. regulations, you could safely eat 40 of these radioactive diamonds a day, but you cannot wear even one for at least 3,000 years. Clearly, the problem has nothing to do with health or safety. It is simply a political issue.

W. WM. HANNEMAN, Ph.D.
Castro Valley, California

FLUX-GROWN SYNTHETIC RED AND BLUE SPINELS FROM RUSSIA

By Sam Muhlmeister, John I. Koivula, Robert C. Kammerling, Christopher P. Smith, Emmanuel Fritsch, and James E. Shigley

Examination of red and blue samples of a relatively new flux synthetic spinel from Russia established criteria by which they can be separated from their natural counterparts. The flux synthetic blue spinels can be recognized on the basis of their inclusions, ultraviolet luminescence, and visible absorption spectrum. Magnification is sufficient to identify the flux synthetic red spinels when flux or metallic inclusions are present; in the absence of such inclusions, however, chemical analysis is required. Red and blue natural spinels both contain significantly more zinc than their flux synthetic counterparts. Also, trace amounts of Pb (from the flux) and Pt and Ir (from the crucible) were found in some of the flux synthetic spinels.

A

new type of synthetic spinel, grown by the flux method, was first encountered as red crystals by gemologists in the late 1980s. Now commercially available, this material can be difficult to identify by standard gem-testing methods. Preliminary studies indicate that most of the gemological properties of these red synthetic spinels (excluding the presence of possible flux or metallic inclusions) overlap those of natural gem spinels of similar color (see Bank and Henn, 1990; Brown et al., 1990; Koivula et al., 1991; Henn and Bank, 1992). This situation contrasts greatly with that of flame-fusion synthetic spinels—the only type of synthetic spinel previously available commercially—which are easily identifiable even when faceted, on the basis of their distinctive refractive index and specific gravity.

These new Russian flux synthetic spinels are also available in blue and have been grown in other colors that, in some cases, do not correspond to natural spinels. This article reports on identification criteria by which these new, commercially available red and blue Russian flux synthetic spinels (figures 1 and 2) can be separated from their natural counterparts. Other colors are briefly discussed in box A.

BACKGROUND

Synthetic spinel was first produced in the mid-1800s—not by flame fusion as is usually thought, but by flux growth (Nassau, 1980). These first, small flux synthetic spinel crystals were accidentally grown during an attempted synthesis of corundum. Although they were commercially insignificant at the time, the basic method for growing flux synthetic spinels has been known for almost a century (Wood and White, 1968; Wang and MacFarlane, 1968).

Flame-fusion (“Verneuil”) synthetic spinels have been marketed as faceted stones since the 1920s (Nassau, 1980; Webster, 1983), primarily in light blue colors as an aquamarine substitute. They can be easily separated from natu-

ABOUT THE AUTHORS

Mr. Muhlmeister is a research associate, Dr. Fritsch is manager, and Dr. Shigley is director of GIA Research, Santa Monica, California. Mr. Koivula is chief research gemologist, and Mr. Kammerling is director of identification and research, at the GIA Gem Trade Laboratory, Santa Monica, California. Mr. Smith is senior staff gemologist at the Gübelin Gemmological Laboratory, Lucerne, Switzerland.

Acknowledgments appear at the end of the article.

Gems & Gemology, Vol. 29, No. 2, pp. 81-98.
© 1993 Gemological Institute of America



Figure 1. These faceted Russian flux-grown synthetic red spinels (the largest is 2.27 ct) are representative of those examined during this study. Photo © Tino Hammid and GIA.

ral blue spinel with magnification. It is reportedly far more difficult to grow synthetic red spinel by this method (see Schiffmann, 1972; Brown et al., 1991), because it requires the incorporation of up to five times the amount of alumina normally contained in the spinel crystal structure (Nassau, 1980). As a result of this dramatic difference in composition, most flame-fusion synthetic red spinels have some very distinctive gemological properties, such as a higher index of refraction, as well as a pattern of anomalous birefringence, or internal strain, seen with polarized light (the so-called "cross-hatch effect" or "tabby extinction"—see Webster, 1983; Hurlbut and Kammerling, 1991). Consequently, the separation of natural red

and blue spinels from most flame-fusion synthetic spinels is usually very straightforward.

In contrast, flux growth produces synthetic spinels with the same (one-to-one) $MgO:Al_2O_3$ ratio as natural spinel (see, e.g., Nassau, 1980); as such, their gemological properties are expected to be very similar. During the past decade, the flux method has been improved by researchers in Russia, with the result that flux synthetic spinels in red and blue are now commercially available in crystals suitable for faceting. GIA researchers first encountered this material in the trade in 1989, when a 17.19-ct red crystal was purchased by one of us (JIK) for gemological investigation (see Koivula and Kammerling, 1989, 1990a; Koivula et al., 1991). Other red crystals as large as 17.96 ct (fashioned to an 8.58-ct cushion antique step cut; J. Fuhrbach, pers. comm., 1990), as well as faceted blue flux-grown synthetic spinels as large as 5.40 ct (Henn and Bank, 1991), have also been reported.

Pinky Trading Co. of Bangkok signed a joint-venture agreement with the Academy of Sciences of the USSR (now the Academy of Sciences of Russia) in the fall of 1989 to market flux-grown synthetic red and blue spinel. They reported to us that as of early July 1993 the following quantities had been marketed: approximately 5,000 ct of rough and 2,700 ct of faceted "red" (actually, light pink to dark red) flux-grown synthetic spinel, and about 1,000 ct of rough and 540 ct of faceted blue material. The faceted stones have included both calibrated and noncalibrated goods, the most popular being ovals and cushion shapes. In red, the most popular sizes have been in the 2–5 ct range, while the greatest demand for blues has been in the 0.5–2 ct range. Pinky Trading also reported that they had no immediate plans to market any additional colors of this material.

The presence of these flux synthetic spinels in the gem market has prompted concern regarding their identification, as evidenced by several brief articles and laboratory alerts issued by the International Colored Gemstone Association (ICA—Bank and Henn, 1989; Koivula et al., 1990a; Henn and Bank, 1991, 1992), and thus the present study.

Note that the blue flux synthetic spinels resemble in color the "cobalt blue" natural spinels found in Sri Lanka. Shigley and Stockton (1984) described but did not clearly define this rare natural gemstone. To provide better identification criteria, we distinguish "cobalt blue" natural spinels

Figure 2. All of these faceted Russian flux-grown synthetic blue spinels (the largest is 1.73 ct) were examined during this study. Photo © Tino Hammid and GIA



from the more common grayish blue natural spinels on the basis of the former's saturated color, red luminescence to both visible light and long-wave U.V. radiation, and visible absorption spectrum (which always contains a combination of features due to both Co and Fe, with increasing absorption below about 430 nm and broad absorption bands at about 458, 480, 550, 560–600, and 620–650 nm). In contrast, the more common "blue" natural spinels (i.e., those with a desaturated grayish blue color that is caused by iron) do not luminesce red and have a different visible absorption spectrum (with increasing absorption below about 430 nm, and broad absorption bands at about 458, 480, 555, 590, 635, and 670 nm). There exists

a continuous series from iron- to cobalt-containing natural blue spinels (Schmetzer et al., 1989).

MATERIALS AND METHODS

The study sample included four red and 16 blue flux-grown synthetic spinel crystals. All of the crystals we examined were euhedral, with relatively flat, smooth faces and sharp edges. At the base of each crystal was an irregular surface in a location normally occupied by a termination of the octahedron (see figure 3). This surface appears to be the point either of attachment or growth nucleation of the crystal; on some specimens, a small secondary crystal that undoubtedly developed during growth of the larger crystal could be seen (figure 4). The

BOX A: FLUX SYNTHETIC SPINELS OF OTHER COLORS

Besides the red and blue samples described in this article, Russian laboratories have grown other colors of flux synthetic spinel, apparently on an experimental basis (W. Barshai, pers. comm., 1991). We studied three brownish yellow octahedra or octahedral fragments ranging from 0.29 to 3.76 ct, one 3.34-ct greenish blue crystal, one 0.80-ct purple elongated octahedron, and one 1.43-ct pale pink crystal (figure A-1). Their indices of refraction and specific-gravity values were within the ranges measured for red and blue natural and flux synthetic spinels, as described in the article text (except for the pink crystal, which had a low S.G., 3.55). These other colors all showed slight anomalous birefringence ("strain"); three exhibited "snake-like bands" under crossed polarizers. All but the inclusion-free purple and pale pink stones displayed typical orange-brown flux inclusions.

The three brownish yellow spinels fluoresced a weak to moderate chalky yellowish green to long-wave U.V. radiation, and had either a weaker reaction or were inert to short-wave U.V. The larger crystal exhibited a moderate green transmission luminescence when excited by visible light. All three crystals showed weak absorption bands at approximately 430 and 460 nm (in the handheld spectroscope). These absorptions were confirmed by absorption spectrophotometry: The color is predominantly related to a regularly increasing absorption toward the ultraviolet, but the precise cause is unknown. Superimposed on this major feature was a sharp absorption band at approximately 427 nm and two broader bands with apparent maxima at about 458 and 490 nm. EDXRF analysis proved that these crystals contain some Mn. The absorption spectra and luminescence are typical of Mn^{2+} in tetrahedral coordination, as is found in Mn-doped flame-fusion synthetic spinel (Schmetzer et al., 1989), although the absorption bands are slightly shifted in the flux synthetic material.

The greenish blue flux synthetic spinel crystal was inert to ultraviolet radiation, but showed two bands in the handheld spectroscope, at approximately 590 and 635 nm. EDXRF analysis demonstrated the presence of Ni, Fe, and traces of Mn and V. Visible absorption spectroscopy revealed increasing absorption toward the ultraviolet with a weak, broad band at 470 nm, a broad band with two apparent maxima at 593 and 635 nm, and another one with a maximum at about 875 nm. These features are similar to those recorded by Wyon et al. (1986) on Czochralski-pulled synthetic spinel doped with Ni, and are typical of Ni^{2+} in octahedral coordination. Therefore, the greenish blue color of this spinel is essentially due to Ni^{2+} .

The purple crystal emitted a weak red when



Figure A-1. Russian laboratories have produced flux-grown synthetic spinels in a variety of colors other than red and blue. These samples, reportedly grown on an experimental basis, range from 0.80 to 3.76 ct. Photo by Maha DeMaggio.

exposed to long-wave U.V. radiation, with a faint red fluorescence to short-wave U.V. It also exhibited a strong red luminescence when excited by visible light, and appeared dark red through the Chelsea color filter. When we examined it with the handheld spectroscope, we noted absorption bands at approximately 590 and 635 nm, as in the greenish blue spinel described above. There were also broad absorptions from about 530 to 590 nm and 660 to 690 nm, and a sharp line at approximately 690 nm. EDXRF analysis revealed the presence of Ni, Fe, and Cr, as well as traces of V, Zn, and Ga. The color is due to the combination of Cr^{3+} and Ni^{2+} absorptions.

The pale pink crystal fluoresced a weak to moderate, slightly chalky orange to long-wave U.V. radiation, with a yellower reaction of the same intensity to short-wave U.V. It showed no lines in the handheld spectroscope, but an absorption spectrum obtained with a spectrophotometer showed one very weak broad band centered at about 560 nm, very similar to that seen for Cr in the red flux synthetic spinels, but considerably weaker in intensity. EDXRF analysis revealed V, Mn, Fe, Ni, Zn, Ga, and possibly Cu as impurities.

Because of their unusual coloring agents, such as Ni and Mn, these other colors of Russian flux synthetic spinels do not duplicate spinels found in nature. In particular, even these experimental crystals do not reproduce the blue component that iron causes in the color of many natural spinels. It would appear that doping synthetic spinels with unusual impurities may produce crystals with attractive colors, but generally these colors would not correspond to those of natural spinels.

red crystals ranged from 6.19 to 45.14 ct, with the largest one (to our knowledge, the largest crystal of its kind reported so far) measuring $23.76 \times 20.86 \times 12.88$ mm. The blue crystals ranged from 1.06 to 14.30 ct, with the largest one measuring $13.10 \times 12.81 \times 11.83$ mm.

We also examined nine red and 12 blue faceted Russian flux synthetic spinels (see, e.g., figures 1 and 2), which ranged from 0.19 to 8.58 ct. Included as well were two (one rough and one faceted) blue flux synthetic spinels from Russia, loaned by Dr. Henry Hänni, that were known to have a higher iron content than our samples.

In addition to the Russian flux-grown synthetic samples, we examined the following gemologically and/or chemically for comparison: (1) 28 red-to-pink or purple and eight blue natural spinels (including four "cobalt blue" samples from Sri Lanka and four grayish blue spinels—one from Sri Lanka and three of uncertain origin); (2) one flux synthetic blue spinel, two flux synthetic red spinels, and five flux synthetic blue and red-to-pink gahnites (ZnAl_2O_4) grown on an experimental basis at Bell Laboratories in New Jersey; and (3) one red and three blue flame-fusion synthetic spinels. The natural red-to-pink or purple spinels reportedly came from the following localities: Africa—2, Myanmar (Burma)—16, Sri Lanka—3, Tajikistan (Pamir Mountains)—2, Tanzania—3, and Thailand—2. The range of color was chosen to determine if any identification criteria established would be valid for other colors of spinel with a distinct red component. The natural and synthetic blue spinels include some of those examined by Shigley and Stockton in 1984.

The gemological properties of all the Russian flux-grown synthetic spinels were determined using the following instruments and methods. Refractive-index readings were taken with a Duplex II refractometer and a near-monochromatic, sodium-equivalent light source. The specific gravity was determined hydrostatically (average of three separate measurements). We also used pure methylene iodide, with a room-temperature specific gravity of 3.32, to estimate specific gravity and determine the usefulness of standard sink-float testing. Ultraviolet luminescence was examined under darkroom conditions, using both long-wave and short-wave ultraviolet radiation, with the sample placed against a nonfluorescent black background. Contrast control goggles were worn during the testing procedure to help eliminate secondary reflections.

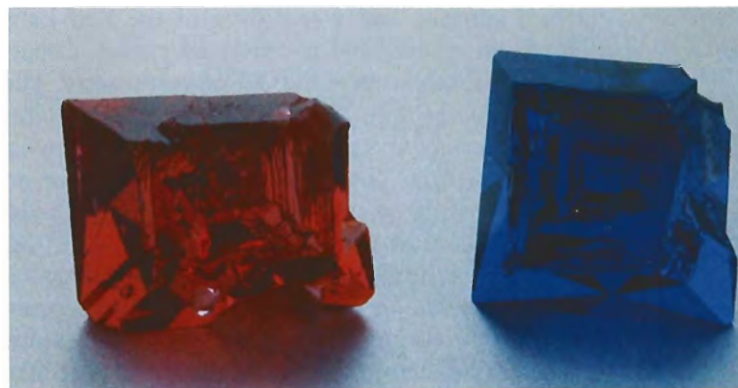


Figure 3. The irregular surface at the base of each Russian flux synthetic spinel crystal (red = 17.19 ct; blue = 14.30 ct) appears to be the point of attachment or growth nucleation. Photo by Maha DeMaggio.

A Beck prism spectroscope and a GIA GEM "DISCAN" digital-scanning diffraction-grating spectroscope were used to observe the visible absorption spectra. The synthetic spinels were also examined spectroscopically with light passed through a flask of copper sulfate solution so that any emission (fluorescence) lines might be seen.

Two methods were used to test the samples for luminescence to visible light, a property referred to in gemology as "transmission luminescence." In the case of the blue spinels, where the visible-light luminescence color differs from the body color of the stone, each sample was placed on the end of a 150-watt tungsten-halogen fiber-optic light wand. This method, however, is not effective when the body and transmission luminescence colors are the same, as is the case for red spinels. For these samples, then, we used the crossed-filters technique (see, e.g., Webster, 1983; Hodgkinson, 1991), with a saturated copper sulfate solution and a red no. 25A photographic filter.

A gemological microscope was used with a variety of illumination techniques, including dark-field, transmitted light, polarized light, shadowing, and oblique illumination. A Zeiss research microscope was used to examine the surface features of the rough crystals, and to compare them to surface characteristics found on natural spinel crystals. Visible absorption spectra were recorded over the range of 350 to 750 nm using a Hitachi model U4001 spectrophotometer, at a scan speed of 120 nm/minute and a slit width of 2.00 nm.

We determined the chemical composition of 12 red and six blue flux-grown synthetic spinels, 28

natural spinels, and a sampling of the Bell Labs flux-grown spinels and gahnites by energy dispersive X-ray fluorescence (EDXRF) spectrometry. The EDXRF spectrometer used was a Tracor X-ray (currently Spectrace Instruments) Spectrace 5000 with a rhodium-target X-ray tube. Typical excitation conditions were: a tube voltage of 30 kV, a tube current of 0.35 mA, a 0.5-mm-thick rhodium filter, and a vacuum atmosphere. These excitation conditions were chosen because they were appropriate for detecting elements between potassium (K) and molybdenum (Mo) in general, and zinc (Zn) in particular (Jenkins, 1980), which are known to occur in natural and synthetic spinels. With EDXRF analysis, we both determined the elements present in each sample tested and compared the relative peak areas of an element from one sample to the next. To confirm the EDXRF results, a quantitative analysis of three flux synthetic red spinel crystals and three faceted natural pink or red spinels was carried out using a Jeol model 733 electron microprobe at the California Institute of Technology.

GEMOLOGICAL CHARACTERISTICS OF THE FLUX SYNTHETIC SPINELS

Tables 1 and 2 summarize the gemological properties of the Russian flux-grown synthetic red and blue spinels we examined during this study, as well as those of natural and flame-fusion synthetic spinels previously reported in the literature (see, e.g., *GIA Gem Property Chart A*, 1985; Hurlbut and Kammerling, 1991) and confirmed by the authors' experience. Specific features are discussed below.

Color. The body color in daylight of the red flux synthetic spinels (both rough and faceted) examined was a vivid, medium dark, slightly purplish red (figures 1 and 3). In incandescent light, the two largest crystals and all but the largest faceted stone showed a very slight orange to brown component. With fluorescent lighting, this orange to brown component was absent, and the purple secondary hue appeared more pronounced.

The body color in daylight of all but one of the rough crystals and all of the faceted samples of blue flux synthetic spinel was a saturated, medium dark to dark, very slightly violetish blue (figures 2 and 3). The exception, a 1.85-ct crystal, was a significantly more saturated blue. In incandescent light, all of the rough crystals and faceted blue stones

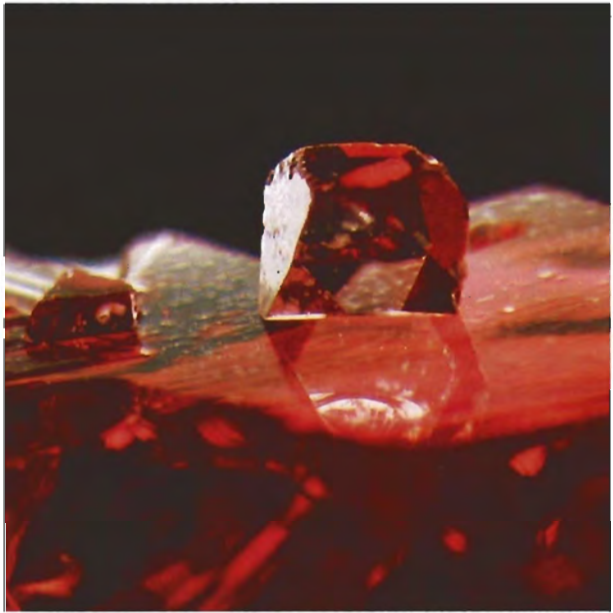


Figure 4. Two small synthetic red spinel crystals are attached to an octahedral face of this crystal. The largest of these small crystals measures 1.2 mm on a side. Photomicrograph by John I. Koivula.

appeared evenly colored with slight red flashes noted when they were rocked in the light. With fluorescent lighting, we observed a slight gray color component.

Index of Refraction. The R.I.'s of the red flux synthetic spinels we examined agree with published values (see, e.g., Brown et al., 1990; Henn and Bank, 1992), and are within the range of R.I. values for natural red spinel.

The R.I.'s of the blue flux synthetic spinels we examined are somewhat lower than the 1.719 value reported for a Russian blue flux synthetic crystal by Henn and Bank (1991, 1992), and are within the R.I. range (1.710–1.720) previously determined for natural "cobalt blue" spinels (Shigley and Stockton, 1984). The faceted blue flux synthetic spinel from Dr. Hänni had an R.I. of 1.717—higher than that of our other blue flux synthetic spinels—probably because of its high iron content.

Specific Gravity. The range of S.G. values for all the flux synthetic spinels tested was within the range for natural spinels. If a hydrostatic balance is not available, a gemologist can estimate the S.G.

using heavy liquids. All of the samples readily sank in methylene iodide (S.G. 3.32) when they were submerged just below the liquid's surface and released.

Ultraviolet Luminescence. In general, we observed a strong purplish red to slightly orangy red reaction to long-wave U.V. radiation—with a weaker, slightly orangy red reaction to short-wave U.V.—in the flux synthetic red spinels examined. With short-wave U.V., some edges between faces on the rough crystals appeared superficially chalky and, in certain directions, more yellowish orange. No phosphorescence was detected following exposure to either source.

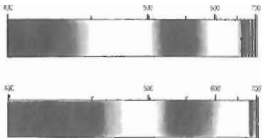
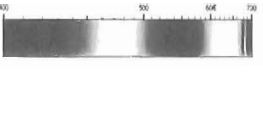
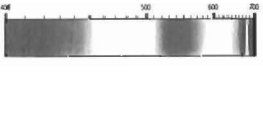
With the exception of the slight chalkiness to short-wave U.V. shown by some of the crystal edges, the ultraviolet luminescence of these flux red spinels is essentially identical to that of natural red-to-pink spinels from Burma and Sri Lanka

(Webster, 1983; Liddicoat, 1990), and is consistent with information previously reported on these flux synthetics (see, e.g., Henn and Bank, 1992).

For the blue flux synthetic spinels we examined, the long-wave U.V. fluorescence varied from weak to moderate, slightly chalky, red to reddish purple. The short-wave U.V. fluorescence was slightly stronger, but the same color. Again, no phosphorescence was detected. The long-wave U.V. behavior is similar to that of "cobalt blue" natural spinels we have tested (but which are inert to short-wave U.V.). In contrast, flame-fusion synthetic spinels of the same bright blue color exhibit strong red fluorescence to long-wave U.V., but mottled blue to bluish white fluorescence to short-wave U.V. (see table 2; also, Schwarz, 1981; Webster, 1983).

Visible-Light Spectroscopy. When examined with a handheld spectroscope, all of the red synthetic

TABLE 1. Gemological characteristics of natural, flame-fusion synthetic, and Russian flux-grown synthetic red spinels.^a

| Property | Natural red | Flame-fusion synthetic red | Flux-grown synthetic red |
|---------------------------|---|---|---|
| Index of refraction | 1.718 (+0.017)(-0.008) | 1.722 (±0.003) | 1.719 (±0.003) |
| Specific gravity | 3.60 (+0.10)(-0.03) | 3.59 (±0.01) | 3.61 (±0.03) |
| Polariscope reaction | Singly refractive (SR); possible weak to moderate anomalous double refraction (ADR) | Singly refractive (SR); strong anomalous double refraction (ADR); "cross hatch" pattern | Singly refractive (SR); possible weak to moderate anomalous double refraction (ADR) |
| Chelsea filter reaction | Red | Red | Red to orangy red |
| Fluorescence ^b | | | |
| Long-wave | Weak to strong, red or orange | Strong red | Strong, purplish red to slightly orangy red |
| Short-wave | Inert to weak, red or orange-red | Inert to moderate red | Moderate to strong slightly orangy red |
| Transmission luminescence | Red | Red | Red to orangy red |
| Inclusions | Most commonly octahedra either singly or in a fingerprint pattern; other inclusions might consist of apatite and dolomite | Curved color banding and curved striae; gas bubbles that occasionally contain a secondary phase | Orangy brown to black flux inclusions occurring singly or in a fingerprint pattern; also metallic platelets |
| Spectra |  |  |  |

^a Properties for natural and flame-fusion synthetic red spinels are as reported in GIA Gem Property Chart A (1985) and Hurlbut and Kammerling (1991), and as determined by the authors' experience. Properties for the Russian flux-grown synthetic spinels are based on the examination of four crystals and nine faceted red samples.

^b No phosphorescence was observed to either wavelength.

spinel showed general absorption in the violet and blue from the ultraviolet to about 450 nm, and a broad absorption band between approximately 510 and 580 nm. We also noted a fluorescent line in the red between 680 and 685 nm. These absorption features are similar to those observed in a natural red Burmese spinel (see table 1—lower spectrum).

Note that none of the flux synthetic red spinels examined exhibited the “organ-pipe” fluorescence emission spectrum of sharp lines (as seen in the red portion of the top spectrum for natural red spinel in table 1) reported for a number of natural red spinels when viewed with a handheld spectroscope (Webster, 1983, p. 134).

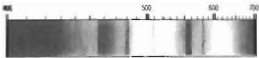
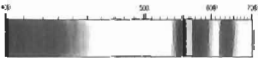
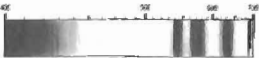
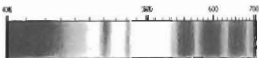
All of the flux synthetic blue spinels examined displayed strong absorption bands between approximately 535 and 550, 560 and 590, and 615 and 635 nm. In some of the larger samples, we saw a very weak sharp line at about 690 nm. There was also a weak absorption below about 430 that increased toward the ultraviolet (see table 2).

Transmission Luminescence/Filter Reactions. Both the red and blue flux synthetic spinels exhibited a red to orangy red “transmission” luminescence to visible light. The intensity of this luminescence appears to be directly proportional to that of the ultraviolet fluorescence. This is the same reaction we have seen with “cobalt blue” natural spinels.

Both the red and blue flux synthetic spinels displayed a red to orangy red color when exposed to an intense incandescent light source and viewed with a Chelsea color filter. This is almost identical to the reaction of natural red spinels. Natural “cobalt blue” spinels exhibit a weak orange-to-red reaction, while natural blue spinels colored by iron do not show any color when tested by this method, presumably because luminescence is quenched by the iron present.

Magnification. Many of the red and blue crystals and faceted flux synthetic spinels contained metal-

TABLE 2. Gemological characteristics of natural, flame-fusion synthetic, and Russian flux-grown synthetic blue spinels.^a

| Property | Natural blue | Flame-fusion synthetic blue | Flux-grown synthetic blue |
|---------------------------|--|---|---|
| Index of refraction | 1.718 (+0.017)(-0.008) | 1.728 (+0.012)(-0.008) | 1.714 (±0.002) |
| Specific gravity | 3.60 (+0.10)(-0.03) | 3.64 (+0.02)(-0.12) | 3.62 (±0.04) |
| Polariscope reaction | Singly refractive (SR); possible weak to moderate anomalous double refraction (ADR) | Singly refractive (SR); strong anomalous double refraction (ADR); “cross hatch” pattern | Singly refractive (SR); possible weak to moderate anomalous double refraction (ADR) |
| Chelsea filter reaction | Fe: Inert Co: Weak orange-to-red | Red | Red to orangy red |
| Fluorescence ^b | | | |
| Long-wave | Fe: Inert Co: Weak to moderate red | Strong red | Weak to moderate, slightly chalky red to reddish purple |
| Short-wave | Fe: Inert Co: Inert | Mottled blue to bluish white | Same color as long-wave U.V. but slightly stronger |
| Transmission luminescence | Fe: Inert Co: Red | Red | Red to orangy red |
| Inclusions | Octahedra either singly or in a fingerprint pattern; other crystal inclusions might include graphite, dolomite, and sphene | Tiny “bread-crumbs” inclusions; gas bubbles | Orangy brown to black flux inclusions occurring singly or in a fingerprint pattern; also metallic platelets |
| Spectra | | | |
| Fe type: |  |  |  |
| Co type: |  | | |

^a Properties for natural and flame-fusion synthetic blue spinels are as reported in GIA Gem Property Chart A (1985) and Hurlbut and Kammerling (1991), and as determined by the authors' experience. Properties for the Russian flux-grown synthetic spinels are based on the examination of 16 crystals and 12 faceted blue samples.

^b No phosphorescence was observed to either wavelength.



Figure 5. Dark reddish to orangy brown, jagged-edged flux inclusions (with gas bubbles), such as this 3-mm-long example, provide proof that the host stone is synthetic. Note how the inclusions taper to a point. Photomicrograph by John I. Koivula.

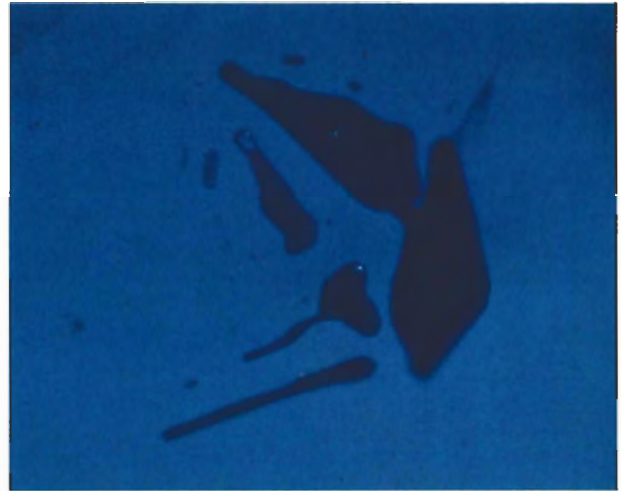


Figure 6. Gas bubbles were also evident in the flux inclusions seen in some of the blue synthetic spinels. Photomicrograph by John I. Koivula; magnified 40x.

lic or flux inclusions that were deep orangy brown to almost black. These inclusions exhibited sharply angular to jagged profiles, which were sometimes slightly rounded and tapered to points; some contained gas bubbles (figures 5 and 6). These bubbles presumably were caused by contraction of the flux as it cooled, as described in Kashan synthetic ruby by Burch (1984). The flux inclusions could be seen as colorless to white to slightly yellowish or orangy brown net- or fingerprint-like patterns (figures 7 and 8), similar to those observed in some flux-grown synthetic rubies (see, e.g., Burch, 1984).

Some of the flux particles noted were very small and, though still distinctly orangy brown (fig-

ure 9), these might be mistaken for natural inclusions by those not familiar with this new synthetic.

A few of the faceted stones contained minute triangular grayish silver inclusions, which exhibited a distinctly metallic luster when observed with oblique surface-incident light (figure 10). Because they were located deep within the host material, they could not be analyzed by X-ray diffraction. From their general appearance and the results of EDXRF chemical analysis on the host stones, we believe that they consist of platinum or iridium derived from the crucibles in which the synthetic spinels were grown.

Figure 7. Flux inclusions formed net- or fingerprint-like patterns in some of the flux synthetic red spinels. Photomicrograph by John I. Koivula; magnified 20x.

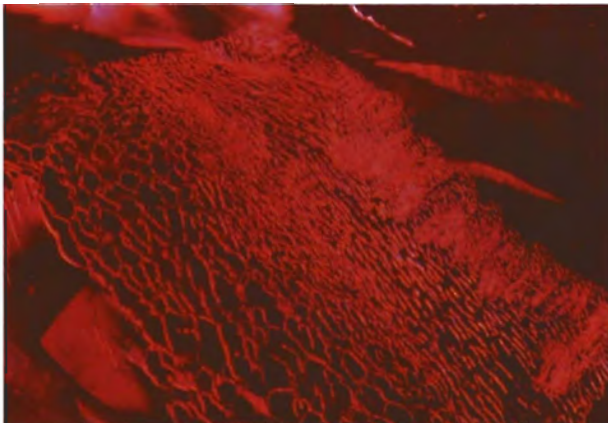
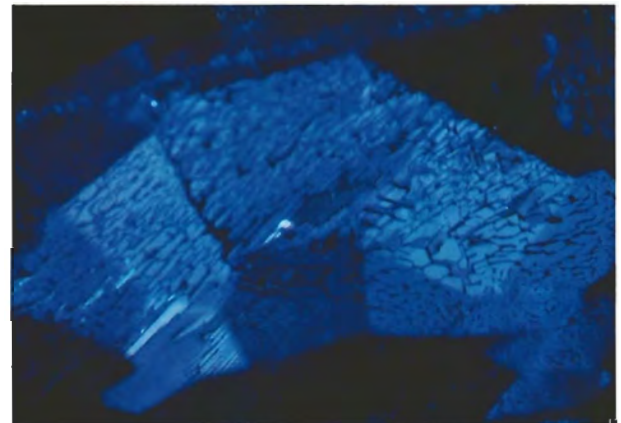


Figure 8. A distinctive net-like pattern of flux inclusions was also typical of the flux synthetic blue spinels. Photomicrograph by John I. Koivula; magnified 15x.



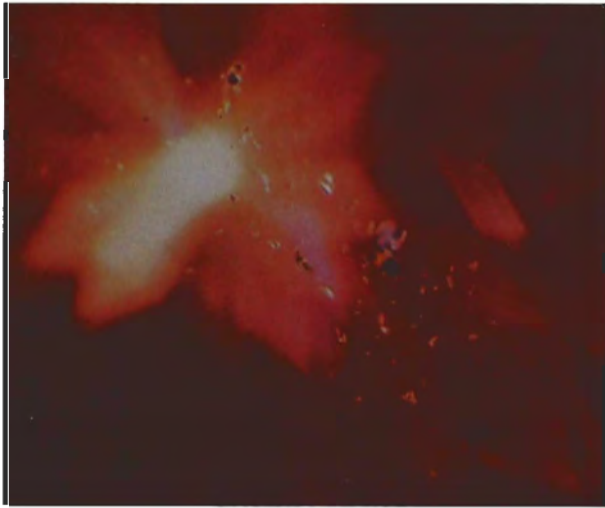


Figure 9. Tiny flux particles such as these might be mistaken for natural inclusions by those not familiar with this flux synthetic spinel. Photomicrograph by John I. Koivula; magnified 25 \times .

A specific crystallographic orientation of the flux inclusions could not be determined in any of the faceted stones. In some of the crystals, however, the larger flux inclusions formed pyramid-shaped phantoms in near-perfect alignment with the external faces and edges of the octahedra. This

Figure 10. Minute, triangular solid inclusions with distinct metallic luster—probably platinum or iridium—were observed in a few stones. Photomicrograph by John I. Koivula; magnified 20 \times .

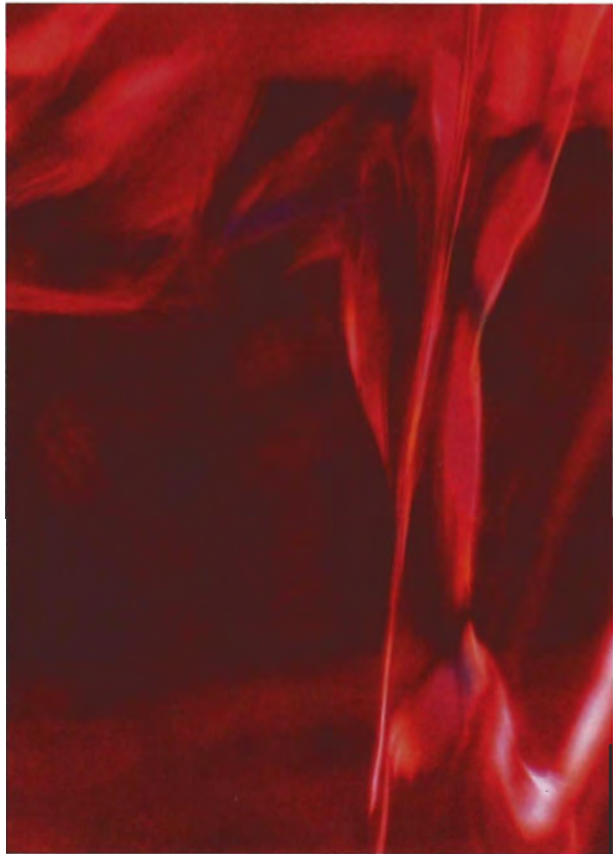


Figure 11. In several of the samples, iridescence was noted in air-filled fractures. Photomicrograph by John I. Koivula; magnified 25 \times .

orientation is consistent with the growth of the synthetic spinel crystal along octahedral planes. Some of these inclusions were centered just under the flat surfaces (again, see figure 3) that appear to form the plane of crucible attachment of the crystal during growth.

In some of the samples, we observed mirror-like air-filled fractures that appeared iridescent when viewed in certain directions (figure 11). As expected, polarized light revealed an anomalous birefringence ("strain") pattern in association with these fractures (as well as with some of the flux inclusions).

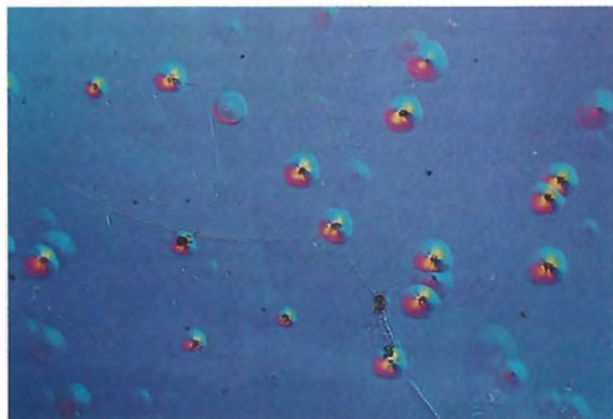
We examined the synthetic spinel crystals by means of Nomarski differential interference contrast microscopy to compare their surface features to those of natural spinel crystals. Most natural crystals that have not been subjected to some form of erosion or abrasion show either very smooth surfaces or slight signs of chemical dissolution in

Figure 12. Natural spinel crystals like this one commonly have triangular etch features. Photomicrograph by John I. Koivula; magnified 80×



the form of minute triangular "etch pits" on their octahedral faces (figure 12). Although the octahedral surfaces of the three red synthetic crystals appeared relatively smooth to the unaided eye, on closer inspection they were found to be decorated with roughly circular to semicircular growth hillocks (figure 13) of a type not yet observed by the authors on the surfaces of natural spinel crystals. Their appearance suggests that they represent slightly triangular growth spirals around a screw-type dislocation (I. Sunagawa, pers. comm., 1993).

Figure 13. In contrast to the triangular etch features noted on the surface of natural spinels (figure 12), circular to semicircular growth hillocks were noted on the octahedral faces of the three Russian flux-grown synthetic crystals. Photomicrograph by John I. Koivula; magnified 80×



One feature that seems to be relatively rare and was only seen in the blue flux synthetic spinels is an unusual "dendritic" inclusion that forms distinctly shaped, extremely thin, delicate fans of varying sizes (figure 14). These "fans" appear opaque in darkfield or transmitted light, and have an obvious metallic luster when observed in reflected light. Because destructive testing would have been necessary and results could not be guaranteed, we could not establish the nature of these dendritic inclusions.

We did not observe any color zoning in either the crystals or the faceted samples.

CHEMICAL COMPOSITION

EDXRF chemical analysis of the Russian flux synthetic spinels revealed differences in their compositions from those of natural spinels of similar colors (figures 15 and 16). Due to the excitation conditions used, the magnesium (Mg) and aluminum (Al) present as intrinsic components in spinels do not produce well-defined peaks, but they also have no diagnostic value in this context. Other elements, present as impurities in spinel, can be divided into "major" and "minor." The former have relatively large X-ray peak areas, whereas the latter always have smaller peak areas.

In the Russian flux synthetic red spinels we tested (e.g., figure 15A-B), chromium (Cr) and iron (Fe) were major impurities, with Cr content being relatively constant but Fe varying from one sample to the next. When they were present, nickel (Ni),

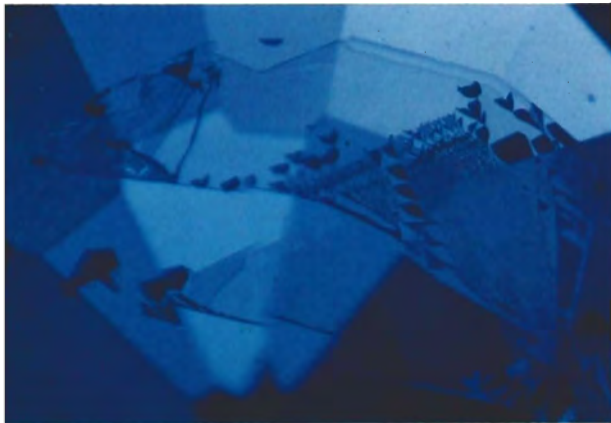


Figure 14. Dendritic inclusions, such as this one, appear to be rare; among the flux synthetic spinels we examined, they were only seen in the blue material. Photomicrograph by John I. Koivula; magnified 15 \times .

vanadium (V), zinc (Zn), gallium (Ga), and lead (Pb) were all minor impurities, with the exception of one sample in which Ni was a major impurity. We did not detect Pb in any of the natural spinels. Two flux synthetic red spinels grown at Bell Laboratories, although both similar in color to one another, as well as to the Russian samples, contained Cr and Fe in one instance and Mn in the other.

In contrast, all 28 natural red-to-pink or purple spinels we analyzed had more Zn than the flux synthetics (compare spectra 15A–B to 15C–E). Cr and Fe varied in content, with generally more Cr than Fe in red spinels from Myanmar, and more Fe than Cr in pink spinels from Myanmar and other localities. The minor impurities titanium (Ti), V, Ga, Ni, and copper (Cu) varied in content in natural spinels from one locality to the next, but generally V was greater than Ti. The Ga content differed from one natural spinel to the next, even when they were from the same locality. Ni and Cu were the least abundant impurities we detected. Cu was not detected in either of the samples for which spectra are illustrated in figure 15A–B.

In the nine flux synthetic blue spinels we analyzed (figure 15A–B), we always found cobalt (Co) and Fe, with Co greater than Fe. The minor impurities V, Cr, manganese (Mn), Pb, Ni, Zn, and Ga occurred in most samples but in varying contents. Fe, Co, Ga, and Pb were present in the one flux synthetic blue spinel from Bell Laboratories that

we analyzed. In contrast, the four Sri Lankan “cobalt blue” natural spinels examined contained Fe and Zn as major impurities, Ga as a minor impurity, and Ni, V, Cr, Mn, and Cu as trace impurities in varying amounts (figure 16C–E). Cu was detected in samples 1791 and 1807 but is not visible in the spectra illustrated. Note that the peak for Co cannot be distinguished from other element peaks in the EDXRF spectra of these natural blue spinels due to the low concentration of Co and the overlap of its characteristic peaks with those of other elements (Koivula et al., 1990b). Nonetheless, there is a sufficient amount (as shown by the spectral data discussed below) to give rise to the saturated blue color.

Finally, iridium (Ir) was found only in the red flux synthetic spinels, and platinum (Pt) occurred only in the blue flux synthetic spinels.

For comparison with these qualitative EDXRF results, table 3 presents quantitative microprobe analyses of three natural faceted pink-to-red spinels and three flux synthetic red spinel crystals. These samples were chosen to represent the lowest Zn concentration detected among the natural spinels and the highest Zn levels among the flux synthetic spinels. The EDXRF and microprobe results are consistent. Furthermore, these microprobe data confirm the similarity in MgO:Al₂O₃ ratios of natural and flux synthetic spinels. We did not do microprobe analysis on the blue spinels, since chemical analysis is not necessary to separate natural from synthetic “cobalt blue” spinels.

VISIBLE ABSORPTION SPECTROPHOTOMETRY

Figure 17 compares the visible absorption spectra (labeled A through F) for three natural, one flame-fusion synthetic, and two flux synthetic (one each Russian and Bell Laboratories) blue spinels, both as recorded with GIA’s Hitachi spectrophotometer and as seen with a handheld spectroscope. We recorded similar spectra for natural and synthetic red spinels (flux and flame-fusion), but these are not shown because the spectral curves were virtually identical, and therefore, are not diagnostic (see the comparison of the spectra obtained with a handheld spectroscope in table 1).

Examination of the six spectral curves in figure 17 reveals differences between the “iron blue” and “cobalt blue” natural spinels mentioned above. Spectra A and B (for grayish blue natural spinels)

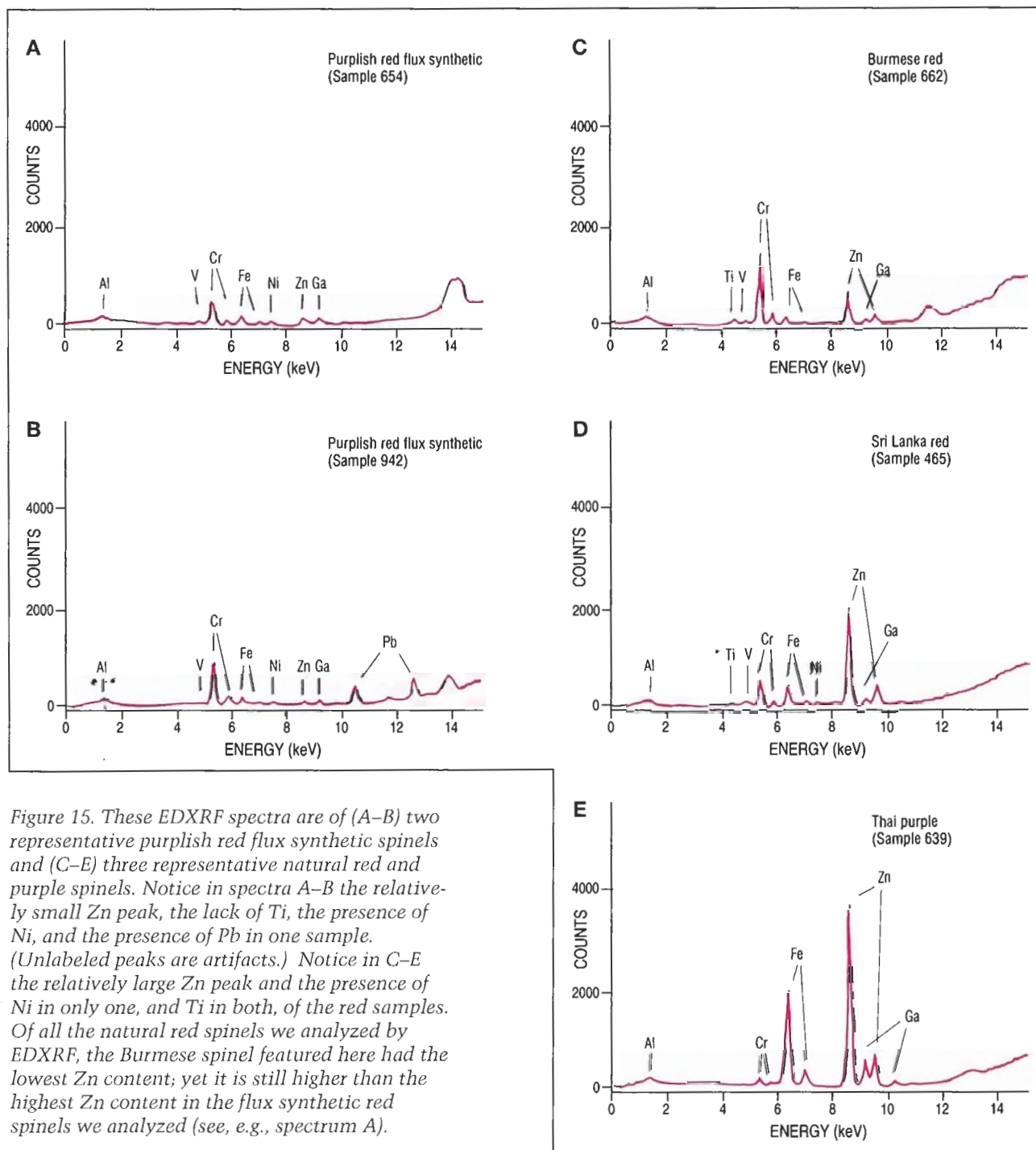


Figure 15. These EDXRF spectra are of (A–B) two representative purplish red flux synthetic spinels and (C–E) three representative natural red and purple spinels. Notice in spectra A–B the relatively small Zn peak, the lack of Ti, the presence of Ni, and the presence of Pb in one sample. (Unlabeled peaks are artifacts.) Notice in C–E the relatively large Zn peak and the presence of Ni in only one, and Ti in both, of the red samples. Of all the natural red spinels we analyzed by EDXRF, the Burmese spinel featured here had the lowest Zn content; yet it is still higher than the highest Zn content in the flux synthetic red spinels we analyzed (see, e.g., spectrum A).

exhibit absorption bands throughout the visible range and increasing absorption below about 430 nm that have been attributed to iron (Schmetzer et al., 1989, p. 166). With increasing Fe content, all of these absorption bands become more pronounced, so much so that those between 550 and 670 nm can begin to be seen with a handheld spectroscope (spectrum B).

Spectrum C is for a natural “cobalt blue” spinel from Sri Lanka in the GIA reference collection. This particular spinel was used to prepare the spectrum labeled as “type 1” in the article on “cobalt blue” natural spinels by Shigley and Stockton (1984). The spectrum shows the weaker bands between 350 and 500 nm due to Fe, as well as a group of three broad, more intense bands (at

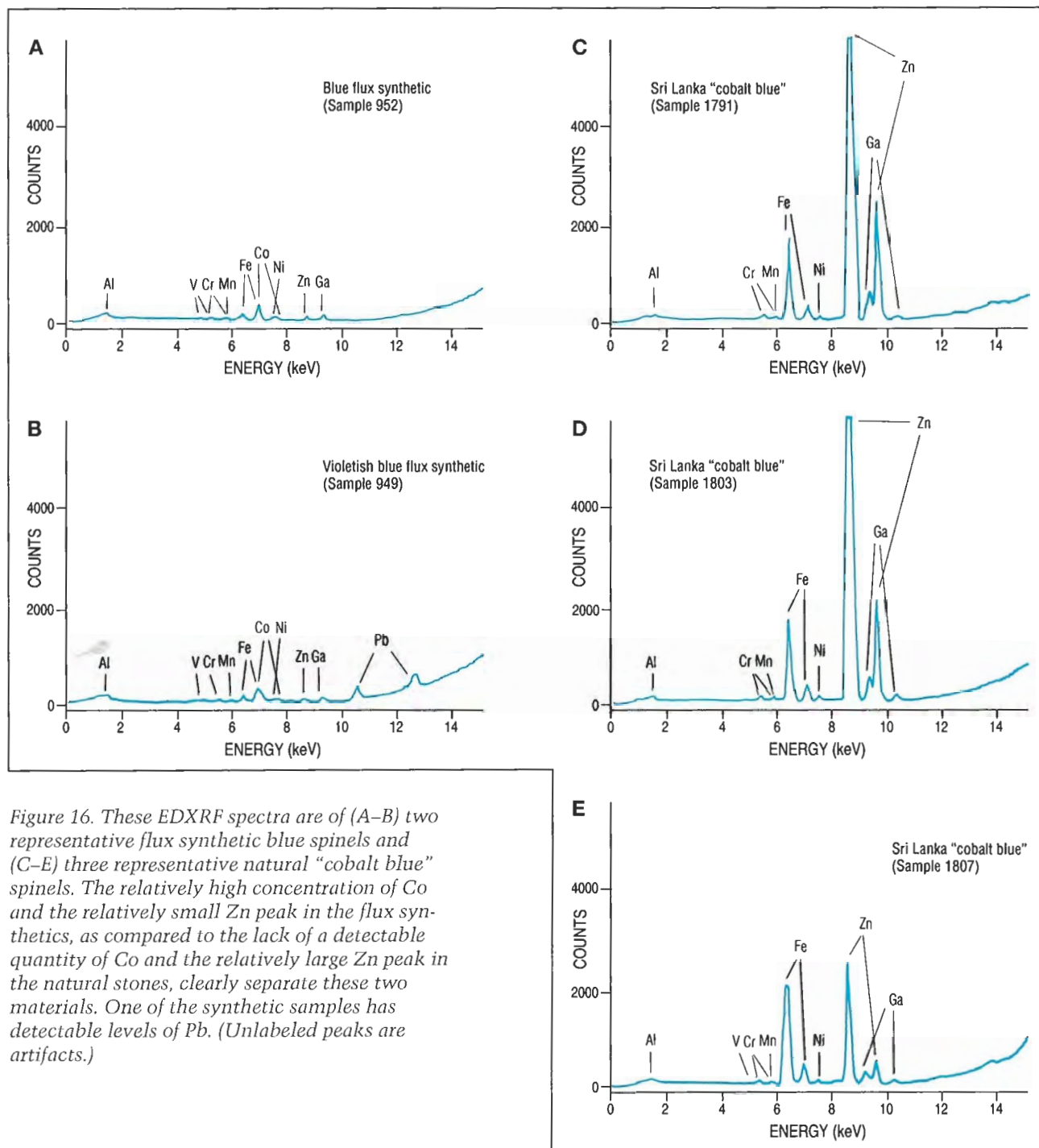


Figure 16. These EDXRF spectra are of (A–B) two representative flux synthetic blue spinels and (C–E) three representative natural “cobalt blue” spinels. The relatively high concentration of Co and the relatively small Zn peak in the flux synthetics, as compared to the lack of a detectable quantity of Co and the relatively large Zn peak in the natural stones, clearly separate these two materials. One of the synthetic samples has detectable levels of Pb. (Unlabeled peaks are artifacts.)

about 550, 585, and 625 nm) that are all attributed to cobalt (Schmetzer et al., 1989). Note that these cobalt features completely overlap and obscure the weaker Fe features between 500 and 700 nm that can be seen in spectra A and B. Three spectral features, when seen in combination, establish these “cobalt blue” spinels as natural: (1) the presence of the Co absorption bands between 500 and 600 nm,

(2) the weak absorption bands due to Fe below 500 nm, and (3) the increasing absorption below about 430 nm also due to Fe.

Spectra D, E, and F are for a Russian flux-grown synthetic, a flame-fusion synthetic, and a Bell Laboratories flux synthetic blue spinel, respectively. All three spectra show the series of stronger absorption bands from 500 to 650 nm due to cobalt

(again, see Schmetzer et al., 1989). The three spectra are very similar (in respect to the location of features) to that of the natural "cobalt blue" spinel (spectrum C) in the region between 500 and 700 nm, but they lack the iron-related spectral features, most notably below 500 nm (even though Fe is detected in them by EDXRF; see figure 16A).

DISCUSSION

Because of the similarities in chemical composition between flux synthetic and natural spinels, their indices of refraction and specific gravity are nearly identical, thus providing no means of separation. In the case of red flux synthetic spinels, flux or metallic inclusions, when present, are the only diagnostic gemological properties; in the case of red natural spinels, only the "organ pipe" luminescence lines in the visible absorption spectrum, when present, are diagnostic (note that the presence of only one fluorescent line or a doublet would be of no help in making a separation). In a stone that lacks characteristic inclusions or a characteristic absorption spectrum, chemical analysis is critical to the separation of natural from flux synthetic red spinels.

All of the natural red spinels we analyzed by EDXRF showed a more intense Zn peak than their

flux synthetic counterparts. Microprobe analyses confirmed that there is no overlap (and that, in fact, there is a significant gap) between the ranges of Zn concentration detected in natural (0.05 to 0.10 wt.% ZnO) and flux synthetic spinels (no more than 0.01 wt.% ZnO). Therefore, the presence of a comparatively large amount of Zn is proof of natural origin. However, there is a complete series within the spinel group to a Zn end member, gahnite, which has also been grown in the laboratory (see box B). The differences in Zn concentration between natural and flux synthetic spinels are large enough that this separation can be done solely using EDXRF analysis; there is no need to use the electron microprobe or other quantitative procedures. Using a more sensitive, quantitative analytical technique known as optical emission spectroscopy, Schwarz (1981) studied the differences in chemistry between flame-fusion synthetic spinels of various colors (none of which were pink to red) and natural pink-to-red spinels from Myanmar and Sri Lanka. He, too, found significantly more Zn in natural spinels than in the flame-fusion synthetics.

We also found Ti only in the natural red spinels. Therefore, the presence of Ti indicates a natural origin. Fe was more abundant in the natural

TABLE 3. Electron microprobe analyses of representative pink-to-red natural spinels and Russian flux-grown synthetic spinels^a.

| Oxide | Natural spinels (wt.%) | | | Russian flux-grown synthetic spinels (wt.%) | | |
|--------------------------------|--------------------------------|--------------------------------|-------------------------------|---|---------------------------|---------------------------|
| | No. 646 ^b (Pink) | No. 647 ^b (Pink) | No. 662 ^c (Red) | No. 656 (Purplish red) | No. 695 (Purplish red) | No. 654 (Purplish red) |
| MgO | 27.72 | 27.81 | 28.17 | 27.70 | 27.38 | 27.59 |
| Al ₂ O ₃ | 69.46 | 69.62 | 67.24 | 70.64 | 70.31 | 71.07 |
| TiO ₂ | 0.01 | 0.02 | 0.41 | BDL ^d | BDL | BDL |
| V ₂ O ₃ | 0.05 | 0.04 | 0.38 | 0.05 | 0.04 | 0.03 |
| Cr ₂ O ₃ | 0.06 | 0.05 | 3.09 | 0.47 | 0.49 | 0.34 |
| MnO | BDL | 0.01 | 0.01 | BDL | 0.02 | BDL |
| FeO | 0.48 | 0.31 | BDL | BDL | 0.05 | 0.04 |
| NiO | 0.01 | BDL | BDL | BDL | BDL | BDL |
| ZnO | 0.07 | 0.10 | 0.05 | 0.01 | 0.01 | BDL |
| Ga ₂ O ₃ | 0.04 | 0.02 | BDL | 0.02 | BDL | 0.03 |
| Total | 97.90 | 97.98 | 99.35 | 98.89 | 98.30 | 99.10 |

^a Electron microprobe analyses were performed on an automated, five-crystal JEOL 733 spectrometer operating at a beam-accelerating potential of 15 kV and a current of 40 nA. K-alpha lines were analyzed for each element. Standards include: (Mg, Al)—spinel, (Si, Ca)—anorthite, (K)—microcline, (Ti)—TiO₂, (V)—V₂O₅, (Cr)—Cr₂O₃, (Mn)—Mn olivine, (Fe)—fayalite, (Ni)—Ni olivine, (Zn)—ZnO, and (Ga)—GaAs. Two analyses at different locations were performed on each sample. Total iron is shown as FeO; total manganese as MnO. The microprobe data were corrected using the program CITZAF (Armstrong, 1988) employing the absorption correction of Armstrong (1982), the atomic number correction of Love et al. (1978), and the fluorescence correction of Reed (1965; as modified by Armstrong, 1988). Analyses performed by Paul Carpenter.

^b From Tajikistan.

^c From Myanmar.

^d BDL = below the detection limits of the instrument (less than 0.01 wt.% oxide).

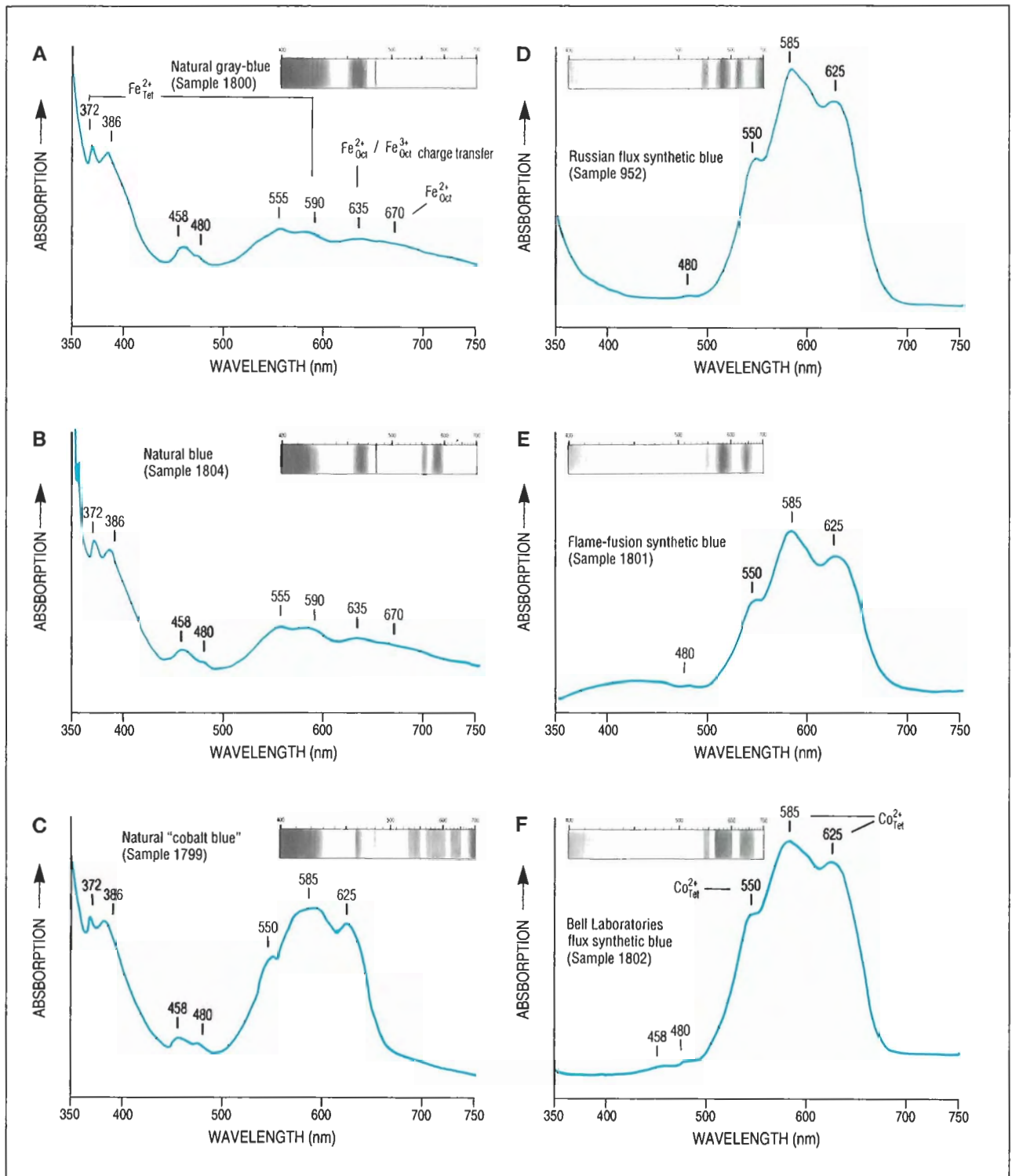


Figure 17. These visible absorption spectra for three natural and three synthetic blue spinels, as recorded with a Hitachi spectrophotometer and seen with a handheld spectroscope, illustrate the evolution from Fe-related features to Co-related features. (For details see text.) Spectrum A is of a 2.11-ct natural gray-blue spinel; spectrum B is of a 2.88-ct natural blue spinel; and spectrum C is of a 1.92-ct natural "cobalt blue" spinel. Spectrum D is of a 0.83-ct faceted Russian flux synthetic blue spinel; spectrum E is of a flame-fusion synthetic blue spinel fragment; and spectrum F is of a 0.15-ct flux synthetic blue spinel crystal grown at Bell Laboratories. Spectra A, C, E, and F were labeled as "spectra types" II, I, III, and IV, respectively, in Shigley and Stockton (1984).

BOX B: SYNTHETIC GAHNITE

Gahnite, $ZnAl_2O_4$, the zinc equivalent of spinel ($MgAl_2O_4$), has been grown in various colors by the flux method, but only on an experimental basis (Nassau, 1980). This rare synthetic was mentioned in the gemological literature as early as 1967 by Liddicoat. As part of our study, we analyzed several pink-to-red flux synthetic gahnites grown in the 1970s at Bell Laboratories (figure B-1). Not surprisingly, the colors result from doping this material with Cr.

Since both synthetic spinel and gahnite crystals can be grown by the flux method, in similar pink-to-red colors, it appears that one could possibly grow a synthetic spinel crystal containing an amount of zinc similar to that detected in natural spinels (see, e.g., Wood and White, 1968). However, it is uncertain whether crystal growers would spend the time and money that would undoubtedly be required to alter their current growth methods simply to circumvent a particular gem identification method. In addition, the new product might have other distinctive gemological properties. We have no evidence that such pink-to-red spinel containing abundant Zn has been synthesized.



Figure B-1. These flux synthetic gahnites (0.47–23.25 ct) were grown on an experimental basis at Bell Laboratories. Courtesy of Dr. Kurt Nassau; photo by Robert Weldon.

red spinels (except for those from Myanmar), and Ga was sometimes more abundant (but with significant overlap in concentration level) in the natural than in the flux synthetic red spinels. Ni was found as a trace impurity in both groups. Cr and V were recorded in both the natural and the flux synthetic red spinels, but in varying relative quantities. Finally, the presence of either Ir (from the crucible) or Pb (from the flux) proves synthetic origin.

Magnification is the key gemological test in separating blue flux synthetic from similar-colored natural spinels, both Fe- and Co-containing. If characteristic inclusions are not present, Fe bands in the visible-light spectrum and an inert reaction to short-wave U.V. radiation will identify both Fe- and Co-containing spinels as natural (table 2). The more common Fe-containing natural blue spinels can also be separated on the basis of their absence of transmission luminescence, of fluorescence to long-wave U.V. radiation, or of a reaction to the Chelsea color filter. Natural blue spinels contain more Zn, and generally more Fe and Ga, whereas the flux synthetic spinels contain more Co and, in some cases, they contain Pb or Pt (with the presence of either of the latter two elements constituting proof of synthetic origin).

CONCLUSION

In this article, we have described the gemological properties and chemical characteristics of the new flux synthetic red and blue spinels from Russia. For blue flux synthetic spinels, microscopy, visible-light spectroscopy, and short-wave U.V. fluorescence will suffice for separation from both Fe-containing and Co-containing natural spinels. Red flux synthetic spinels can be identified gemologically only if flux or metallic inclusions are present. In either case, qualitative chemical analysis by EDXRF appears to provide definitive proof, as it did for all the spinels examined for this study.

The commercial availability of Russian flux synthetic spinels in a range of colors and significant faceted sizes will require that gemologists consider a variety of tests to identify this material. For some stones, they will need to use a combination of both standard gem-testing methods and advanced chemical analysis. This situation has already been demonstrated in the case of natural and synthetic ruby (see, e.g., Muhlmeister and Devouard, 1991). In the absence of definitive gemological tests, this article points out the growing importance of rapid, nondestructive, EDXRF chemical analysis to modern gem testing.

Acknowledgments: The authors thank Bill Vance and John Fuhrbach for allowing examination of their synthetic spinels. Russian scientists and crystal growers Dr. G. V. Bukin and the late Dr. A. S. Lebedev provided samples for this study (obtained through Prof. Dr. N. V. Sobolev of the Russian Academy of Sciences in Novosibirsk). Several rough and faceted flux synthetic spinels were obtained from Walter Barshai of Pinky Trading Co. Ltd. in Bangkok and Kyle Christianson Ltd. of Sylvania, Ohio. Dr. Kurt Nassau loaned flux synthetic spinel and synthetic gahnite crystals grown at Bell

Laboratories in New Jersey. Dr. Henry Hänni loaned two blue flux synthetic spinels. Patricia Maddison of the GIA Gem Trade Laboratory gemologically tested many of the faceted stones, while Mike Moon and Meredith Mercer of GIA Research prepared some of the initial visible absorption spectra. Paul Carpenter carried out the electron microprobe analysis at the California Institute of Technology in Pasadena, California. This study was made possible in part by funds from the Dr. Byron C. Butler Fund for Inclusion Research.

REFERENCES

- Armstrong J.T. (1982) New ZAF and α -factor correction procedures for the quantitative analysis of individual microparticles. In K.F.J. Heinrich, Ed., *Microbeam Analysis—1982*, San Francisco Press, San Francisco, CA, pp. 175–180.
- Armstrong J.T. (1988) Quantitative analysis of silicate and oxide materials: Comparison of Monte Carlo, ZAF and $\phi(\rho z)$ procedures. In D.E. Newbury, Ed., *Microbeam Analysis—1988*, San Francisco Press, San Francisco, CA, pp. 239–246.
- Bank H., Henn U. (1989) Flux grown synthetic red spinel from U.S.S.R. *ICA Early Warning Laboratory Alert*, No. 26, December 8.
- Bank H., Henn U. (1990) Untersuchung eines im Flussmittelfverfahren hergestellten synthetischen roten spinells aus der UdSSR. *Zeitschrift der Deutschen Gemmologischen Gesellschaft*, Vol. 39, No. 1, pp. 45–48.
- Brown G., Beattie R., Snow J. (1991) Verneuil synthetic red spinel. *Australian Gemmologist*, Vol. 17, No. 9, pp. 344–347.
- Brown G., Kelly S.M.B., Sneyd R. (1990) Russian flux-grown synthetic spinel. *Australian Gemmologist*, Vol. 17, No. 8, pp. 315–317.
- Burch C.R. (1984) Some observations on a Kashan synthetic ruby. *Journal of Gemmology*, Vol. 19, No. 1, pp. 54–61.
- GIA Gem Property Chart A (1985). Gemological Institute of America, Santa Monica, CA.
- Henn U., Bank H. (1991) Flux-grown synthetic red and blue spinels/USSR. *ICA Early Warning Laboratory Alert*, No. 26, December 11.
- Henn U., Bank H. (1992) Über die Eigenschaften von im Flussmittelfverfahren hergestellten synthetischen roten und blauen Spinellen aus Russland. *Zeitschrift der Deutschen Gemmologischen Gesellschaft*, Vol. 41, No. 1, pp. 1–6.
- Hodgkinson A. (1991) Synthetic red spinel. *Australian Gemmologist*, Vol. 17, No. 11, pp. 466–468.
- Hurlbut C.S., Kammerling R.C. (1991) *Gemology*, 2nd ed. John Wiley and Sons, New York.
- Jenkins R. (1980) *An Introduction to X-ray Spectrometry*. Heyden & Son Inc. Philadelphia, PA.
- Koivula J.I., Kammerling R.C. (1989) Gem news: Flux synthetic spinel. *Gems & Gemology*, Vol. 25, No. 4, p. 250.
- Koivula J.I., Kammerling R.C. (1990a) Flux-grown synthetic red spinel/USSR. *ICA Early Warning Laboratory Alert*, No. 26, January 12.
- Koivula J.I., Kammerling R.C. (1990b) Gem news: Color-change cobalt spinel. *Gems & Gemology*, Vol. 26, No. 4, pp. 305–306.
- Koivula J.I., Kammerling R.C., Fritsch E. (1991) Gemmological investigation of a synthetic spinel crystal from the Soviet Union. *Journal of Gemmology*, Vol. 22, No. 5, pp. 300–304.
- Liddicoat R.T. Jr. (1967) Developments and highlights at the gem trade lab in Los Angeles: Unusual gem materials. *Gems & Gemology*, Vol. 12, No. 5, pp. 151.
- Liddicoat R.T. Jr. (1990) *Handbook of Gem Identification*, 12th ed. rev., 3rd printing. Gemological Institute of America, Santa Monica, CA.
- Love G., Cox M.G., Scott V.D. (1978) A versatile atomic number correction for electron-probe microanalysis. *Journal of Physics D*, Vol. 11, pp. 7–27.
- Muhlmeister S., Devouard B. (1992) Determining the natural or synthetic origin of rubies using energy-dispersive X-ray fluorescence (EDXRF). In A.S. Keller, Ed., *Proceedings of the International Gemmological Symposium 1991*, Gemological Institute of America, Santa Monica, CA, pp. 139–140.
- Nassau K. (1980) *Gems Made by Man*. Chilton Book Co., Radnor, PA.
- Reed S.J.B. (1965) Characteristic fluorescence correction in electron-probe microanalysis. *British Journal of Applied Physics*, Vol. 16, pp. 913–926.
- Schiffmann C.A. (1972) Observations on synthetic red spinel grown by the Verneuil method. *Lapidary Journal*, Vol. 26, September, pp. 926–931.
- Schwarz D. (1981) Chemismus und Fluoreszenzverhalten natürlicher und synthetischer Spinelle. *Uhren Juwelen Schmuck*, No. 20, pp. 57–60.
- Schmetzer K., Haxel C., Amthauer G. (1989) Colour of natural spinels, gahnospinels, and gahnites. *Neues Jahrbuch für Mineralogie, Abhandlungen*, Vol. 160, No. 2, pp. 159–180.
- Shigley J.E., Stockton C.M. (1984) "Cobalt blue" gem spinels. *Gems & Gemology*, Vol. 20, No. 1, pp. 34–41.
- Wang C.C., MacFarlane S.H. III (1968) Growth and characterization of large stoichiometric magnesium aluminate spinel single crystals. *Journal of Crystal Growth*, Vol. 3, No. 4, pp. 485–489.
- Webster R. (1983) *Gems, their sources, descriptions, and identification*, 4th ed. Revised by B.W. Anderson, Butterworths, London.
- Wood J.D.C., White E.A.D. (1968) Growth stoichiometric magnesium aluminate spinels crystals by flux evaporation. *Journal of Crystal Growth*, Vol. 3, No. 4, pp. 480–484.
- Wyon C., Aubert J.J., Auzel F. (1986) Czochralski growth and optical properties of magnesium-aluminium spinel doped with nickel. *Journal of Crystal Growth*, Vol. 79, pp. 710–713.

Back Issues of GEMS & GEMOLOGY

Limited quantities of these issues are still available.

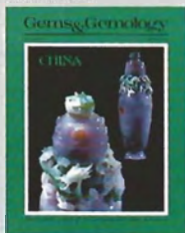
Spring 1985



Summer 1985



Spring 1986



Summer 1986



Fall 1986



Winter 1986



Spring 1987



Summer 1987



Fall 1987



Winter 1987



Spring 1988



Summer 1988



Fall 1988



Winter 1988



Spring 1989



Summer 1989



ORDER NOW!

Complete your back issues of Gems & Gemology NOW!

| | |
|--------------------|-----------------------------|
| Single Issues:* | \$ 9.00 ea. U.S. |
| | \$ 12.50 ea. elsewhere |
| Complete Volumes:* | |
| 1986, 1987, | \$ 32.00 ea. vol. U.S. |
| 1989, 1991, | \$ 42.00 ea. vol. elsewhere |
| 1992 | |
| Three-year set | \$ 85.00 U.S. |
| | \$ 110.00 elsewhere |
| Five-year set | \$ 140.00 U.S. |
| | \$ 180.00 elsewhere |

*10% discount for GIA Annual Fund donors at the Booster's Circle and above.

Spring 1986

A Survey of the Gemstone Resources of China
The Changma Diamond District, China
Gemstone Carving in China: Winds of Change
A Gemological Study of Turquoise in China
The Gemological Characteristics of Chinese Peridot
The Sapphires of Mingxi, Fujian Province, China

Summer 1986

The Coscuez Mine: A Major Source of Emeralds
The Etahera Gem Field of Central Sri Lanka
Some Unusual Sillimanite Cat's-Eyes
An Examination of Four Important Gems
Green Glass Made of Mount Saint Helens Ash?

Fall 1986

A Simple Procedure to Separate Natural from Synthetic Amethyst on the Basis of Twinning
Pink Topaz from Pakistan
Carbon Dioxide Fluid Inclusions as Proof of Natural-Color Corundum
Specific Gravity—The Hydrostatic Method
Colombage-Ara Scheelite

Winter 1986

Sumitomo Gem-Quality Synthetic Yellow Diamonds
Art Nouveau: Jewels and Jewelers
Contemporary Intarsia: The Medvedev Approach

Spring 1987

"Modern" Jewelry: Retro to Abstract
Infrared Spectroscopy in Gem Identification
A Study of the General Electric Synthetic Jadeite Iridescent Orthoamphibole from Greenland

Summer 1987

Gemstone Durability: Design to Display
Wessels Mine Sugillite
Three Notable Fancy-Color Diamonds
The Separation of Natural from Synthetic Emeralds by Infrared Spectroscopy
The Rutilated Topaz Misnomer

Fall 1987

An Update on Color in Gems. Part I
The Lennix Synthetic Emerald
Kyocera Corp. Products that Show Play-of-Color
Man-Made Jewelry Malachite
Inamori Synthetic Cat's-Eye Alexandrite

Winter 1987

The De Beers Gem-Quality Synthetic Diamonds
Queen Conch "Pearls"
The Seven Types of Yellow Sapphire and Their Stability to Light

Summer 1988

The Diamond Deposits of Kalimantan, Borneo
An Update on Color in Gems. Part 3
Pastel Pyropes
Three-Phase Inclusions in Sapphires from Sri Lanka

Fall 1988

An Economic Review of Diamonds
The Sapphires of Penglai, Hainan Island, China
Iridescent Orthoamphibole from Wyoming
Detection of Treatment in Two Green Diamonds

Winter 1988

Gemstone Irradiation and Radioactivity
Amethyst from Brazil
Opal from Opal Butte, Oregon
Kyocera's Synthetic Star Ruby

Spring 1989

The Sinkankas Library
The Gujjar Kilil Emerald Deposit
Beryl Gem Nodules from the Bananal Mine
"Opalite:" Plastic Imitation Opal

Summer 1989

Filled Diamonds
Synthetic Diamond Thin Films
Grading the Hope Diamond
Diamonds with Color-Zoned Pavilions

Fall 1989

Polynesian Black Pearls
The Capoeirana Emerald Deposit
Brazil-Twinned Synthetic Quartz
Thermal Alteration of Inclusions in Rutilated Topaz
Chicken-Blood Stone from China

Winter 1989

Emerald and Gold Treasures of the Atocha
Zircon from the Harts Range, Australia
Blue Pectolite
Reflectance Infrared Spectroscopy in Gemology
Mildly Radioactive Rhinestones and Synthetic Triplets

Spring 1990

Gem Localities of the 1980s
Gemstone Enhancement and Its Detection
Synthetic Gem Materials of the 1980s
New Technologies: Their Impact in Gemology
Jewelry of the 1980s

Summer 1990

Blue Diffusion-Treated Sapphires
Jadeite of Guatemala
Tsavorite Gem Crystals from Tanzania
Diamond Grit-Impregnated Tweezers

Winter 1990

The Dresden Green Diamond
Identification of Kashmir Sapphires
A Suite of Black Diamond Jewelry
Emeraldolite

Spring 1991

Age, Origin, and Emplacement of Diamonds
Emeralds of Panjshir Valley, Afghanistan

Summer 1991

Fracture Filling of Emeralds: Opticon and "Oils"
Emeralds from the Ural Mountains, USSR
Treated Andamooka Matrix Opal

Fall 1991

Rubies and Fancy Sapphires from Vietnam
New Rubies from Morogoro, Tanzania
Bohemian Garnet—Today

Winter 1991

Marine Mining of Diamonds off Southern Africa
Sunstone Labradorite from the Ponderosa Mine, Oregon
Nontraditional Gemstone Cutting
Nontransparent "CZ" from Russia

Spring 1992

Gem-Quality Green Zoisite
Kilbourne Hole Peridot
Fluid Inclusion Study of Querétaro Opal
Natural-Color Nonconductive Gray-to-Blue Diamonds
Peridot as an Interplanetary Gemstone

Summer 1992

Gem Wealth of Tanzania
Gamma-Ray Spectroscopy to Measure Radioactivity
Dyed Natural Corundum as a Ruby Imitation
An Update on Sumitomo Synthetic Diamonds

Fall 1992

Ruby and Sapphire Mining in Mogok
Bleached and Polymer-Impregnated Jadeite
Radiation-Induced Yellow-Green Color in Grossular Garnet

Winter 1992

Determining the Gold Content of Jewelry Metals
Diamond Sources and Production
Sapphires from Changle, China

Some issues from the 1984 and 1985 volume years are also available. Please call the Subscriptions Office for details.

TO ORDER: Call toll free (800)421-7250, ext. 394 or (310) 829-2991, ext. 3
OR WRITE: GIA, 1660 Stewart Street, Santa Monica, CA 90404,
Attn: G&G Subscriptions

EMERALDS AND GREEN BERYLS OF UPPER EGYPT

By Robert H. Jennings, Robert C. Kammerling, André Kovaltchouk, Gustave P. Calderon,
Mohamed K. El Baz, and John I. Koivula

Egypt is the most ancient of sources for emerald. More than 2,000 years ago, emerald deposits in upper Egypt were supplying gems throughout the Graeco-Roman Empire. A recent visit to this emerald province revealed that the emeralds occur within a northwest-southeast trending belt of schistose rocks in the Red Sea Hills, near the port town of Marsa Alam. At the time of the visit, there was no official commercial mining of emerald in the region, although there was evidence of sporadic activity by Bedouin tribespeople. Gemological examination of 14 cut emeralds and green beryls revealed properties consistent with those of material from similar geologic environments.

ABOUT THE AUTHORS

Mr. Jennings is former senior geologist, Mr. Kovaltchouk is former chief geophysicist, and Mr. El Baz is former staff geologist, ARCO Suez Inc., Cairo, Egypt; Mr. Kammerling is director of Identification and Research, Mr. Calderon is a staff gemologist, and Mr. Koivula is chief research gemologist, GIA Gem Trade Laboratory, Santa Monica, California.

Acknowledgments: The authors thank C. A. Barker and M. J. Welland for their support and permission to use ARCO vehicles and equipment. Ali Khorassany accompanied the research group in the field and provided study material. The hospitality of the Egyptian Geological Survey and Mining Authority in Marsa Alam is greatly appreciated. Derek Content kindly provided the text for box A. Sam Muhmeister and Mike Moon of GIA Research gathered the EDXRF and infrared spectroscopy data, respectively. Carol Silver did the map artwork.

*Gems & Gemology, Vol. 29, No. 2, pp. 100-115.
© 1993 Gemological Institute of America*

The legendary "Cleopatra's Mines" were the single most important source of emeralds for most of recorded history, with the earliest known production dating to the fourth century B.C. In fact, until the Spaniards' 16th-century discovery of emerald deposits in what is now Colombia, Egypt was the only significant source of this beryl variety as a gem material (Sinkankas, 1981). Yet in spite of their long history, relatively few early Egyptian emeralds are known (figure 1), with only a small number having been found in ancient tombs (Gregorietti, 1969). Sinkankas (1981) concludes from this relative scarcity of historic stones that large quantities were not produced from these mines, and the stones recovered were small and of "mediocre" quality. He further speculates that such material was probably used primarily in amulets or was crushed for medicinal use. The mines themselves have been largely inactive for more than 700 years, with 19th- and 20th-century attempts to reestablish commercial operations singularly unsuccessful.

Consequently, relatively little has been published on Egypt's emerald deposits—especially maps of the various occurrences and reports of current recovery—or on the gemology of the gems themselves. Although Grubessi et al. (1990) provided some gemological and crystallographic data for beryl crystals from Gebel Zabara, there has been no detailed gemological characterization of the gem-quality fashioned material that is available today.

It is commonly believed that the commercial potential of the Egyptian emerald deposits is low because of the generally poor quality of the material and the remoteness of the area, its harsh climate, and the consequent high cost of mining. Nevertheless, limited quantities of emeralds are recovered from the region today. No production figures are available, but small amounts of faceted and cabochon material are occasionally available for purchase in the town of Luxor, in the Nile Valley of upper Egypt. Rough and fashioned material from the region is also sometimes sold in Cairo's Khan il Khalili Bazaar.



Figure 1. This Egypto-Roman necklace and Graeco-Roman ring, both containing emeralds believed to be from upper Egypt, help illustrate the historic significance of the gems from this source. The loose stones are typical of the emeralds and green beryls that have been produced from this region over the centuries. The emerald in the ring, which is courtesy of Th. Horovitz © Cie., is 8.88 × 5.90 mm. The necklace and loose stones are courtesy of Derek Content, Inc., Houlton, Maine. Photo © Harold © Erica Van Pelt.

Some of this material is quite attractive, especially when enhanced by fracture filling (figure 2).

Four of the authors (RHJ, RCK, AK, MEB) traveled to the Zabara, Sikheit, Nugrus, and Umm Kabu emerald localities of upper Egypt from November 30 to December 7, 1991. The objectives of this excursion were to: (1) determine the current extent of emerald recovery in this region; (2) update existing locality maps and draft new ones for areas previously not surveyed (such as Umm Kabu); and (3) if possible, obtain material for gemological study.

This article briefly reviews access to, and the geology of, some of the localities where emeralds and green beryls have been mined in upper Egypt, as well as what is known of past and present recovery activities. Revised locality maps of the mining areas that were visited are presented, as is a previously unpublished access map to the mines of the Umm Kabu region, where most of the current recovery activity appears to be focused. The gemological characteristics of fashioned emeralds recently obtained from the region are described.



Figure 2. This 14.56-ct emerald cabochon was obtained recently in Egypt and subsequently fracture filled. Photo © GIA and Tino Hammid.



Figure 3. Dating from the first century A.D., this Roman intaglio (8 × 6.4 × 3.5 mm; impression shown in inset) has been carved from emerald that undoubtedly came from Egyptian mines. From the collection of the J. Paul Getty Museum, Malibu, CA; photos by Ellen Rosenbery.



HISTORICAL BACKGROUND

With the exception of one bead from Nubia dating to predynastic times, the beryls that have survived in Egyptian jewelry date from the Graeco-Roman Period (332 B.C.–395 A.D.; again, see figure 1) and later (Aldred, 1978; Andrews, 1991). In the earliest—Hellenistic—part of this period, one of the important innovations in jewelry was the use of color. Among the stones favored by the Greeks were emeralds (Black, 1981).

Emerald also played a role in the jewelry of imperial Rome, and it is believed that the emeralds discovered in the ruins of Pompeii and Herculaneum, two Italian towns destroyed by the eruption of Mt. Vesuvius in 79 A.D., came from upper Egypt (Rogers and Beard, 1947). Among the treasures found in Pompeii, and now in the National Museum in Naples, is a gold mesh necklace set with mother-of-pearl and emeralds (Gregoriotti, 1969). The emeralds clearly exhibit their natural, hexagonal prismatic form, which is typical of Egyptian emeralds used in ancient jewelry.

By the end of the Roman Empire, there was significant use of gemstones in jewelry, especially emeralds from the Egyptian mines. Among the Roman jewelry in the collections of the British Museum is a necklace from the second century A.D., which consists of gold links with cut-out patterns alternating with prismatic emerald crystals. Such Roman jewelry is also found in the archeological record of Carthage, in what is now Tunisia in North Africa. One example is a third-century A.D. emerald-inlaid hair ornament (Tait, 1987).

Occasionally, emeralds were engraved in Roman times for use as ring stones (Gregoriotti, 1969). A first-century A.D. oval intaglio that is now in the J. Paul Getty Museum shows an unbearded comic mask (Spier, 1992; figure 3). What is described as one of the best examples of a carved emerald (Middleton, 1891) is a cameo of Medusa's head, cut from a large stone around the time of Emperor Hadrian (76–138 A.D.).

Emeralds are also featured in the jewelry history of Roman Britain. Among the items from the Late Roman Thetford Treasure (all dating to the late fourth century A.D.; Caygill, 1985) is a gold ring with a large bezel that is set with an amethyst in the center and surrounded by alternating garnets and emeralds. Still later, Byzantine jewelry from Egypt, which dates to circa 600 A.D., includes a gold necklace and earrings, all set with emerald crystals, sapphires, and pearls (Tait, 1987). It might reasonably be argued that the prismatic emeralds in a talisman that was buried with Emperor Charlemagne in 814 A.D. were also of Egyptian origin (Black, 1981). Emeralds were used

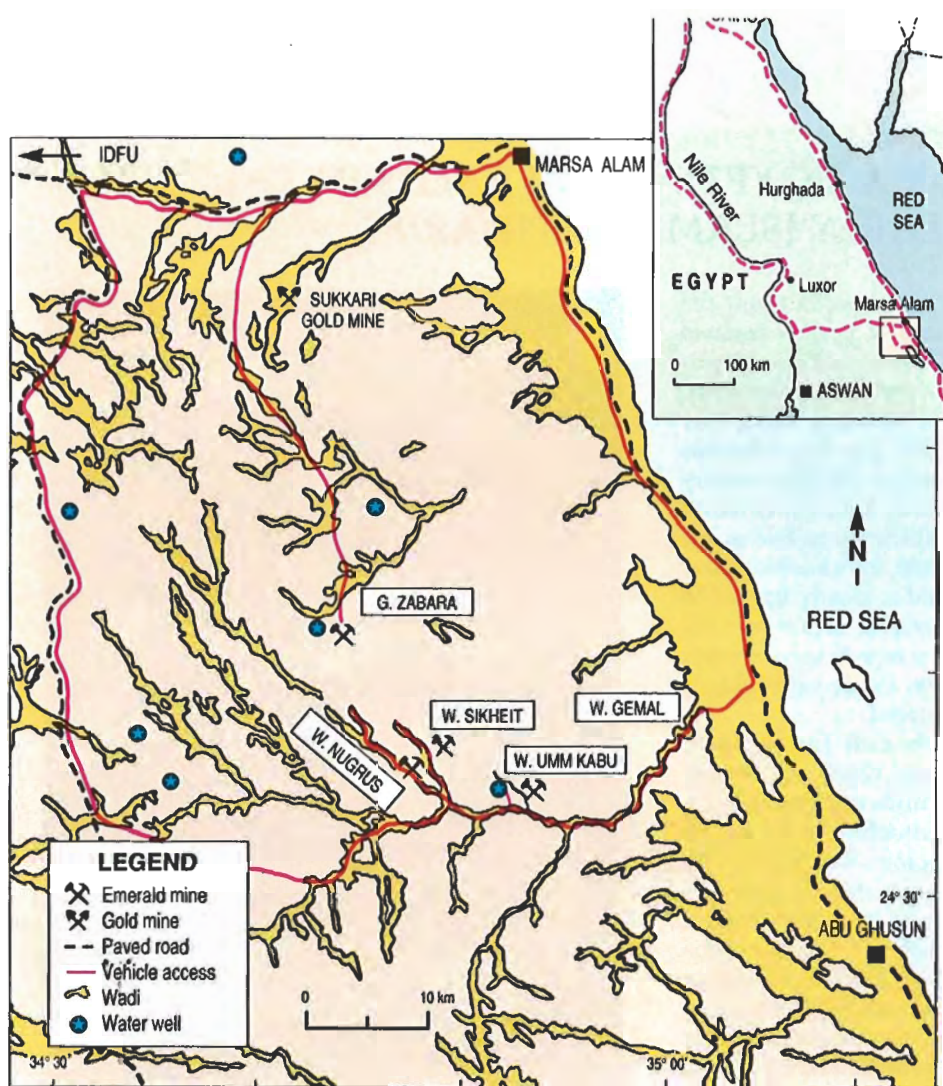


Figure 4. The emerald-bearing province of upper Egypt lies in the hills inland from the coast of the Red Sea. From Cairo, the mines are most easily reached by vehicle via the paved highway that runs along the coast to the small port community of Marsa Alam (see inset). The primary route to the Sikkheit, Nugrus, and Umm Kabu localities is through Wadi Gemal, a narrow, sinuous wadi that cuts through the Red Sea Hills to the coast. The most direct route to Gebel Zabara is via a desert track that heads south from the paved road between Marsa Alam and Idfu, past the ancient Sukkari gold mine. A guide is essential to find any of the workings. Passage south of Marsa Alam requires a military permit.

extensively in the early Islamic cultures as well. In fact, a number of treatises discussing the value of emeralds have been written in Arabic (see box A).

Although many fine accounts of the historic record of emerald mining in Egypt have been published, exactly when these deposits were first exploited remains a mystery. An excellent review is provided by John Sinkankas (1981). According to Sinkankas, there is some evidence suggesting that emeralds were being mined in upper Egypt as early as the 12th Dynasty (2000–1788 B.C.). However, most historians agree only that the emerald deposits were extensively exploited from 330 B.C. (during the Graeco-Roman period) until 1237 A.D. (during the reign of Sultan al-Kamil).

The emerald mines may have been worked sporadically after this date, but we know of no written record of such activities. By approximately 1740, the emerald mines had been abandoned. Their location was virtually unknown until their rediscovery by French explorer Frédéric Cailliaud in 1816 (Sinkankas, 1981).

From 1816 to 1928, various attempts were made to exploit the emerald deposits commercially. An interesting account of one of these—an expedition

mounted to assess the economic feasibility of the deposits for Streeter and Company, London jewelers—was reported by D. A. MacAlister (1900). All of these attempts, however, ultimately were unsuccessful. In fact, there has been no successful commercial mining of the Egyptian deposits in modern times.

Although some general geologic information of value was acquired during this period, more detailed geologic data were obtained later through extensive study and subsequent reporting by Hume (1934), Basta and Zaki (1961), and Hassan and El-Shatoury (1976). An extensive geologic analysis of the Nugrus and Zabara areas was published by Soliman (1986). Most recently, a detailed account of beryllium mineralization in Egypt was published by Hussein (1990). Geologic studies of the area are currently being conducted by the Egyptian Geological Survey and Mining Authority (EGSMA), to assess the gem and mineral resources (Rohr, 1990).

LOCATION AND ACCESS

The mines are best reached from the small port community of Marsa Alam (see figure 4). The distance from Cairo to Marsa Alam is around 700 km (430

BOX A: EGYPTIAN EMERALDS IN EARLY ISLAMIC LAPIDARIES

The main textual sources of information about the ancient and medieval workings of Egypt's emerald mines are the lapidaries—books describing the perceived properties of gemstones and related materials. These range from the earliest surviving treatise by Theophrastos (written ca. 315 B.C.), to Pliny's famous *Natural History* (written in Italy in the first century A.D.), to the medieval English and Continental European treatises, some of which are as late as the 16th century. However, specific information about Egyptian emeralds is sparse and is mostly limited to vague descriptions of the geographic area where the mines were located. For more comprehensive sources we must turn, not surprisingly, to the early Islamic lapidaries, of which there are several.

The value of emeralds in the early Islamic period is discussed by Al-Biruni (d. ca. 1050), in his great work about gemstones and mineralogy *Kitab al-Djamahir fi Ma'rifat al-Djawahir* [*Book of the Manifold Knowledge of Precious Stones*]; by Al-Akfani (d. 1348), in his *Kitab Irshad al-Kasid* [*Treatise on Precious Stones*]; and, to a lesser extent, by several other writers cited by Wiedemann in his *Über den Wert von Edelsteinen bei den Muslimen* [*Concerning the Value of Gemstones by the Muslims*] (Strasburg, 1911). However, most relevant to our subject is the chapter on emeralds attributed to Ahmad Al-Tifashi (d. 1253).

The translation below was made by Nahla Nassar using the Arabic text printed in 1818 in Florence titled *Kitab Azhar al-Afkar fi Jawahir al-Ahjar / Fior di Pensieri sulle Pietre Preciose di Ahmed Teifuscite* [*Flowers of Thoughts on Precious Stones from Ahmad Al-Tifashi*] (edited and translated from Arabic into Italian by Antonio Raineri).

CHAPTER III: EMERALDS

FORMATION: Pliny the Elder mentioned that emeralds are essentially rubies; as they were going through the process of formation, they were red all over. The red color deepened and became more dense, so that it acquired a blackness, and they became azure in color. The intensity and harshness of the dryness forced the blue color to be concentrated in the center; the pure redness rose to the surface and became yellow. Thus

mi.) along the coastal highway, about nine hours.

The mines are located in the Red Sea Hills some 40–60 km southwest of Marsa Alam. Access is by four-wheel-drive vehicle along a complex system of narrow, sandy-bottomed, dry river beds, or washes, called wadis. These wadis often wind around the



Figure A-1. This reassembled strand of emerald crystals with amethyst and colorless quartz beads is typical of early Islamic jewelry. Note that the large emerald at the bottom center is 27.69×12.27 mm. Courtesy of Derek Content, Inc., Houlton, Maine; photo by Shane F. McClure.

the surface became yellow and the center blue. As the heat increased, the two colors were cooked and mixed together, and both the surface and the center became green. . . .

MINES WHERE IT IS FORMED: Emeralds are formed in the bordering regions between Egypt and the Sudan. Behind Aswan is a long mountain where pieces of emeralds are mined. The head miner in Egypt,

mountains in a complex maze and are subject to dangerous flash flooding. The localities where emeralds have been mined are named after prominent gebels (hills) and associated wadis in the area, namely, Gebel Zabara, Gebel Sikheit, Wadi Nugrus, and Wadi Umm Kabu. There are other known occurrences of emerald in

appointed in charge of this mine by the Sultan [probably Ayyubid Sultan Al-Malik al-Kamil, d. 1238], said that the first emerald minerals that appear are known as *talf*; these are black stones that change into golden pyrite when heated. If one mines deeper, one comes across a loose soft red soil in which emeralds are found. Those which are found in the soil are known as *fass* ["a stone for a ring"]; those which are found still attached to a vein are known as *qasab* ["a longer stone for jewels"], in the language of jewelers and mineralogists.

GOOD AND BAD VARIETIES: There are four varieties of emeralds: al-Dhubabi, al-Rihani, al-Silqi and al-Sabouni. The most precious and valuable, and the most superior in all its qualities, is al-Dhubabi. This is a very dark green, untainted by any other color; it is of good pigment and clarity. It was called Dhubabi in relation to the flies [Ar. *dhubab*] that are found on roses in springtime. These flies are of the purest and most intense green hues. Al-Rihani is of a lighter green color, similar to the color of sweet basil [*Ocinum basilicum*, Ar. *rihan*]; the Silqi is the same color as green chard [Ar. *silq*]; the Sabouni, which is beneath it in quality, is the color of soap [Ar. *saboun*]. We have already mentioned that the Dhubabi is the best variety in clarity and brilliancy, and the most beautiful. :

IMPERFECTIONS ASSOCIATED WITH EMERALDS: One of the greatest shortcomings of emeralds is the variation in color between stones mined in different places. This applies to all varieties, including al-Dhubabi. Another is unevenness in shape; this is common in emeralds, rubies, sapphires and all other gemstones. An imperfection inherent in emeralds is cracking: these are concealed cracks that appear in the stones.

CHARACTERISTICS AND BENEFITS: Dhubabi emeralds have a very important characteristic which is particular to this variety, and is used to test real from fake specimens. If a snake looks upon a real Dhubabi emerald, and lays its eyes on it, they will burst on the spot. Ahmad Al-Tifashi said: "I used to come across this characteristic of emeralds in books on gemstones, so I tried it myself. I hired a snake gatherer to hunt a snake. I placed the snake in a basin. I took an arrow and placed a piece of wax on its tip; to that I

this region, such as at Umm Harba and Umm el Dabaa (Sinkankas, 1981), which we did not have time to visit. To reach the emerald localities, a local guide is essential and can be hired (as we did) through the EGSMa office in Marsa Alam. Military permits to travel to the area must be obtained in Cairo.

stuck a piece of pure Dhubabi, and put it near the snake's eyes. At first, the snake persisted in moving towards the emerald with a forceful movement that showed a desire to get out of the basin. When the stone was brought even nearer to its eyes, I heard a gentle crackling, and saw that the eyes of the snake had melted and were clearly protruding. . . ."

Other characteristics are softness, easy decomposition and lightness in weight; it is also smooth and polished. A beneficial characteristic of emeralds is driving weariness of the eye away from anyone who looks intently upon them. The best Dhubabi will also protect anyone who wears it in a necklace or a ring from epilepsy, especially if it is worn before the oncoming of the disease. Another characteristic is that if it is given in drink to someone who has been bitten or poisoned, it will save him from death. It is also beneficial for excessive discharge of blood; or dysentery if worn on a spot above the liver, and stomach aches if worn above the stomach. It will also prevent poisonous animals from coming near anyone who wears it, or a place where it is found. It helps in difficult births. Another of its characteristics is that devils do not come near anyone who carries it, and will flee the place where it is found. A property of emeralds is that their color intensifies if they are mounted onto a backing.

VALUE AND PRICE: It should be noted that all the above mentioned characteristics belong exclusively to al-Dhubabi emeralds, and not to any of the other varieties. It is for this reason that the price for this variety is high. . . . The price increases with the weight of the stone and the presence of the above mentioned descriptions. But the price of a smaller stone does not depreciate as much as small stones of other varieties because of the nobility of this gem and the greatness of its qualities, and the fact that they are more so in a larger stone. Other varieties have no value whatsoever.

[Although, the author adds] . . . Al-Tifashi told that he once bought a Rihani emerald from a merchant; after cutting and polishing, it weighed twelve mithqals. He had paid 1,000 dirhams for the uncut stone. Later he took it to the Sultan al-Malik al-Kamil when he was in Damascus, where it was valued at 30,000 dirhams cash; but it was worth much more.

Derek J. Content
Houlton, Maine

CARTOGRAPHIC PROCESS

To accurately navigate the remote labyrinth of canyon-like wadis and produce reliable maps of the mine locations, we used surface geologic maps and satellite imagery of the region in conjunction with a Global Positioning System (GPS). This pocket-calculator-

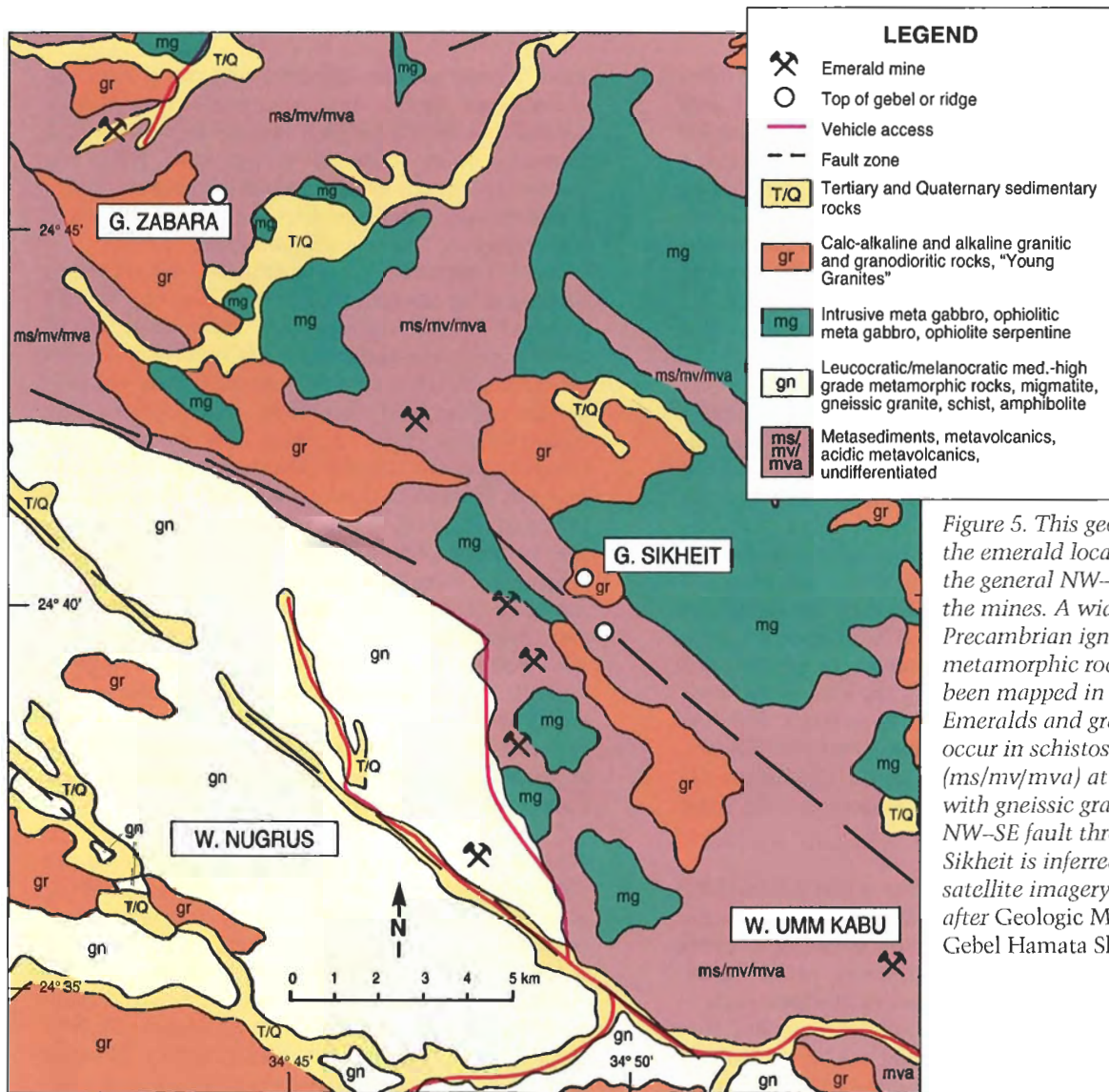


Figure 5. This geologic map of the emerald localities shows the general NW-SE trend of the mines. A wide variety of Precambrian igneous and metamorphic rocks have been mapped in the region. Emeralds and green beryls occur in schistose rocks (ms/mv/mva) at their contact with gneissic granite (gn). A NW-SE fault through Wadi Sikheit is inferred, based on satellite imagery. Modified after Geologic Map of Egypt, Gebel Hamata Sheet (1987).

sized, fully portable, battery-operated electronic device provides access to a radio-navigation system operated by the U.S. Department of Defense. Now available from several manufacturers, the GPS allows a user on the ground to triangulate his/her position anywhere in the world by receiving radio signals from satellites orbiting the Earth.

In the Red Sea Hills environment, the twisting nature and steep walls of the wadis, which often extend hundreds of meters above the canyon floor, make dead-reckoning navigation impossible and measurements with other instruments too slow and impractical. With the GPS device, the coordinates of specific points on the ground were recorded in seconds to within 100 m laterally and were later plotted to reconstruct the maps of the mines shown here. In addition, this invaluable instrument helped the authors

find their way back to base camp at night, when all recognizable markers had disappeared in darkness.

GEOLOGY AND OCCURRENCE OF THE EMERALD DEPOSITS

A comprehensive review of previously published work on the geology of the emerald mines of upper Egypt is beyond the scope of this article, and the reader is referred to the work of Basta and Zaki (1961), Hassan and El-Shatoury (1976), Soliman (1986), and Hussein (1990), for further details. The following overview is a summary of the geologic setting of the emerald deposits at the localities that were visited: Zabara, Sikheit, Nugrus, and Umm Kabu.

A wide variety of igneous and metamorphic rock types have been mapped in the region (figure 5). Basement rocks consist of metasediments and

metavolcanics (designated ms/mv/mva in figure 5) intruded by granites (Hassan and El-Shatoury, 1976). The emerald deposits of upper Egypt occur within a northwest-southeast trending belt of emerald-bearing schistose rocks that extends for some 45 km from Gebel Zabara in the northwest to Wadi Umm Kabu in the southeast.

Beryl mineralization is associated with the intrusive contact between a gneissic biotite granite and overlying mica schists (Soliman, 1986). The emeralds and other beryls occur as crystals in biotite schists, biotite-actinolite schists, and biotite-tourmaline schists along this contact, as well as in the quartz veins and pegmatite dikes that commonly cut the emerald-bearing zones in these mica schists. The ancient emerald mines were located where stream erosion had exposed a concentration of emerald along the contact zone and where emerald fragments were abundant in the alluvial deposits of the resultant wadi. It appears that most such concentrations in the region were found and worked long ago, with little left behind for today's collectors.

The linear distribution of beryl mineralization in the region, as indicated by the NW-SE linear distribution of the emerald mines, is generally attributed to the presence of a NW-SE trending deep-seated tectonic zone of Precambrian age. Soliman (1986) speculated that the beryl mineralization is due to pneumatolytic-hydrothermal processes associated with the episodic emplacement of granites during the Precambrian along this NW-SE trending deep-seated tectonic zone. Further speculations on beryl mineralization are given in Hassan and El-Shatoury (1976) and Hussein (1990).

ZABARA

The Gem-Bearing Deposits. The geology of the beryl occurrences in the Zabara area has been described in detail by Basta and Zaki (1961) and Hassan and El-Shatoury (1976). A locality map of the ancient mined areas that were visited is shown in figure 6. Emerald and green beryl were mined from schistose rocks at their contact with the underlying gneissic granite. The contact is commonly obscured where it has been covered by talus from the steep canyon walls. However, the contact is exposed on both sides of the narrow wadi, and there are numerous shafts along its entire length. The contact plunges below ground level to the northeast, where Wadi Zabara joins a larger, unnamed wadi (figure 7). Numerous quartz veins and fractures cut across the schists and underlying gneissic granites. Mica schists along the contact at some of

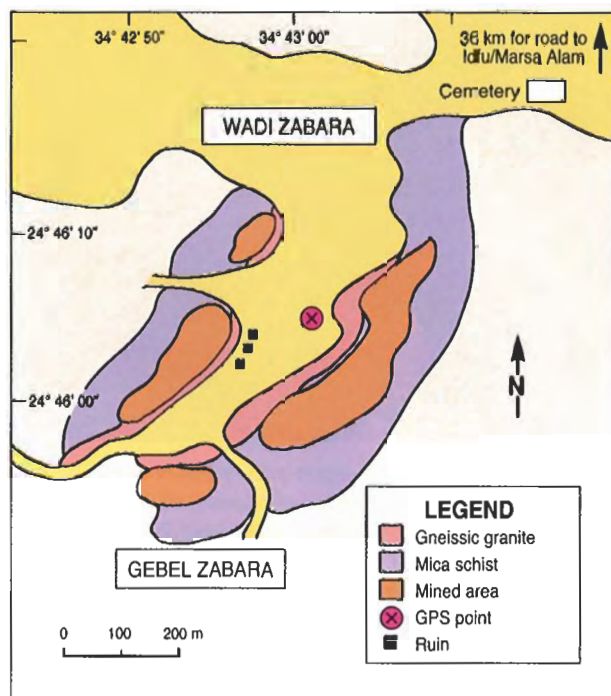


Figure 6. This sketch map of the emerald mines near Gebel Zabara was constructed using GPS navigation. Gneissic granite is exposed near the floor of the wadi. The emeralds occur in overlying mica schists on both walls.

the mines contained some beryl crystals; however, there were no obvious mappable zones of mica schists with abundant beryl mineralization. Rather, it appears that beryl mineralization occurred in limited, discontinuous zones along the contact. Fragments of emerald and green beryl were also recovered from the tailings associated with the mines and from alluvial gravels in the floor of the narrow wadi.

Mine Workings. Simple but extensive mine shafts have been sunk below the workings into the schist-gneissic granite contact on both sides of the wadi; we entered workings on the north side. Several near-vertical shafts (up to 15 m [approximately 50 ft.] deep) sunk along the contact here connected at depth to a large area where rooms with pillars had been created to facilitate removal of the mica schists (figure 8). The miners probably used hand tools to remove the ore, which they then carried to the entrance of the mine, at which point the material was broken and worked for emerald. There was no indication that a mappable emerald-bearing zone or reef had been systematically mined. Nor was there evidence of recent



Figure 7. The intrusive contact and emerald workings can be seen here, looking northeast, in one wall of Wadi Zabara. The true strike and dip of the contact are unknown. The contact plunges to the northeast below ground level at the entrance to the wadi (to the left on the photograph). Emerald workings occur above this contact, with the mine tailings extending from below the workings and down to the wadi floor. Note the cars on the far left for scale. Photo by Robert Jennings.

mining *in situ*, although shallow pits with unweathered dirt in the mine tailings and alluvial gravels of the wadi floor indicate recent activity.

According to Cairo gem dealer Ali Khorassany, the Bedouin of the area work the wadi gravels from November to March, when the region receives most of its scant rainfall. When it rains in the desert, there can be substantial flooding in the wadis. This natural process results in a "float," as the floods wash through the wadis carrying huge volumes of sand and gravel. The floods are usually brief and, soon after they subside, the Bedouin visit the wadis that drain the emerald workings to sort through the surface gravels by hand, looking for the green gems.

SIKHEIT AND NUGRUS

The Gem-Bearing Deposits. The workings along Wadi Sikheit and Wadi Nugrus are near Gebel Sikheit. The geology of the beryl occurrences in the Sikheit/Nugrus localities has been described in detail by MacAlister (1900), Hume (1934), Basta and Zaki (1961), and Hassan and El-Shatoury (1976). MacAlister (1900) sketched one of the more accurate maps ever produced of this locality (shown in figure 9, modified using GPS navigation). Our GPS recording changed the mapped orientation of some wadis and indicated that there is no vehicular connection between Wadi Abu Rushaid and Wadi Sikheit. A geologic map of this locality was pub-



Figure 8. This view is inside one of the mines on the north wall of Wadi Zabara, entered through a near-vertical shaft excavated along the schist-gneissic granite contact. Note the chisel marks and the pillar, approximately 1 m in diameter, left as support. Photo by Robert C. Kammerling.

lished by Hassan and El-Shatoury (1976). Grubessi et al. (1990) published one of the more recent accounts of an excursion to this locality, commenting on the many fine ancient ruins (dwellings and temple) to be seen. The main temple at Wadi Sikheit, carved into the canyon walls, has served as a landmark for many travelers (figure 10). Unfortunately, graffiti has tarnished some of its aesthetic beauty.

The most extensive emerald workings at this locality can be found (1) on the southwest slopes of Gebel Sikheit, along the upper reaches of Wadi Sikheit; (2) midway along Wadi Sikheit, near the temple and associated ruins (both sides of the wadi); and (3) on the northeast side of Wadi Nugrus, near the ruined dwellings. The occurrence of beryl in these two wadis is restricted to the mica schist-gneissic granite contact zone (Hassan and El-Shatoury, 1976). Beryl is concentrated in discontinuous zones in schistose rocks along this contact, and in quartz veins cutting the schists and underlying gneissic granites. As at Zabara, this contact is often obscured by alluvium or by tailings from the numerous mines. In most places, the contact between the beryl-bearing schistose rocks and the underlying gneissic granite is inferred. The beryl-bearing schists are exposed on the slopes of Gebel Sikheit, and to the southeast along Wadi Sikheit, toward the ruins. According to MacAlister (1900) and Hume (1934), the deposits on the slopes of Gebel Sikheit occur in four bands of mica schist and talc schist. These schists are mapped in fault contact with the gneissic granite in Hume (1934). No new geologic mapping was conducted in this area other than to confirm the rock types and mineral associations that had previously been described.

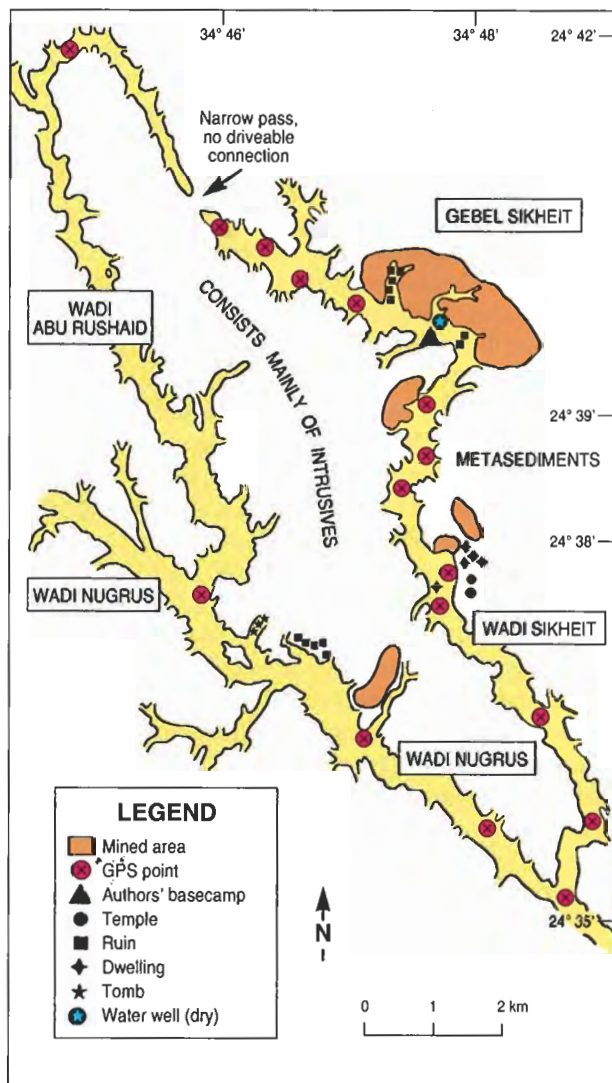


Figure 9. This map of the emerald mines of Wadi Sikheit and Wadi Nugrus is modified from GPS navigation after a sketch map of D. MacAlister (1900). The authors' global positioning survey changed the mapped orientation of some of the wadis and indicated there was no vehicular connection between Wadi Abu Rushaid and Wadi Sikheit.

Mine Workings. The abundance of ancient shafts, adits, and associated mine tailings in the Sikheit/Nugrus localities suggests that this area was extensively worked in the past. Mine shafts and adits occur in groups, probably where stream erosion along the wadis exposed the emerald-bearing rocks. Some groups of mines were worked more than others, as evidenced by their large chambers and interconnected tunnels. The extensive ruins in Wadi Sikheit and Wadi Nugrus also indicate that there was a high level of emerald-mining activity in the past, considerably more than at Zabara.

There is evidence that some of the mines at this



Figure 10. This temple, carved into the canyon wall and dating to Ptolemaic times (circa 300 B.C.), is at the entrance to Wadi Sikheit. It has long served as a landmark for travelers in the region. Photo by Robert C. Kammerling.

locality have been worked in more recent times. Some of the mine shafts and adits at Sikheit are marked with wooden survey stakes, and the entrances to a few of the larger mines are numbered with paint (figure 11). In addition, unweathered tailings piles of limited extent were seen at the entrances to some of the workings along the lower part of Wadi Sikheit. Goat and camel droppings and fire pits indicated that Bedouin camps had been set up relatively recently. However, the small size of the unweathered tailings suggests that recovery has not been systematic. No mines in the area we visited could be considered active.

There is also considerable evidence, in the form

Figure 11. The authors came across some evidence that mines on the slopes of Gebel Sikheit had been worked in more recent times. Note the number painted here at a mine entrance on the southwest slope of Gebel Sikheit. Photo by Robert Jennings.



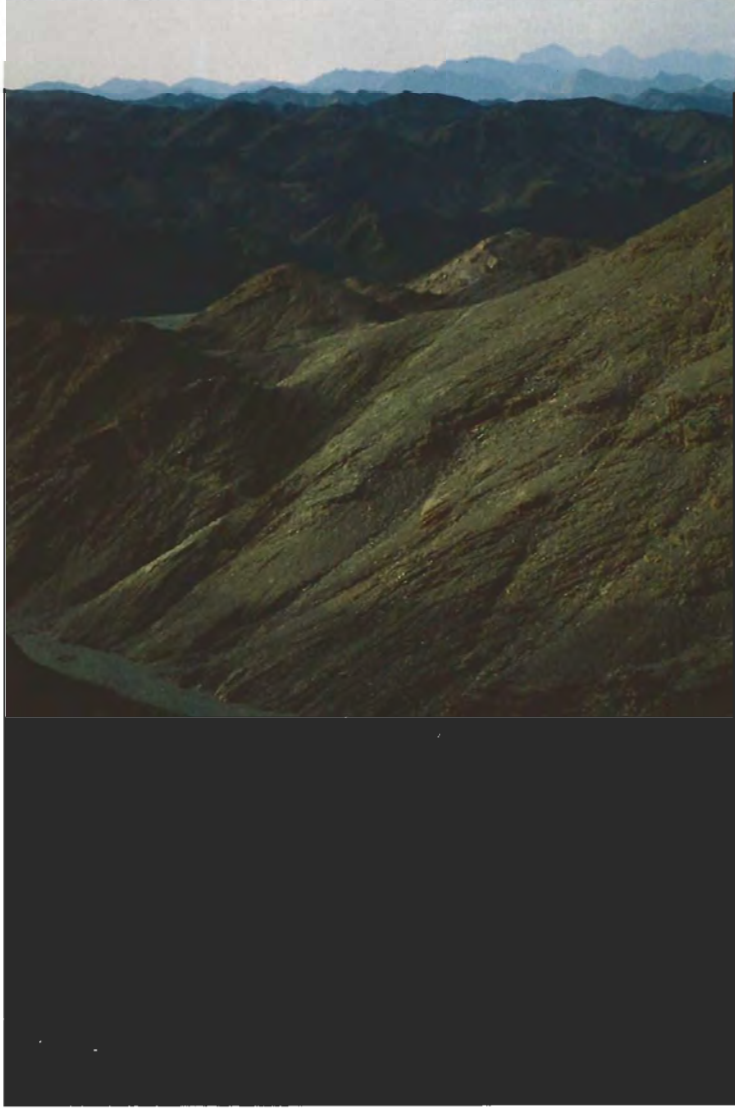


Figure 12. This narrow wadi, just north of Wadi Nugrus and below extensive mine workings on the ridge, provides key drainage for the extensive emerald workings. Such wadis often form narrow, sinuous canyons as they cross the Red Sea Hills. Photo by Robert Jennings.

of abandoned camps and shallow, unweathered diggings, that the gravels that drain the mine tailings are still worked periodically (figure 12).

It is interesting to note that many of the ruins of dwellings at Wadi Sikheit and Wadi Nugrus appear to be situated adjacent to or on mine tailings and caved-in adits. It is possible that the early miners constructed habitats in such proximity to the workings to maintain security.

UMM KABU

Description of the Gem-Bearing Deposits. The location of the Umm Kabu workings is shown in figure 13. The emerald mines are accessed from two wadis that branch north-northeast from Wadi Gemal. Both of these wadis are extremely narrow (5-30 m) and sinu-

ous, and both contain additional stone ruins near the workings. We noted very recent vehicle tracks on the northern side of the workings, which suggests that vehicular access is possible via another wadi on the north or northeast flank of the mined area.

Very little information has been published on Umm Kabu, although the geology was briefly described by Hume (1934) and by Hassan and El-Shatoury (1976), the latter including a geologic sketch map of part of the area. Even so, the workings here are as extensive as those at Sikheit/Nugrus, which suggests that they were once a major source of emerald. The occurrence of beryl at Umm Kabu, as at the other localities, is believed to be due to the emplacement of granites into mica schists (Hassan and El-Shatoury, 1976; Soliman, 1986). There is very little evidence here, however, of this intrusive contact. Cobbles of gneissic granite, white granite, hornblende gneiss, and serpentinite were observed in the alluvial fill of the wadis leading to the emerald workings, as were numerous types of mica schists and beryl. A few small exposures of gneissic granite and white granite were found in the lower reaches of Wadi Umm Kabu. It is assumed that the occurrences of beryl here are indicative of the occurrence of intrusives very close to the surface at this locality.

Abundant fragments of green beryl and emerald were found along both of the narrow wadis that lead to the emerald workings of Umm Kabu. Emerald was found as small (a few millimeters in diameter), loose, hexagonal prisms, as well as single crystals and occasional clusters embedded in quartz and biotite schist. The emeralds embedded in biotite schist seemed to have the best color. Fragments of green beryl and emerald were also found in the tailings piles.

Mine Workings. The ancient mine workings at this locality are considerable, as can be seen by the extensive tailings (figure 14). Most of the shafts are now caved in, but those that are partially open indicate that they were nearly vertical. As at Sikheit and Nugrus, the mine shafts were located to excavate obvious zones of emerald-bearing mica schist.

Piles of cobbled material—emerald and green beryl in quartz and in biotite schist—were seen around the ruins at the entrance to Umm Kabu. The cobbling appeared to be fresh, with no evidence of weathering, which suggests that the material had been transported down the wadis from an active working relatively recently. However, we could not determine the source of the emeralds. It is possible that cobbling was done on old material.

The footpaths along both of the wadis that lead to

and across the ancient workings at Umm Kabu are well worn, and there is considerable evidence that Bedouin visit the area frequently with their camels and goats. Several campsites were evident along both wadis and at the ancient mines.

In the few days we walked between the entrances of these two wadis and the ancient emerald workings, we found a few dozen small crystals and crystal fragments of emerald and green beryl. It is possible that these gravels could yield considerable amounts of similar material if they were systematically worked.

Figure 13. The emerald mines of Umm Kabu are accessible only by foot from Wadi Gemal. The two main wadis shown drain the mined area. Abundant emerald fragments were recovered by the authors from alluvial gravels along the entire length of the narrow wadis. This original sketch map was constructed from GPS points recorded in the field at locations shown.

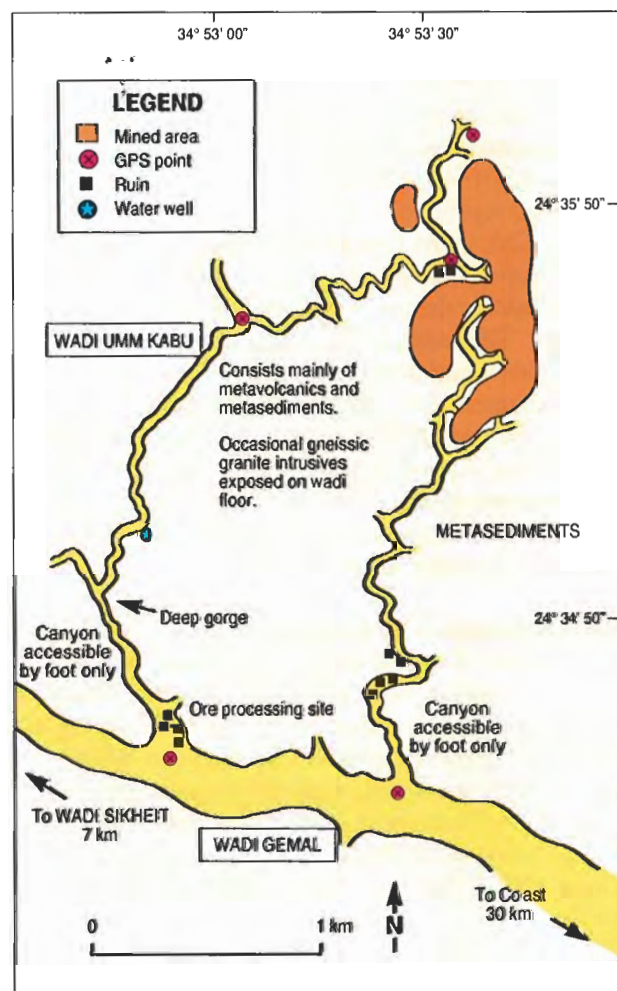


Figure 14. The ancient mine workings at Umm Kabu are considerable, as can be seen from the extensive tailings. Photo by Robert Jennings.

THE CURRENT STATUS OF PRODUCTION

At the time of the authors' visit, no commercial mining was being carried out on a mining exploitation license issued by the Egyptian Geologic Survey and Mining Authority at any of the localities visited. Recent discussions with merchants in Cairo indicate that EGSMa has awarded an Egyptian firm a two-year exploration license for the Sikheit region. However, we were unable to obtain official confirmation of this.

It is interesting to note that several exploitation licenses have reportedly been awarded by the Egyptian government in the last 10–15 years to mine mica in the Zabara region (A. Khorassany, pers. comm., 1991). EGSMa is currently encouraging individuals to invest in gem mining in the emerald-bearing region, but taxes, interference by local authorities, and, no doubt, the generally low quality of the material have so far discouraged activity. Interest by local investors is also affected by the fact that most Egyptians prefer gold and diamonds for jewelry. To attract foreign investment, EGSMa is currently conducting new studies in this region to evaluate the potential of the gem deposits.

Most gem materials recovered today are by Bedouin who pick through the ancient tailings and material weathered from the host rock and deposited in the wadis. Many are employed by the geologic survey and thus have acquired considerable knowledge of the location of many gems and minerals. Production

figures are unknown, as none of the emerald-bearing deposits is mined officially.

According to Ahmed Hussein Moustafa of the Zagloul Bazaar in Luxor (pers. comm., 1991), emerald crystals are hand carried to the towns of Idfu and Luxor, where they are sold to merchants for fashioning. Most of the material is not gem quality and, at present, there does not appear to be enough gem-quality emerald to justify much more activity. However, Mr. Moustafa has made a few trips to Idar-Oberstein in Germany to have some of the better-quality material fashioned. Most of the fashioned material has been cut *en cabochon* and is sold to tourists in Luxor. The Bedouin also bring other gem materials to Idfu and Luxor—such as amazonite, amethyst, chrysoprase, fluorite, and peridot—from the Red Sea Hills surrounding Wadi Gemal.

GEMOLOGICAL AND SPECTROSCOPIC CHARACTERISTICS

Materials and Methods. Fourteen specimens of emerald and green beryl from Upper Egypt were acquired for the gemological study performed at the GIA Gem Trade Laboratory in Santa Monica, California. These specimens (see, e.g., figure 15), which are from unspecified mining localities in upper Egypt, were obtained from two sources: (1) Ali Khorassany, who both personally collected rough from the mining areas and acquired specimens from local Bedouin; and (2) Ahmed Hussein Moustafa, who purchased specimens from Bedouin who also reportedly collected them in the mining areas. Thirteen of the specimens are cabochons and range from 0.38 to 17.50 ct; the 14th specimen is a 2.28-ct emerald cut. None of the crystal fragments found by the authors on site was large enough or of high enough quality for gemological testing.

The specimens ranged in diaphaneity from translucent to semitransparent, as a result of being moderately to heavily included, and in color from medium-light to dark green. With regard to the latter, it should be noted that Egyptian emeralds are variously described in the literature as ranging from "very pale bluish green or yellowish green to the intense green hue" (Sinkankas, 1981) and as "light-coloured" (Webster, 1983), although darker material has also been reported (again, see box A). Because Egyptian stones are described as often being light toned, the question has arisen as to whether they are properly classified as emeralds rather than green beryls. The staff of the GIA Gem Trade Laboratory determined that, on the basis of color, 12 of the 14 specimens used in the

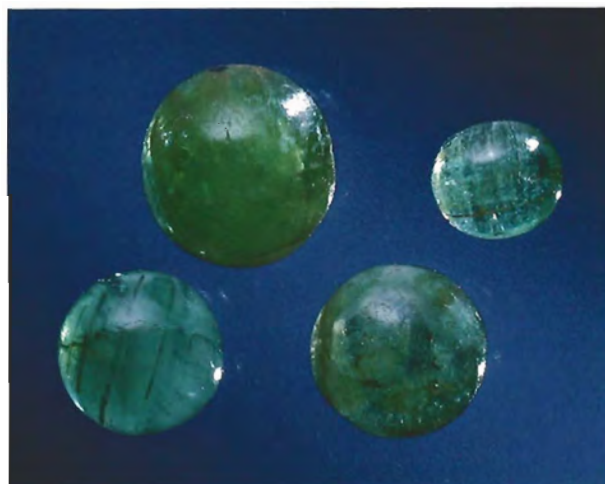


Figure 15. These emerald cabochons (0.46–1.72 ct), used in the gemological investigation, are typical of the Egyptian emeralds/green beryls currently available in limited quantities. Photo © Tino Hammid and GIA.

gemological study were appropriately called emerald, while the other two qualified as green beryl.

Refractive indices were taken with a Duplex II refractometer; pleochroism was determined with a Polaroid-filter-type dichroscope; specific gravity was measured hydrostatically; microscopic examination used a GIA GEM Instruments Mark VII GemoLite microscope; and spectra were observed with a GIA GEM desk-model unit fitted with a Beck prism spectroscope. The results of gemological testing are reported in table 1 and discussed below.

The chemical composition of five of the samples was determined qualitatively using a Tracor Spectrace 5000 X-ray fluorescence (EDXRF) analysis system. Mid-infrared spectra (400–4000 cm^{-1}) of two of the samples were recorded using a Nicolet 60SX Fourier-transform infrared spectrometer.

Refractive Index. Spot readings on the cabochons were 1.57 to 1.58. The one faceted specimen, on which a flat-facet reading could be obtained, yielded refractive indices of $e = 1.581$ and $o = 1.588$, with a birefringence of 0.007. These latter values lie between the 1.573–1.580 values previously reported for emeralds mined along the eastern side of Wadi Sikheit, the 1.577–1.585 values reported for stones recovered from the base of Gebel Sikheit (Basta and Zaki, 1961; Sinkankas, 1981), and the 1.590–1.596 reported for stones from Gebel Zabara by Grubessi et al. (1990). These values are also

within the documented range for emeralds from numerous other localities (Sinkankas, 1981).

Pleochroism. Although all of the specimens were moderately to highly included, it was possible to resolve their pleochroic colors. The weak to moderate dichroism of yellowish green and bluish green observed in all the stones is consistent with that observed in emeralds from other localities (Sinkankas, 1981).

Ultraviolet Fluorescence. All 14 specimens were inert to short-wave ultraviolet radiation, but the 13 cabochons displayed faint to weak yellowish green luminescence to long-wave U.V. The long-wave reaction may be the result of residual substances (oils?) used to fill surface-reaching fractures (see below). The fluorescence of green beryls and emeralds is known to be variable and, in general, weak (Sinkankas, 1981).

TABLE 1. Gemological characteristics of emeralds and green beryls from upper Egypt.^a

| Property | Observations |
|----------------------------------|--|
| Color | Medium-light to dark green |
| Clarity | Translucent to semitransparent |
| Refractive indices | 1.57 to 1.58 (spot) ^b e = 1.581, o = 1.588 ^c |
| Birefringence | 0.007 ^c |
| Pleochroism | Weak to moderate dichroism; yellowish green (ordinary ray) and bluish green (extraordinary ray) |
| U.V. fluorescence | |
| Long-wave | Inert or faint to weak yellowish green ^d |
| Short-wave | Inert |
| Chelsea filter reaction | Negative (i.e., yellowish green) to weak to moderate pink |
| Specific gravity | 2.62–2.73 |
| Optical absorption spectrum (nm) | Typical "emerald" absorption spectrum (Liddicoat, 1989). Key features: 683.5 and 680.5 doublet and lines at 662 and 646 ^c |
| Internal features | Numerous partially healed fractures composed of two-phase (liquid and gas) inclusions, unhealed fractures stained with a yellowish brown substance (limonite?), growth tubes running parallel to the optic axis (some with yellowish brown staining), translucent brown tabular inclusions (biotite?), oxidized amphibole "stalks," and possibly decomposed filling material in surface-reaching fractures |

^a Study sample includes 13 cabochons and one faceted stone.

^b Spot readings determined on 13 cabochons.

^c Flat facet reading determined on one faceted stone.

^d Fluorescent reactions possibly due to fracture-filling residues.

^e The three lightest-colored stones exhibited only two weak absorption lines, at 683.5 and 680.5 nm.

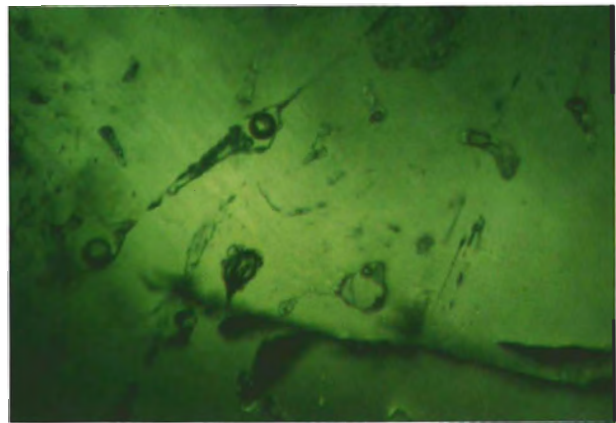


Figure 16. Two-phase fluid inclusions such as these were noted in most of the emeralds and green beryls examined by the authors. Photomicrograph by John I. Koivula; magnified 50 \times .

Chelsea Filter Reaction. When viewed through the Chelsea color filter, 11 of the specimens gave a "positive" reaction, ranging from weak to moderate pink. The remaining three stones—the three lightest-color specimens—gave a negative (yellowish green) reaction. While emeralds from many localities give a positive (red) reaction to the Chelsea filter, emeralds from India and some African localities also have a negative reaction (Webster, 1983).

Specific Gravity. The range of S.G. values is consistent with those for emeralds from many localities (Sinkankas, 1981). The variation in S.G. values may be at least partly explained by the differing degree to which individual stones are fractured and/or contain fluid and mineral inclusions. Previous documentations of Egyptian emeralds report a specific gravity of 2.75 (Basta and Zaki, 1961; Sinkankas, 1981; Grubessi et al., 1990).

Magnification. All of the stones contained numerous partially healed fractures, which were composed of two-phase, liquid and gas, inclusions (figure 16). Several of the stones also had unhealed fractures stained by a yellowish brown substance, possibly limonite. Another distinctive feature common to most of these specimens was the presence of growth tubes running parallel to the c-axis, some of which also exhibited yellowish brown staining (figure 17). Parallel growth tubes in emerald have been reported from several localities, including Brazil (Gübelin and Koivula, 1986) and Pakistan (Gübelin, 1982).



Figure 17. Growth tubes running parallel to the *c*-axis were also noted in some of the specimens used in this study. Some, like those shown here, contained what appears to be epigenetic limonite staining. Photomicrograph by John I. Koivula; magnified 15 \times .

Six of the specimens contained translucent brown tabular inclusions that resemble biotite (figure 18). Biotite in emerald is associated with metamorphic deposits such as those in the Ural Mountains of Russia (Schmetzer et al., 1991), Austria, India, Mozambique, Norway, Zimbabwe, and Brazil (Gübelin and Koivula, 1986). In addition, one of the specimens had a cluster of oxidized amphibole "stalks" (figure 19), an internal feature that has also been observed in emeralds from the Habach Valley, Austria, and from Sverdlovsk in the Ural Mountains (Gübelin and Koivula, 1986). Given that the inclusions observed in these specimens also occur in emeralds from numerous other localities, we believe that Egyptian emeralds and green beryls cannot be conclusively identified as to their locality on the basis of these characteristics.

It was interesting to note that some of the stones contained what appears to be decomposed filling material in their surface-reaching fractures. It is possible that the fractures were treated with oil to enhance the apparent clarity. With time, the oil could decompose, leaving behind a dry residue. As suggested above, this could explain the yellowish green long-wave U.V. fluorescence noted in some of the stones. The historic use of oil to treat emeralds in Egypt has been documented. Schneider (1892) quotes Schehab ed-din Abul Abbas Achmed from his work *Mesa-Lek Al-Absar*, written in the Middle Ages: "When an emerald is found it is thrown into hot oil, then in wood shavings and wrapped in linen or some other material." One of the cabochons had a green filling material in surface-reaching fractures.

Absorption Spectra. Eleven of the specimens exhibited a typical "emerald" absorption spectrum (Liddicoat,

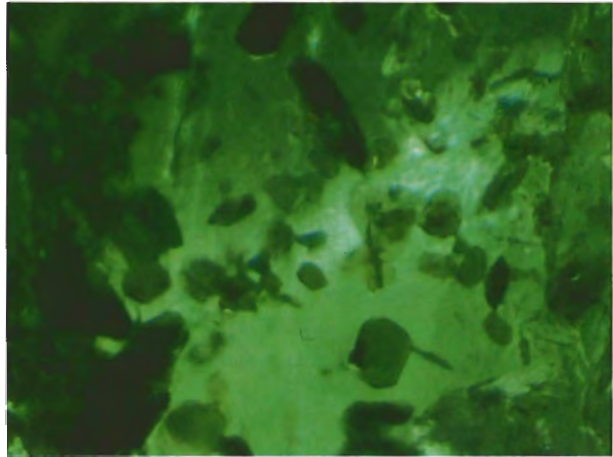
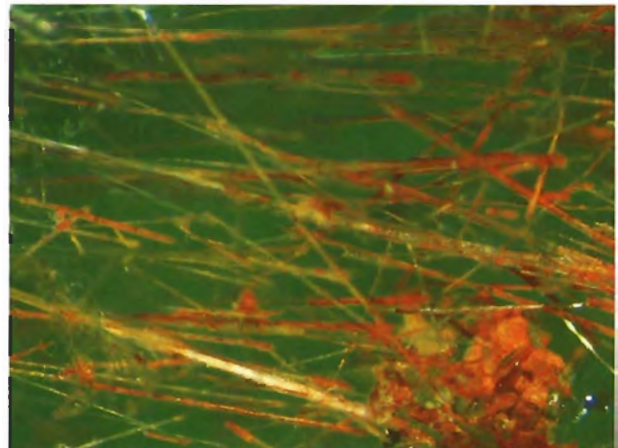


Figure 18. Translucent, brown, tabular inclusions were another internal feature noted in the Egyptian emeralds/green beryls. Photomicrograph by John I. Koivula; magnified 30 \times .

1989), key features of which are a doublet at 683.5 and 680.5 nm, as well as absorption lines at 662 and 646 nm. The three lightest-color specimens, however, had only two weak absorption lines at 683.5 nm and 680.5 nm. This type of spectrum is typical of lighter green beryls such as Brazilian stones of pegmatitic origin (Liddicoat, 1989).

EDXRF and U.V.-Visible Analyses. Besides the expected aluminum and silicon, EDXRF analysis revealed the presence of chromium, vanadium, and iron in varying amounts, with the XRF peak for iron being greater or equal in height to the XRF peak for chromium, and

Figure 19. Oxidized amphibole "stalks," typical of emeralds from such localities as the Ural Mountains of Russia and the Habachtal Valley, Austria, were seen in one of the Egyptian specimens studied. Photomicrograph by John I. Koivula; magnified 25 \times .



both being higher than the vanadium XRF peak. Smaller XRF peaks for potassium, calcium, cesium, and titanium were also detected in one or more samples. A quantitative chemical analysis (by electron microprobe) of an Egyptian emerald from Gebel Zabara (Grubessi et al., 1990) lists each of these elements except vanadium and cesium. All of the elements we detected in these samples are common in emeralds from many localities that we and others have analyzed.

The infrared spectra of these Egyptian emeralds appear to be similar to those of other natural emeralds and, not surprisingly, different from the spectra of flux- and hydrothermally grown synthetic emeralds (see Stockton, 1987). The spectra of one of the emeralds displayed features similar to those seen in emeralds that have been fracture filled. This supports the observations made regarding long-wave U.V. radiation and magnification.

CONCLUSION

The emerald and green beryl localities of upper Egypt have been mined, formally and informally, for more than 2,000 years. They are undoubtedly the earliest source of emeralds on record in the Western world.

Although there is no systematic mining at the present time, nomadic Bedouin pick through rain-washed gravels and ancient tailings to retrieve the small quantities of emeralds seen in local markets.

Gemological investigation of fashioned specimens obtained in Egypt revealed properties consistent with those reported in the literature for emeralds and green beryls from several other localities. Inclusions noted are typical of emeralds from other metamorphic environments and therefore cannot be used to characterize the locality.

Although many of the fragments seen in the ancient mine tailings and *in situ* at Gebel Zabara were light in tone and therefore more appropriately called green beryl, others were of sufficient depth of color to be called emerald. At present, however, because of the generally poor quality of this emerald as compared to that of emeralds from localities such as Colombia, Brazil, and Zambia, the prospects for increasing the supply of gem-quality emerald would appear to be too low to justify formal mining activity. Their greatest value lies in their role in the history of gemology and in the adornment of some of our early cultures.

REFERENCES

- Aldred C. (1978) *Jewels of the Pharaohs*. Ballantine Books, New York.
- Andrews C. (1991) *Ancient Egyptian Jewelry*. Harry N. Abrams, New York.
- Basta E.Z., Zaki M. (1961) Geology and mineralization of Wadi Sikheit area, South-Eastern Desert. *Journal of Geology, U.A.R.*, Vol. 5, No. 1, pp. 1-38.
- Black J.A. (1981) *A History of Jewelry*. Park Lane, New York, N.Y.
- Caygill M. (1985) *Treasures of the British Museum*. Harry N. Abrams, New York.
- Geologic Map of Egypt, Gebel Hamata Sheet (1987)*. CONOCO/EGPC/TU Berlin Mapping Project, Institut für Angewandte Geodassie, Berlin.
- Gregoriotti G. (1969) *Jewelry Through the Ages*. American Heritage, New York.
- Grubessi O., Aurisicchio C., Castiglioni A. (1990) The Pharaohs' forgotten emerald mines. *Journal of Gemmology*, Vol. 22, No. 3, pp. 164-177.
- Gübelin E.J. (1982) Gemstones of Pakistan: Emerald, ruby, and spinel. *Gems & Gemology*, Vol. 18, No. 3, pp. 123-139.
- Gübelin E.J., Koivula J.I. (1986) *Photoatlas of Inclusions in Gemstones*. ABC Edition, Zurich.
- Hassan M.A., El-Shatoury H.M. (1976) Beryl occurrences in Egypt. *Mining Geology*, Vol. 26, pp. 253-262.
- Hume W.F. (1934) *Geology of Egypt*, Vol. 2, Part 1: The metamorphic rocks. Government Press, Cairo, pp. 105-125.
- Hussein A.A. (1990) Mineral deposits. In Rushdi Said, Ed., *The Geology of Egypt*, A.A. Balkema, Rotterdam, Netherlands, pp. 537-539.
- Liddicoat R.T. (1989) *Handbook of Gem Identification*, 12th ed. rev. Gemological Institute of America, Santa Monica, CA.
- MacAlister D.A. (1900) The emerald mines of Northern Etbai. *Geographical Journal*, Vol. 16, pp. 537-549.
- Middleton J.H. (1891) *The Engraved Gems of Classical Times, with a Catalogue of the Gems in the Fitzwilliam Museum*. Cambridge University Press, London, England.
- Rogers F., Beard A. (1947) *5000 Years of Gems and Jewelry*. J.P. Lippincott Co., Philadelphia and New York.
- Rohr M.K. (1990) Gems—The forgotten industry. *Business Monthly*, Journal of the American Chamber of Commerce in Egypt, Vol. 6, No. 11, pp. 28-29.
- Schmetzer K., Bernhardt H.-J., Biehler R. (1991) Emeralds from the Ural Mountains. *Gems & Gemology*, Vol. 27, No. 2, pp. 86-99.
- Schneider O. (1892) Der Aegyptische Smaragd. *Zeitschrift für Ethnologie*, Vol. 24, pp. 41-100.
- Sinkankas J. (1981) *Emerald and Other Beryls*. Chilton Book Co., Radnor, PA, pp. 542-548.
- Soliman M.M. (1986) Ancient emerald mines and beryllium mineralization associated with Precambrian stanniferous granites in the Nugrus-Zabara Area, Southeastern Desert, Egypt. *Arab Gulf Journal of Scientific Research*, Vol. 4, No. 2, pp. 529-548.
- Spier J. (1992) *Ancient Gems and Finger Rings*. Catalogue of the Collections, J. Paul Getty Museum, Malibu, CA.
- Stockton C.M. (1987) The separation of natural from synthetic emeralds by infrared spectroscopy. *Gems & Gemology*, Vol. 23, No. 2, pp. 96-99.
- Tait H., Ed. (1987) *Jewelry: 7000 Years*. Harry N. Abrams, New York.
- Webster R. (1983) *Gems, Their Sources, Descriptions and Identification*, 4th ed. Revised by B.W. Anderson, Butterworths, London.

REACTOR-IRRADIATED GREEN TOPAZ

By Charles E. Ashbaugh III and James E. Shigley

Examination of samples of faceted "Ocean green" topaz reveals that this material has been irradiated in a nuclear reactor. An earlier reactor-irradiation experiment suggests that temperature conditions during the irradiation of this material may be higher than those used to produce typical "London-blue" topaz. Like such reactor-irradiated blue topaz, this material may be radioactive. In addition, the green color is not stable to direct sunlight.

A relatively new color variety of topaz is being sold under the trade name "Ocean green" topaz (figure 1), with several thousand carats of this material now in the marketplace. Inquiries to dealers revealed that most of the original, untreated topaz comes from Sri Lanka, is currently being irradiated at the research reactor at Texas A&M University, and is being released under their license from the U.S. Nuclear Regulatory Commission (NRC). Material of this same color may also originate from, and be irradiated in, other countries.

GIA's current interest in testing reactor-irradiated blue topaz for radioactivity, and in determining whether it can be released to consumers in compliance with U.S. regulations regarding reactor-irradiated gem materials, now extends to reactor-irradiated green topaz as well. Telephone inquiries to the reactor facility at Texas A&M were unsuccessful in obtaining any information related to the treatment process for

this kind of topaz. Therefore, this article reports the results of our gemological examination, chemical analysis, and radioactivity and color-stability testing of several specimens of this material.

MATERIALS AND METHODS

For this study, we selected five faceted samples of irradiated green topaz to examine in detail (table 1). For color-origin and stability testing, we also examined a variety of additional green and other types of topaz (see table 1 and figure 2). Samples 1-4, 9, and 12-13 represent the Ocean-green topaz being sold commercially at this time. Sample 5 was irradiated by one of us (CEA) in a nuclear reactor in 1986. This treatment was performed in a cadmium-shielded "dry rabbit" type of canister without water cooling (and, therefore, at an elevated temperature) for seven hours. Under these conditions, a bluish green color resulted from a colorless starting material. Green topaz has been reported to occur in nature, but it seems to be rare (Webster, 1983; Deer et al., 1982; Hoover, 1992), and we were unable to obtain natural specimens for examination.

We used standard gemological tests and equipment to characterize green samples 1-5. We then recorded absorption spectra for samples 1-8 over the range of 250-2500 nm using a Hitachi U-4001 spectrophotometer. These spectra were recorded with unpolarized light, with each topaz oriented such that the light beam traveled through the polished girdle. Because it is usually impractical to orient faceted stones optically, we did not attempt to do so; this should be kept in mind when comparing the visible absorption spectra. In addition, we determined the

ABOUT THE AUTHORS

Mr. Ashbaugh is a nuclear engineer and former manager of radiation testing at the GIA Gem Trade Laboratory, Santa Monica, California. Dr. Shigley is director of research at the Gemological Institute of America in Santa Monica.

Acknowledgments: Study samples were kindly provided by: Helmut Zimmermann, Zimmermann BCS Stones, Harxheim, Germany; G. B. Sharma, Gem Center of California, Los Angeles; Virginia Busby, Service Merchandise, New York; and the GIA reference collection. Caesar Habib, of Kaiser Gems in Los Angeles, performed the heat-treatment experiments. In GIA Research, Yan Liu helped interpret the color-stability data, Emmanuel Fritsch helped interpret the visible absorption spectra, and Sam Muhlmeister performed the EDXRF analyses.

Gems & Gemology, Vol. 29, No. 2, pp. 116-121
© 1993 Gemological Institute of America

chemical composition of three samples (nos. 1, 5, and 6) from their polished table facets using a Tracor Spectrace 5000 X-ray fluorescence (EDXRF) analysis system.

We also tested irradiated green topaz samples 1–5, 9, 12, and 13 for radioactivity using GIA's gamma-ray spectroscopy system (Ashbaugh, 1992). Each sample was placed with its table facet positioned above the high-purity germanium (HpGe) detector, and then "counted" for a one-hour period.

TABLE 1. Topaz samples examined.

| Sample no. | Color | Weight (ct) | Comments ^b |
|-----------------|-----------------|-------------|--|
| 1 ^a | Green | 3.85 | Emerald cut, irradiated, (R1154) |
| 2 ^a | Bluish green | 4.34 | Emerald cut, irradiated, (R1155) |
| 3 ^a | Bluish green | 4.71 | Emerald cut, irradiated, (R1614) |
| 4 ^a | Bluish green | 8.70 | Emerald cut, irradiated, (R1613) |
| 5 | Bluish green | 4.10 | Emerald cut, reactor irradiated at elevated temperatures (no cooling), (R1156) |
| 6 | Blue | 3.38 | Emerald cut, irradiated and heat treated, from Sri Lanka, (R1160) |
| 7 | Brownish yellow | 11.26 | Emerald cut, from Brazil, (R1161) |
| 8 | Brown | 14.51 | Oval cut, irradiated, (R1186) |
| 9 ^a | Green | 9.20 | Emerald cut, irradiated, cut in half for control (A) and test (B) samples; one piece (B) heat treated (now blue); half of A subsequently exposed to direct sunlight (now blue) |
| 10 | Brown | 1.84 | Modified triangle cut, linac-irradiated; exposed to direct sunlight (now blue) |
| 11 | Brown | 2.00 | Modified triangle cut, linac-irradiated; heat treated (now blue) |
| 12 ^a | Green | 4.50 | Modified pear shape, irradiated; tested for color stability to combined fluorescent and incandescent light |
| 13 ^a | Green | 4.94 | Modified pear shape, irradiated; tested for color stability to direct sunlight (now blue) |

^a Sample represents the material being sold today as "Ocean green" topaz.

^b Number in parentheses refers to GIA Research sample number. Information after semicolons for samples 9–13 refers to type of color-stability testing, as appropriate.



Figure 1. A new color variety of irradiated topaz has appeared in the trade, and is being sold under the name Ocean-green topaz. These samples (3.85–8.70 ct) show a typical range of color for this material. Photo © GIA and Tino Hammid.

As a preliminary test of color stability to heat, green sample 9 was cut into two pieces, with one half (9A) retained as a control (together with linear accelerator [linac] irradiated brown topaz sample 10). The other half of sample 9 (9B) and brown sample 11 were progressively heated in air over a temperature range of 180°–400°C in 10° increments, with a half-hour period at each step. The stones were visually examined at the end of each period to determine at what temperature a color change occurred.

Last, we tested the color stability of the irradiated green topaz to light. We cut green sample 9A in half again and placed one piece with green sample 13 (and, for comparison, brown sample 10) outdoors in direct sunlight for one day. We exposed green sample 12 to normal indoor lighting—that is, a combination of simultaneous incandescent (30 cm from a 100-watt bulb) and fluorescent lighting—for 48 hours. To determine the extent of the color change, if any, we compared the test stones to Munsell color chips before and after each exposure.



Figure 2. These five samples (from left—nos. 1, 8, 7, 6, and 5) represent the different types of topaz examined in this study and, specifically, those for which absorption spectra are given in figure 3. Photo by Maha DeMaggio.

RESULTS

Gemological Examination. The indices of refraction of green topaz samples 1–5 fell within the range 1.610–1.620, typical values for both untreated and treated topaz (Liddicoat, 1990, p. 208). To long-wave ultraviolet radiation, these samples fluoresced a weak-to-moderate, turbid, yellowish green. The short-wave fluorescence was similar in color but less intense. This U.V. luminescence has been seen in some other colors of topaz (Webster, 1983, p. 141). When the stones were examined with a microscope, no distinctive inclusions or other features were observed.

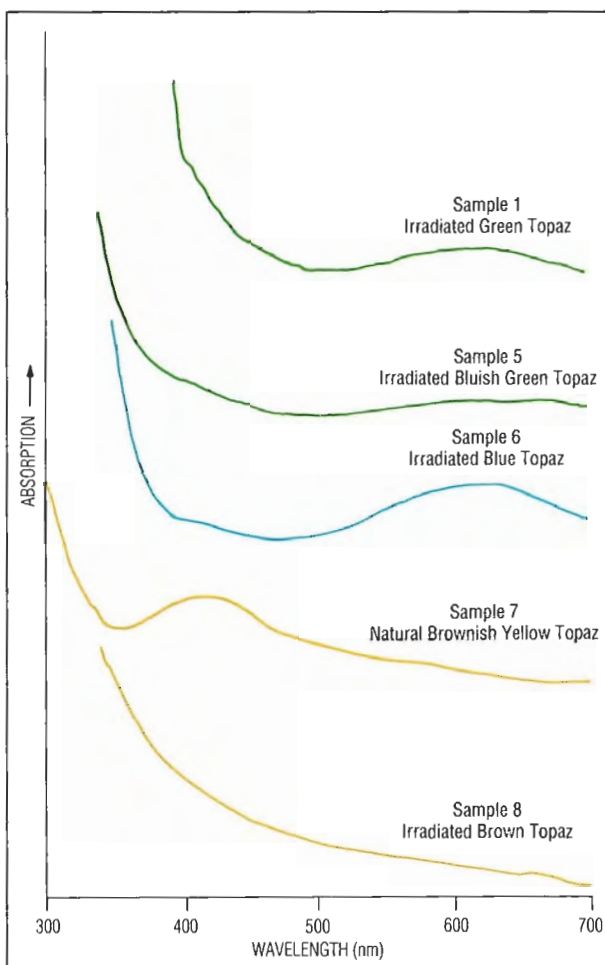
Absorption Spectra and Chemistry. The visible absorption spectra of two representative green topaz samples (nos. 1 and 5) revealed three main features, all of which have been described previously in colored topaz (see, e.g., Petrov, 1977). These three spectral features are all too weak and too broad to be seen as distinct bands with a handheld spectroscope. Comparison of the visible spectra of these samples with those of other colors of untreated and treated topaz (figure 3) provides an explanation for the green color.

The spectrum of each of the two green samples displays a very weak, broad region of absorption between 500 and 700 nm that is centered at about 600 nm. This same broad band is also present in the spectrum of the blue topaz that has been irradiated and heat treated (no. 6; see also figure 5 in Petrov, 1977, p. 296).

The spectra of the two green samples also display a broad and very intense region of absorption centered in the ultraviolet, a portion of which extends into the visible region up to about 500 nm. This

appears to be the same as the prominent feature seen in the spectrum of irradiated brown sample 8. It is also evident, though much weaker, in blue sample 6. Nassau and Prescott (1975) described this broad band as being produced when topaz is irradiated.

Figure 3. These visible and near-ultraviolet absorption spectra of two samples of irradiated green (nos. 1 and 5) and other natural-color (no. 7, brownish yellow) and laboratory-irradiated (nos. 6—blue and 8—brown) topaz samples illustrate the three main absorption features present in the spectra of irradiated green topaz that, in combination, produce the Ocean-green color: (1) a broad, weak absorption centered at about 600 nm (giving rise to the blue component; e.g., sample 6); (2) the broad region of absorption in the ultraviolet and extending into the visible (causing a brown component; sample 8); and (3) the broad, very weak absorption centered at about 425 nm, and seen on the shoulder of the ultraviolet absorption (contributing to a yellow component; sample 7).



The third feature that we observed in the green samples is a very weak, broad region of absorption centered at about 425 nm that appears to be the same as a band that is especially prominent in the spectrum of the natural-color brownish yellow (no. 7) topaz (also see figure 2 in Petrov, 1977, p. 294). In the spectra of the two green topaz samples (nos. 1 and 5), this broad band is barely visible and only as a very weak shoulder on the side of the large absorption band in the ultraviolet.

Besides the expected aluminum and silicon (the fluorine in most topaz cannot be detected by this method), chemical analysis by EDXRF revealed the presence of germanium (Ge) in all three green topaz samples (nos. 1, 5, and 6) analyzed. This trace element substitutes for silicon in the topaz crystal structure in concentrations up to several hundred parts per million (ppm), and is occasionally reported in chemical analyses of topaz (see, e.g., El-Hinnawi and Hofmann, 1966; Deer et al., 1982, p. 806). When this trace element is present in topaz, irradiation in a linear accelerator generates the radionuclide germanium-69 (Ge-69); as a result, the treated stones must be withheld from the market for a few weeks to await radioactive decay (see Ashbaugh, 1988).

Radioactivity. We determined that each of the six green and bluish green topaz samples that registered radioactivity contained the radionuclides commonly found in reactor-irradiated topaz (Schmetzer, 1987; Ashbaugh, 1991). These included scandium-46 (Sc-46), tantalum-182 (Ta-182), and manganese-54 (Mn-54);

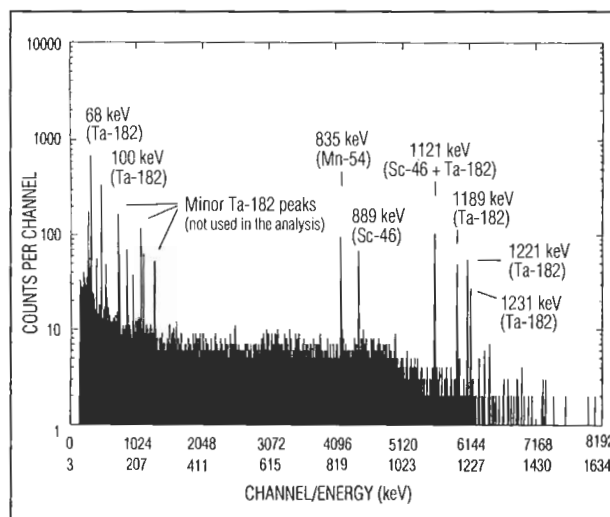


Figure 4. The gamma-ray spectrum of green topaz sample 9 (a one-hour counting period) shows the gamma-ray peaks of Sc-46, Ta-182, and Mn-54. The gamma-ray energy range of the spectrum shown is from 50 to 1500 keV. The radionuclides are represented by peaks in the spectrum. The quantities of each of the radionuclides can be calculated by computer analysis from these counting data.

see the gamma-ray spectrum of sample 9 in figure 4). Sample 1 showed a small amount of cesium-134 (Cs-134). These radionuclides would not likely be found in topaz irradiated by other methods (Ashbaugh, 1991). The concentration levels of these radionuclides in each sample are shown in table 2. The number shown

TABLE 2. Radionuclide data for samples of irradiated green topaz.^a

| Radionuclide | NRC release limit ^b | Sample no. (and carat weight) | | | | | |
|----------------------------|--------------------------------|-------------------------------|-------------------|----------|----------|----------|----------|
| | | 1 (3.85) | 2 (4.34) | 3 (4.71) | 4 (8.70) | 5 (4.10) | 9 (9.20) |
| Sc-46 | 0.4 | Trace ^d | 0.02 | 0.73 | 0.10 | Trace | 0.15 |
| Ta-182 | 0.4 | 0.20 | Trace | 0.28 | 0.20 | Trace | 0.76 |
| Mn-54 | 1.0 | Trace | Trace | 0.17 | 0.14 | Trace | 0.17 |
| Cs-134 | 0.09 | 0.01 | None ^e | None | None | None | None |
| Sum of ratios ^c | 1.0 | 0.61 | 0.05 | 2.70 | 0.89 | 0.01 | 2.45 |

^a Radionuclide data in nanocuries per gram (nCi/gm) of radioactivity. Data collected on October 27, 1992; the radionuclide concentration values will decrease over time due to radioactive decay. Because no radioactivity was detected for samples 12 and 13, they are not included in this table.

^b Current NRC release concentration limits for these radionuclides—see U.S. NRC Rules and Regulations, Title 10, Chapter 1, Part 30.70, Schedule A (August 30, 1991); and Part 20, Appendix B (May 31, 1991).

^c Sum of the ratios = summation of the concentration of each radionuclide present divided by the NRC release limit for that radionuclide. This number must be less than or equal to 1.0 for the individual irradiated topaz sample to be sold or distributed legally in the United States.

^d Trace = trace quantities (less than 0.01 nCi/gm) of these radionuclides were detected.

^e None = the radionuclide was not detected.

in the bottom row (labeled as the "sum of the ratios") must be less than or equal to 1.0 for the topaz sample to be sold or distributed legally in the United States. As can be seen, samples 3 and 9 were above this limit.

Color Stability. With regard to color stability to heat, at about 250°C the brown color of sample 11 became blue; beginning at about 310° up to 375°C, sample 9B changed progressively from green to blue, with no residual green color present above the latter temperature (C. Habib, pers. comm., 1992; figure 5). According to our experience, blue topaz is most color stable to heat, while irradiated brown and (now) green topaz are less stable.

The two green topazes (no. 13 and the portion of 9A) and one brown (no. 10) sample that were tested for stability to direct sunlight all became blue within one day of exposure (see, e.g., figure 6). Subsequent exposure of two additional Ocean-green topaz samples not in the original study gave the same result: Both turned blue in the course of one day in direct sunlight. However, there was no change in the green color of sample 12 after 48 hours of exposure to a combination of simultaneous incandescent and fluorescent (normal indoor) lighting. The visible absorption spectrum of sample 13, after it had turned blue in the sunlight, was identical to that of irradiated blue topaz (see, e.g., the spectrum of sample 6 in figure 3).

DISCUSSION

Because the samples of green topaz that we tested revealed the same radionuclides as are typically found in neutron-irradiated blue topaz, we believe that the

Figure 5. Heat-treatment experiments revealed that exposure to high heat will turn either brown or green topaz blue. On the left are the originally green control (sample 9A) and heat-treated (sample 9B) topaz samples; on the right are the originally brown control (sample 10) and heat-treated (sample 11) topazes. Photo by Maha DeMaggio.



Figure 6. Ocean-green topaz sample 12 (top) showed no color change when exposed to combined fluorescent and incandescent (indoor) lighting. Sample 13 (bottom) changed from green to blue within a day of exposure to direct sunlight. Photo © GIA and Tino Hammid.

green topaz was also neutron irradiated, but probably at a higher temperature. This conclusion is substantiated by the fact that one of us (CEA) produced the bluish green color of sample no. 5 by irradiation in a non-water-cooled area of a nuclear reactor; that is, the topaz was subjected to an irradiation temperature that was higher than is typical in this procedure. We have also seen some green topaz in parcels after electron treatment in a linear accelerator and prior to the heat treatment normally used to produce the "Sky-blue" material (pers. knowledge CEA; D. Duke, pers. comm., 1992). However, this type of irradiation would not have produced the radionuclides found in reactor-irradiated topaz.

The color of this irradiated green topaz can be understood by referring to the visible absorption spectra in figure 3. The green results from the cumulative effect of the causes that individually produce brown, yellow, or blue. In the spectrum of the green topaz, there is the broad absorption in the ultraviolet extending into the visible (causing the brown component), the broad but very weak absorption centered at about 425 nm (providing the yellow component), and a broad, weak absorption centered at about 600 nm



(giving rise to the blue component). This agrees with the interpretation of Petrov (1977).

CONCLUSION

The Ocean-green topaz currently being marketed has been neutron irradiated in a nuclear reactor under conditions that are believed to be different—in terms of a higher irradiation temperature—than the conditions used to produce normal London-blue topaz.

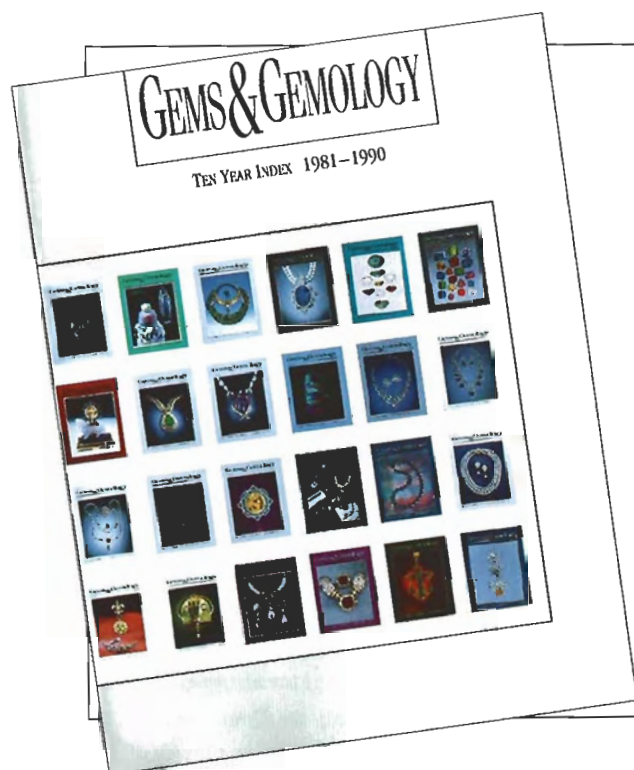
As is the case with reactor-irradiated blue topaz, this green topaz is radioactive when first removed from the reactor. NRC regulations require that it be tested for residual radioactivity before it is made avail-

able for sale to the general public. Two samples tested in this study (nos. 3 and 9) were found to be above the current NRC release limits and, as such, are illegal to sell or distribute in the United States. Therefore, all green topaz should be tested for residual radioactivity by an NRC-licensed testing facility before being placed on the market.

We also found that irradiated Ocean-green topaz turned blue when exposed to direct sunlight for only a day. Exposure to fluorescent and/or incandescent light indoors did not appear to affect the color. Disclosure of the instability of the green color to sunlight should be made in conjunction with any sale of this material.

REFERENCES

- Ashbaugh C.A. III (1988) Gemstone irradiation and radioactivity. *Gems & Gemology*, Vol. 24, No. 4, pp. 196–213.
- Ashbaugh C.A. III (1991) Radioactive and radiation treated gemstones. *Radioactivity and Radiochemistry*, Vol. 2, No. 1, pp. 42–57.
- Ashbaugh C.A. III (1992) Gamma-ray spectroscopy to measure radioactivity in gemstones. *Gems & Gemology*, Vol. 28, No. 2, pp. 104–111.
- Deer W.A., Howie R.A., Zussman J. (1982) *Rock-forming Minerals, Vol. 1A, Orthosilicates*. Longman Group Ltd., London.
- El-Hinnawi E.E., Hofmann R. (1966) Bemerkungen zur Verteilung von Spurenelementen im Topas. *Chemie der Erde*, Vol. 25, pp. 230–236.
- Hoover D.B. (1992) *Topaz*. Butterworth-Heinemann, New York.
- Liddicoat R.T. Jr. (1990) *Handbook of Gem Identification*, 12th ed. rev., 3rd printing. Gemological Institute of America, Santa Monica, CA.
- Nassau K., Prescott B.E. (1975) Blue and brown topaz produced by gamma irradiation. *American Mineralogist*, Vol. 60, No. 7/8, pp. 705–709.
- Petrov I. (1977) Farbuntersuchungen an Topas. *Neues Jahrbuch für Mineralogie Abhandlungen*, Vol. 130, No. 3, pp. 288–302.
- Schmetzer K. (1987) Colour and irradiation-induced defects in topaz treated with high-energy electrons. *Journal of Gemmology*, Vol. 20, No. 6, pp. 362–368.
- Webster R. (1983) *Gems, Their Sources, Description, and Identification*, 4th ed. Revised by B. W. Anderson, Butterworth and Co., London.



Where to Find Everything You Need to Know?

The Gems & Gemology Ten-Year Index, 1981-1990

Thousands of entries lead you to critical information on everything from De Beers gem-quality synthetic diamonds to Kashmir sapphires, from inclusion photography to infrared spectroscopy, from the Muzo mine to Minas Gerais to Mingxi.

An indispensable resource, the Index is your guide to the exciting developments published in *Gems & Gemology* during this decade.

You can get your personal copy for only \$9.95 (plus shipping and handling, and tax where appropriate) or FREE with your new subscription to *Gems & Gemology*.

Supplies are limited. Order NOW.

For more information, Call toll-free (800) 421-7250 x201, or outside the U.S. (310) 829-2991 x201. FAX (310) 453-4478.

Or Write *Gems & Gemology* Subscriptions Dept.,
1660 Stewart St., Santa Monica, CA 90404

GEM TRADE LAB NOTES

EDITOR

C.W. Fryer Gem Trade Laboratory, West Coast

CONTRIBUTING EDITORS

GIA Gem Trade Laboratory, East Coast
G. Robert Crowningshield • Thomas Moses

GIA Gem Trade Laboratory, West Coast
Karin Hurwit • Robert C. Kammerling •
Shane F. McClure

Treated AMBER

Occasionally the laboratory embarks on detective work beyond the straight identification of an item. For example, a client submitted two amber cabochons to the East Coast lab, with the request that we determine why the paler of the two had faded when it was mounted and displayed in a brightly lit showcase. The client reported that the “faded” sample was from the same parcel as the darker one and was originally the same color (figure 1).

In the process of confirming that the samples were amber, we noticed an unusual orange fluorescence and the presence of a layer of minute gas bubbles in swirls just beneath the sur-

face on both pieces (see, e.g., figure 2). In the April 1986 *Journal of Gemmology*, Kenneth Scarratt reported on amber with a dark surface color that showed similar (but straighter) strings of gas bubbles; removal of part of the surface revealed that it was actually a very shallow layer over a very pale core.

The prominent stress fractures (“sun spangles”) in the faded stone are undoubtedly due to exposure to heat. It is known that cloudy amber can be clarified by gradual heating—in 50° increments—to approximately 200°C (see, e.g., Kurt Nassau, *Gemstone Enhancements*, Butterworth's, 1984). It appears that, during heat treatment, the gas bubbles that cause the cloudiness migrate to the surface, the

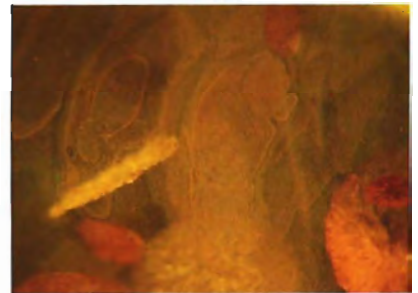


Figure 2. This veil-like plane of minute bubbles was seen just beneath the surface of the faded cabochon in figure 1. Magnified 10×.

Figure 1. These two clarified amber cabochons (each about 25 × 18 mm, 10.50 ct) were from the same lot and, originally, both the same color. The paler specimen (right) had faded over time while displayed in a brightly lit case.



surface darkens, and the color in the center may be almost totally lost. Presumably, the darker brown surface color is due to oxidation caused by the heating. However, the finished product usually has a dull, chalky green (rather than orange) fluorescence to long-wave ultraviolet radiation.

Ken Scarratt has reported (pers. comm., 1993) that this clarification process may be carried out with the stones heated in what he calls “sump oil” (old crankcase oil). With no specimens known to be treated in this fashion available for study, however, we have not been able to investigate this possibility.

Nassau and others also state that

Editor's note: The initials at the end of each item identify the contributing editor who provided that item.

Gems & Gemology, Vol. 29, No. 2, pp. 122-128.

© 1993 Gemological Institute of America



Figure 3. When the brown "skin" was removed from one end of an amber sample from the same lot as the stones shown in figure 1, a near-colorless center was exposed.

amber may be surface colored with organic dyes, and these may fade. However, the detection of an organic dye on an organic substrate, such as amber, commonly requires other than routine gemological procedures and so was beyond the scope of this investigation.

The client subsequently provided us with several more cabochons, all of which had the swirled layer of tiny gas bubbles and fluoresced the unusual orange color noted above. The client also gave us permission to subject the specimens to any tests we felt appropriate. First, we removed a portion of the "skin" from one end of one of them, which revealed that the material underneath is almost colorless (figure 3). Next, we cut another sample in two and placed one half in

Figure 4. Originally, both portions of this 25 × 18 mm cabochon were dark. The section on the right faded when it was exposed to the light from a 14-watt Tensor lamp for approximately 170 hours at close range.



the dark while we left the other approximately 1.5 cm from the bulb of an illuminated 14-watt Tensor lamp for seven days. At the end of that time, the exposed piece had become markedly paler (figure 4). Our work on these two stones confirmed that the fading was probably due to exposure to intense light. GRC

DIAMOND

Extensive, Subtle Fracture Filling in a Diamond

Preliminary examination of a 0.88-ct heart-shaped brilliant submitted to the West Coast lab revealed what appeared to be a filled diamond with extremely low relief "fingerprint" inclusions containing minute voids. Because the GIA Gem Trade Laboratory does not issue grading reports on filled diamonds, the stone was referred to the Identification and Research Department for additional testing and issuance of an identification report.

Further examination with magnification using standard darkfield illumination revealed several transparent, colorless, filled fractures that contained the minute voids mentioned above and showed a very subtle orange-to-blue flash effect. The flash effect in these fractures was particularly difficult to detect because the fractures lay at very shallow angles to the surface of the diamond.

The treatment became more apparent (figure 5) when a pinpoint fiber-optic illuminator was used. This lighting technique revealed the extent of the filled breaks, which included one very large fracture beneath, and nearly parallel to, the table. The intense illumination also made the flash effects significantly more noticeable and revealed hairline fractures in the filling material. With transmitted light, the outlines of the filled areas were easier to detect when a single polarizing filter was placed between the microscope's objective and the diamond.

Qualitative chemical analysis performed by GIA Research, using energy-dispersive X-ray fluorescence (EDXRF), detected lead. This element

had previously been detected in diamond fillings (see J. Koivula et al., "The Characteristics and Identification of Filled Diamonds," in the Summer 1989 issue of *Gems & Gemology*). X-radiography further confirmed the presence of the filling in the form of white, X-ray-opaque areas on the X-radiograph.

It is important to reiterate that, although the diamond contained

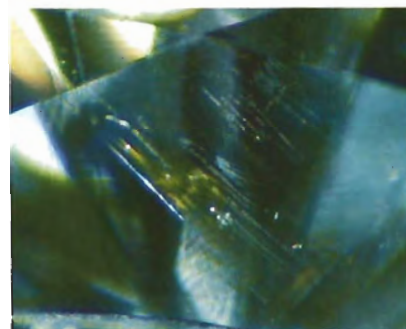


Figure 5. The orange and blue flash effects are very subtle in this extensively filled diamond. Fiber-optic illumination; magnified 40x.

numerous filled fractures, the diagnostic microscopic features were quite subtle. These might have been easily overlooked if only darkfield illumination had been used. It is therefore prudent to use additional lighting techniques, including pinpoint fiber-optic illumination and polarized light, in all cases where fracture filling is suspected. RCK and SFM

Iridescent "Dislocation" in a Diamond

In our experience, iridescence in diamond is almost always associated with very fine fractures. It was thus a pleasant surprise to encounter the unusual internal scene shown in figure 6 in a 1.60-ct round brilliant submitted to the West Coast lab for grading. Here, iridescence revealed a thin-film separation along what appeared to be a "V"-shaped dislocation that reminded us of a "Stealth" fighter aircraft. A visual estimation of the angle

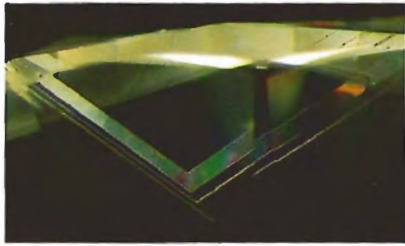


Figure 6. Iridescence can be seen in this "V"-shaped thin film in a diamond. Magnified 30 \times .

led us to believe that the thin film follows a pair of possible dodecahedral planes. The iridescence, visible at some orientations, is apparently due to the narrowness of the separation.

RCK and John I. Koivula

Mounted Diamonds Mistaken for Simulants

The Fall 1991 Gem News section contained an entry on small diamonds set in pendants by means of a transparent, colorless, carbon-based polymer. It was noted that small stones so mounted can give false "simulant" readings on thermal conductivity meters. Other tests, such as magnification, were recommended in such instances.

Recently, the West Coast lab was asked to examine one of these pendants after a jeweler had told the client that the stones were imitations. Testing of one randomly selected stone revealed properties diagnostic of diamond, including typical microscopic features. We also resolved 415.5-nm absorption lines in the spectra of some of the stones, and a number of them fluoresced blue to long-wave U.V. radiation (figure 7), a behavior that is quite typical of diamond, but not of its simulants. Therefore, we concluded that the stones were indeed diamonds.

RCK and Cheryl Wentzell

Treated Green Diamond

Before beginning some alterations on the diamond-set white-metal ring shown in figure 8, a local jeweler sub-

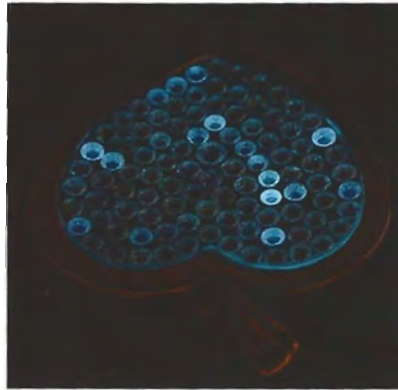
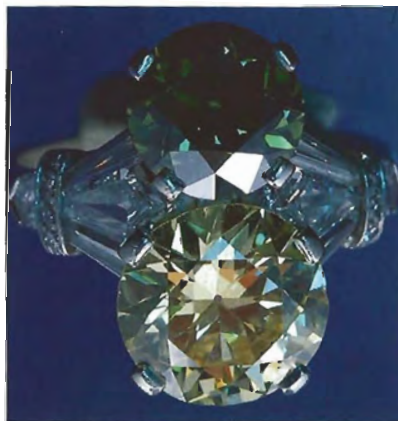


Figure 7. When exposed to long-wave U.V. radiation, several of the stones in this pendant exhibited the blue fluorescence typical of diamond.

mitted the piece to the East Coast laboratory for a report on the origin of color of the green stone. The jeweler's client had indicated that the ring was purchased from a prominent New York City jewelry firm in the 1930s and had been in the family ever since.

Treatments that alter the color of gem diamonds have been known since 1906, and treatment with radioactive compounds became commercial in 1915. Other methods of radiation treatment did not become common until after 1946. However,

Figure 8. The green diamond in this ring measures approximately 8.5–8.6 mm in diameter by 5.3 mm deep and owes its color to a surface treatment with a radioactive compound.

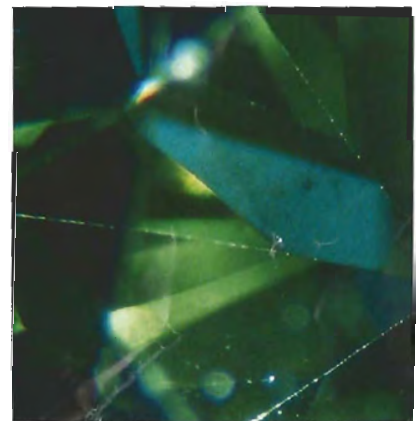


examination of this green diamond with a binocular microscope revealed numerous brown spots and patches on the polished surfaces, especially on the pavilion (figure 9). A distribution of green spots and patches frequently results from surface treatment with a radioactive compound, a process that leaves the diamond itself radioactive. When checked with a hand-held survey meter, the stone exhibited significant radioactivity, with a maximum reading of 42 mR/hour, thus confirming our suspicion of treated color.

Subsequent radionuclide testing at the West Coast lab revealed the characteristic gamma-ray signature of lead-210 (Pb-210) in this green diamond. We know that if lead-210 is present, its radioactive daughter nuclides, bismuth-210 (Bi-210) and polonium-210 (Po-210), must also be present; however, only Pb-210 releases enough gamma rays during decay to be measured quantitatively in our laboratory.

Pb-210 and Bi-210 both decay by emission of beta particles, and Po-210 decays by emission of alpha particles. The penetration of alpha and beta particles is very shallow in diamond—only about 0.01 mm and 1

Figure 9. The patchy brown radiation stains on the pavilion of the green diamond shown in figure 8, seen here through the table, were probably caused by heating after the radiation treatment. Magnified 21 \times .



mm, respectively. The surface stains are one result of this shallow penetration; another is the fact that most of the green color is confined to a layer at, or just below, the surface of the stone. The fact that the surface stains appear brown here, rather than green, indicates that the stone was heated to 550°–600°C at some point after it was irradiated.

These radionuclides occur naturally as part of the uranium-238 (U-238) decay chain. A quantity of Pb-210 and Bi-210, when separated from radium (or uranium), has been known traditionally in the nuclear industry as a "Radium D+E source"; it was once employed as a high-energy beta radiation source for instrument calibration but is rarely, if ever, now used.

Pb-210 is subject to regulation whenever it is separated chemically from uranium ore by artificial means. In the case of this green diamond, the 75 nanocuries of Pb-210 measured in this 2.34-ct (0.468 gram) stone greatly exceeded the U.S. Nuclear Regulatory Commission's exempt concentration limit of 0.001 nanocuries per gram. However, because it was below the exempt quantity limit of 100 nanocuries, we returned it to our client with full disclosure as to what radionuclides are present and in what quantities. Inasmuch as the half-life of Pb-210 is 22.3 years, this treated green diamond would not be legal to sell, or trade, in the United States until around the year 2192. The report also gave the surface dose rate—that is, the amount of radiation someone wearing the ring would receive. In the absence of other exposure, this ring could be worn 357 hours a year without exceeding the U.S. federal recommendation for radiation exposure to the hands for the general public.

*Ilene Reinitz and
Charles E. Ashbaugh*

EMERALD

An Ancient Miniature Carving

On occasion, common gem materials provide challenging identifications due to their surface condition or the

form in which they are fashioned (e.g., carvings). The miniature bust in figure 10 (22.1 × 14.1 mm; 25.36 ct) was submitted to the East Coast lab with an important provenance: It was reported to depict Roman Emperor Nero at approximately 11–13 years of age (49–51 A.D.) and to have been carved during that era.

Because the carving is so intricate, we could not establish the refractive index. Using the hydrostatic method, we determined that the specific gravity was 2.70. Although not strong, the spectrum revealed the chromium absorption typical of emerald. The carving also showed a weak pink color—a reaction seen in natural emeralds from a variety of sources—when examined with the Chelsea color filter. The diaphaneity was semitransparent to translucent and, using fiber-optic illumination, we saw numerous fluid inclusions as well as several small crystals that we could not conclusively identify (although we believe that at least one,

Figure 10. This 22.1-mm-high emerald carving is purported to be of Roman Emperor Nero and to date from approximately the first century A.D.



which had a cleaved section that reached the surface on the side of the "head," is biotite mica). Most of the numerous surface-reaching fissures had yellowish brown staining, probably residue of iron compounds. No evidence of "oiling" was present. From the properties, we concluded that the specimen is natural emerald.

If the provenance of the sculpture is genuine, the emerald is most likely from Egypt. According to John Sinkankas in *Emerald and Other Beryls* (Chilton Book Co., Radnor, PA, 1981), the Egyptian mines were worked extensively during the Graeco-Roman period and beyond, from roughly 330 B.C. to about 1237 A.D. In 1991, Robert C. Kammerling, of the GIA Gem Trade Laboratory, visited a number of the ancient emerald mines in Egypt and obtained samples locally. He reports that the material he obtained is very similar in color and transparency to this carving and shows the same turbidity of fluid inclusions, stained fractures, and biotite-mica crystals (see the article by Jennings et al. in this issue of *Gems & Gemology*). TM

EUCLASE, Colored by Chromium

Color is the first clue in the identification of a gemstone, and normally suggests a number of possibilities. These can then be narrowed down on the basis of further testing. If the gem falls outside its usual color range, however, the final identity can be rather surprising. This was the case when the East Coast lab identified the 1.85-ct, vividly colored, greenish blue, square-emerald-cut stone shown in figure 11 as euclase. Gem-quality euclase is usually colorless, pale blue to green (from Brazil), or sometimes very dark blue (from Zimbabwe).

Although the refractive indices and birefringence of this sample were consistent with published values for euclase, the specific gravity (at 3.14) was slightly higher than the usual range of 3.00 to 3.12. In addition, the



Figure 11. This unusual 1.85-ct greenish blue euclase was found to be colored by chromium.

trichroic colors of purple, blue-green, and colorless were different from the bluish gray, light blue, and colorless usually seen in the pale blue material. Unlike the pale material, which shows no reaction to the Chelsea color filter, this stone appeared red. Like the pale material, however, this stone was inert to both wavelengths of ultraviolet radiation. The stone displayed absorption lines in the hand spectroscope, with a doublet centered at about 460 nm and a sharp line at about 680 nm, as previously reported by B. W. Anderson (*The Gemmologist*, Vol. 24, No. 283, 1955, p. 31).

Because we thought that artificial irradiation was one possible cause of the unusual color, we sent the stone to our West Coast radiation-testing facility. However, no residual radioactivity was detected, thereby eliminating the possibility of recent irradiation in a nuclear reactor, and diminishing the possibility of high-energy electron irradiation.

The origin of color in dark blue euclase from the Miami area of Zimbabwe was assigned to the Fe^{2+} - Fe^{3+} charge transfer by S. M. Mattson and G. R. Rossman (*Physics and Chemistry of Minerals*, Vol. 14, 1987, pp. 94-99). Euclase colored by this process exhibits a broad peak at 670 nm, and peaks at 860 and 1250 nm. E. Gübelin (*Gems & Gemology*, Winter 1978-79, pp. 104-110) attributed the

various other hues (light blue, green, deep yellowish green, and greenish blue) of euclase to various states of iron oxidation, although Anderson had attributed blue in euclase to chromium on the basis of gemological spectroscopy ("The spectroscope and its application to gemology," Parts 10 to 17, *The Gemmologist*, Vol. 23, Nos. 275-282, 1954-55).

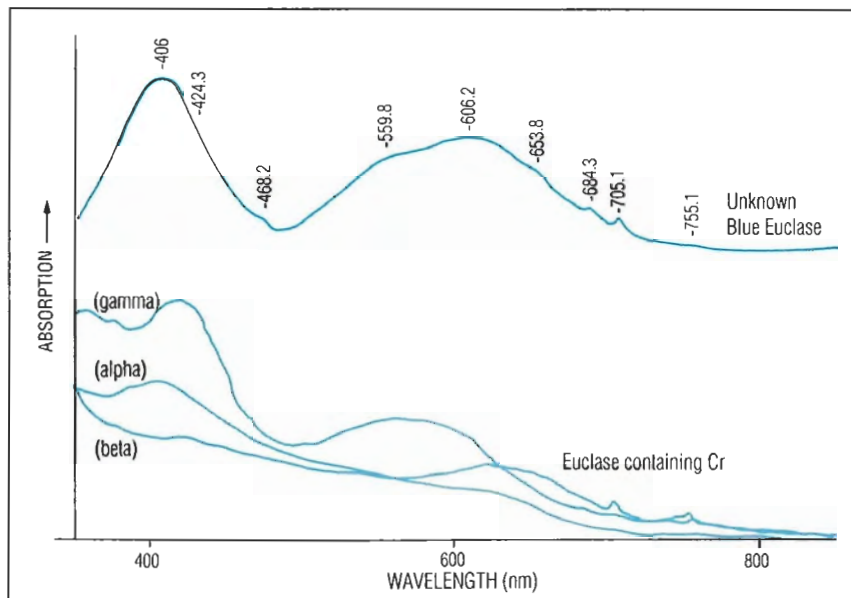
Qualitative energy-dispersive X-ray fluorescence spectrometry performed at GIA Research showed this stone to contain significant amounts of chromium and vanadium, but only trace amounts of iron and titanium. An ultraviolet-visible absorption spectrum of this dark greenish blue euclase (recorded in a random orientation—the top graph in figure 12) shows two broad bands centered at approximately 405 and 605 nm, and weak bands at about 468, 653, 685, 705, and 755 nm. The bands at 468 and 685 correspond to those estimated at 460 and 680 with the handheld spectroscope. The general shape of the spectrum and the position of the weak bands suggest absorption caused by Cr^{3+} . The lower three graphs in figure 12 show the polarized

absorption spectra of a very light bluish green euclase from Villa Roca, in Minas Gerais, Brazil, that was colored by Cr^{3+} . These spectra were provided for comparison purposes by Dr. George R. Rossman of the California Institute of Technology, Pasadena, California. The similarity of the absorption features is striking, and the spectrum of the euclase submitted to us can easily be interpreted as being a combination of the three polarized absorption spectra of the comparison stone. It is uncertain whether or not vanadium contributes to the absorption.

We concluded that the unusual, highly saturated greenish blue color of this 1.85-ct stone is natural and due to chromium, rather than iron as was previously established for other dark blue euclases. The pleochroism of chromian euclase explains why its faceup color varies from greenish blue to bluish green (and possibly purple), depending on the crystallographic orientation of the rough relative to the gem's table.

TM, Emmanuel Fritsch,
Meredith Mercer, and
Ilene Reinitz

Figure 12. The U.V.-visible absorption spectrum at the top is of the 1.85-ct dark greenish blue euclase in figure 11, taken in a random orientation. The three spectra below it are of a very light bluish green euclase, known to be colored by chromium, taken in the three crystallographic directions.



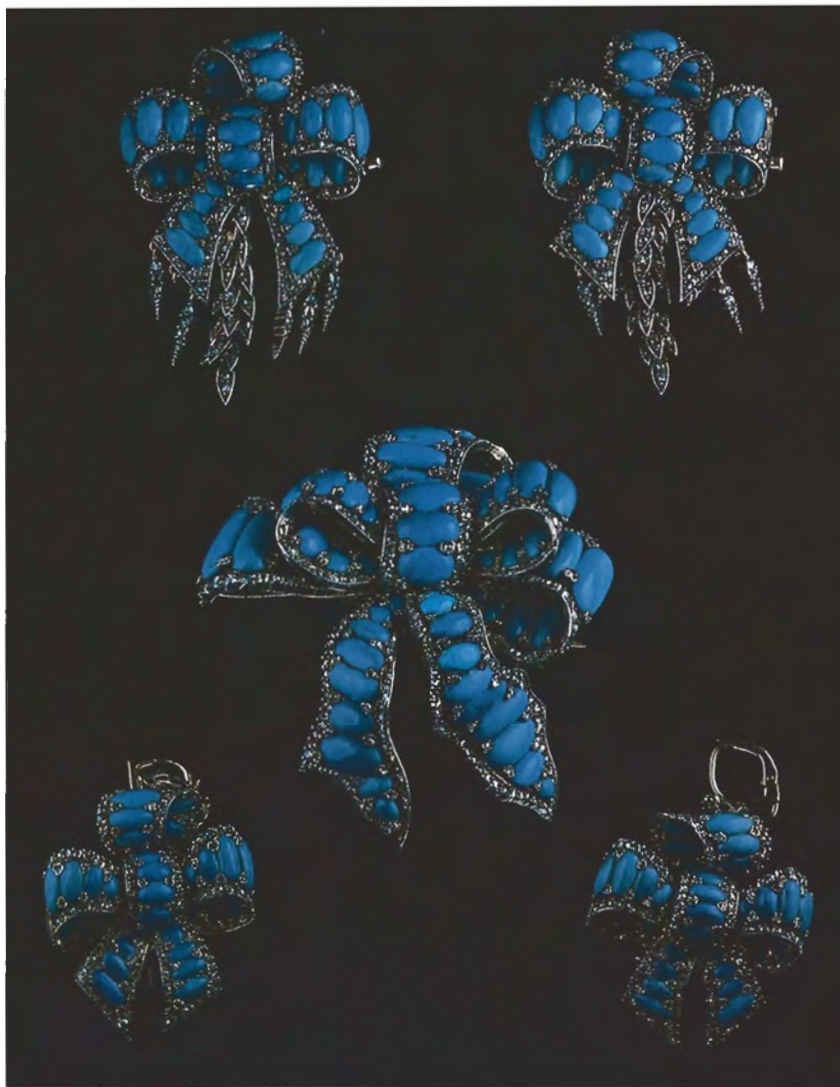


Figure 13. This suite of jewelry, set with diamonds and cabochons of odontolite, turquoise, and at least one glass imitation, is in a style typical of the mid-19th century. The center brooch measures approximately 6×6 cm.

ODONTOLITE

One of the joys for a gemologist is the occasional encounter with a gem material that he or she has read about in textbooks, but has rarely seen. Therefore, it was quite rewarding to be able to identify, with some assistance from GIA Research, the material known as odontolite, or "bone turquoise," among the cabochons in the suite shown in figure 13. Although this writer had seen one some 40 years ago, while studying rare gem materials in museum collections, he had never seen it set in jewelry. The suite of silver jewelry in figure 13, which also contained rose-cut diamonds as well as at least one glass imitation and a number of turquoise cabochons, appears to be in a style that was popular in the mid-19th century.

As the name "bone turquoise"

suggests, odontolite is basically a fossilized organic material—usually the tusks of mammoths or mastodons. The organic material (ivory) is largely replaced by minerals—carbonates, phosphates, or both. Generally, it is green, colored by inclusions of the mineral vivianite, but these cabochons were distinctly blue.

Although the R.I. of 1.61 matched that of turquoise, several other features suggested that some of these samples were not turquoise: their translucency, the parallel banded structure (figure 14), and the lack of a turquoise spectrum in the hand spectroscope.

To determine whether a carbonate was present, with the client's permission we placed a drop of dilute hydrochloric acid on an inconspicuous spot of a sample. With magnifica-



Figure 14. This odontolite cabochon shows the parallel banding frequently seen in this material. Magnified 17x.

tion, we observed a weak effervescence consistent with a carbonate. This was confirmed by the infrared absorption bands located between 2500 and 3000 cm^{-1} , detected with a Nicolet 510 FTIR spectrometer. Additional absorption bands between 1000 and 1600 cm^{-1} suggested that the replacement minerals also included phosphates.

For a short time in the mid-1800s, odontolite was mined commercially in the Department of Gers, in southern France. This might well be the source of the material in these pieces, since their style is consistent with that period. Max Bauer, in his book *Precious Stones* (Charles E. Tuttle Co., Vermont, 1969, reprint of 1904 translation), mentions that when the material in France was mined, it was an unattractive gray-blue color, which became a fine blue with heat treatment. GRC

PEARLS

Natural-Color Black Cultured Pearl with an Unusual Surface

Ideally, the surfaces of both natural and cultured pearls should be smooth and free of blemishes. Although sometimes, to the unaided eye, these ideal conditions appear to be met, usually there are at least some surface blemishes.

The East Coast laboratory recently examined a strand of round, natural-color, black cultured pearls that averaged approximately 13 mm in diameter. All had blemishes of one sort or other, but on some the entire surface was covered with regularly arranged, "dimpled" pits that gave the appearance of a golf ball. The cen-

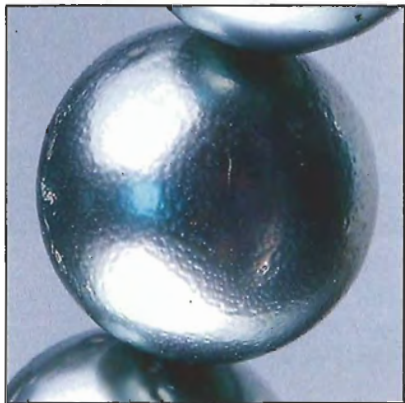


Figure 15. The dimpled surface on this 13-mm black cultured pearl is very unusual.

ter pearl in figure 15 is an excellent example of this effect, which differs from the "hammered" appearance of some natural saltwater pearls.

Examination with magnification revealed the presence of very tiny bumps at the bottoms of these pits (see figure 16). Staff members at the lab do not recall seeing anything similar on other cultured pearls, and have no idea what the cause might be.

GRC

Pearl Care

Wearers of pearl necklaces have been advised for generations to wipe their necklaces with a soft cloth after each wear and avoid cleaning them with liquids, because the capillary attraction of the string may draw substances contaminated by skin acids into the drill holes and cause them to enlarge. This is particularly important for natural pearls, where the drill holes are much finer than in cultured pearls. With both types of pearls, the pearl stringer should wash them thoroughly at the time of restringing and run a length of clean thread through the drill holes to dry them out.

Although customers are com-

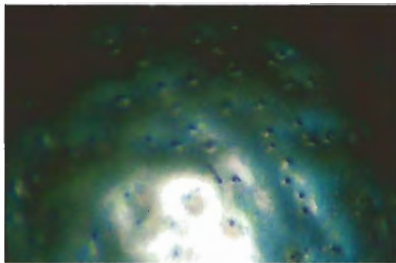


Figure 16. Tiny bumps are seen in the depressions on the pearl in figure 15. Magnified 32x.

monly told that pearls are relatively soft and are damaged by contact with skin acids, instruction in the care of pearls in jewelry other than necklaces has generally been neglected. Since most other pearls in jewelry do not come into direct contact with the skin, instruction for their care usually amounts to gentle warning about their softness and the effects of acids.

Stronger additional caution may be warranted, however. Figure 17 shows the "remains" of a 7-mm half-drilled cultured pearl from a stud earring that was worn constantly. When the pearl was unmounted, it was evident that the portion of the pearl protected from skin acids by the pearl cup now projects out from the area above it, which has been worn away so much that the nucleus is exposed and beginning to wear, too. Wearers of pearl stud earrings should be advised to wash them regularly with mild soap and water, especially if

Figure 18. Half of a 6-mm natural pearl has been set in this diamond clasp.



Figure 17. Note the relationship of the eroded area on this 7-mm cultured pearl to the area protected by the earring cup.

they are worn night and day, as was the case with this earring. GRC

Pearl Half

The GIA Gem Trade Laboratory usually identifies natural and cultured pearls by the structural characteristics as seen on an X-radiograph. It is rare that we get a direct view of the interior of the pearls we are asked to identify. While examining a 6-mm round pearl that graced a diamond clasp (figure 18), the West Coast laboratory staff was surprised to find that the pearl had actually been cut in half before mounting. Figure 19 shows the back of the clasp and the exposed cross-section of the pearl, which clearly reveals its internal structure. Around a conchiolin-rich dark core, numerous darker concentric conchiolin layers have been deposited, beautifully illustrating the characteristic structure of a natural pearl. KH

Figure 19. The back of the half pearl in figure 18 shows perfectly the concentric nacreous layers that form from the center outward in a natural pearl.

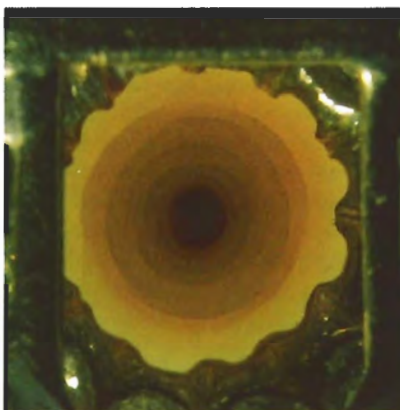


PHOTO CREDITS

Nicholas DelRe took the pictures in figures 1-4, 8, 9, and 13-17. Maha DeMaggio furnished figure 7. John I. Koivula made the photomicrograph for figure 6 and the photographs for figures 18 and 19. Shane F. McClure is responsible for the photos in figures 5 and 11. Figure 10 is compliments of Christie's. Emmanuel Fritsch provided the top spectrum in figure 12.

THANK YOU, DONORS

The Gemological Institute of America extends its sincerest appreciation to all of the people and firms who contributed to the activities of the Institute in 1992 through donations of gems to the Gemstone Collection for reference, research, and classroom use, as well as donations of written materials to the Richard T. Liddicoat Gemological Library and Information Center. We are pleased to acknowledge many of you below.

N. W. Ayer Inc.
Mark Baldridge
Walter Barshai
Allan Bassett
The Bell Group, Inc.
K. C. Bell
Ben Bridge Jewelers
Anne Blumer
James Botsford
Mark Castagnoli
Chatham Created Gems
Shiv Chokhani
Donald Clary
Jo Ellen Cole
Jim Costa
Craftstones
Archie Curtis
Diamond Cutters
of Western New York
Nancy Levy Diamond
(*in memoriam*)
Stanley Dick
Paul Downing
David B. Dubinsky
Ron Dufault
Robert Dunnigan
Ente Fiera di Vicenza
DW Enterprises
Pascal Entremont
Erin & Company
Peter V. Fankboner
Howard Fradkin
Mr. and Mrs. Leonard
Friedman
Emmanuel Fritsch
C. W. Fryer

Edward A. Gabriel
Brad Garman
Gem Resources Inc.
Gem Search International
Susan Goldstein
Gretchen A. Graham
Harold Greenberg
Mark E. Greene
Carl W. Grover
Eva Mae Duit Haru
(*in memoriam*)
Taketoshi Hayakawa
D. B. Hoover
Italian Jewelry Guild, Inc.
D. F. Jayakody
J. Rukin Jelks
Robert H. Jennings
Natalie Johnson
Robert C. Kammerling
Robert and Holly Kane
Akira Kawai
Kyle Kisseberth
Hannes Kleynhans
Kummel Geological
Sciences Library, Harvard
Brian Kvasnik
Richard Larson
Douglas S. Le Grand
Charlotte Lewis
Robert Louis Loeb (*in memoriam*)
Richard Lua
Tom and Phyllis Malicki
Gerald L. Manning
Yianni Melas
Paul Merkel
George and Patricia Messersmith

Anna Miller
Robert Mitchell
Noman Mohammedi
My Humble House
Himiko Naka
Kurt Nassau
Oda E. Nowrath
Erin Orgel
C. D. Parsons
King Plutarco
Precision Cutting Company
Michael Randall
Ronald Ringsrud
Ralph Rosen
Michael Ross
Royal Irish Academy
Hiroshi Saito
Pierre Salerno
Kenneth Scarratt
Betty Schile
Josephine L. Scripps
(*in memoriam*)
Sherris Cottier Shank
James E. Shigley
Weijun Sun
Messele Tadease
Varig Airlines
V.O.I.C.E. of Gold
William Videto
Frank D. Walker
Joseph Wenckus
David Widess
Donald T. Wilson
John Woodbury
Melvin M. Zelnick



GEM NEWS

JOHN I. KOIVULA, ROBERT C. KAMMERLING, AND EMMANUEL FRITSCH, EDITORS

DIAMONDS

Botswana produces large diamond. A 446-ct diamond, recovered earlier this year from the Jwaneng mine in Botswana, is the largest diamond to date from this southern African nation. The stone is being evaluated by Debswana, a firm owned by the government of Botswana and De Beers. (*Mining Journal*, April 9, p. 259)

De Beers now marketing high-quality, high-pressure synthetic diamond products . . . De Beers's work on high-quality synthetic diamond crystals, qualified for years as being purely experimental, is now being applied to the commercial production of industrial materials. As reported in the January 1993 issue of *Industrial Diamond Review*, Dr. Corrie Phaal, senior technical executive of the De Beers Industrial Diamond Division, revealed that

Figure 1. De Beers is now promoting a line of high-quality industrial synthetic diamonds under the trade name Monocrystal®. The display shown here, part of the De Beers industrial diamond exhibit at the 1992 Japan International Machine Tool Fair in Tokyo, included a 34.80-ct yellow synthetic diamond (upper center) that has since been sawn into plates for industrial tooling research. Photo courtesy of De Beers.



research and development efforts in the high-pressure, high-temperature synthesis of diamond have led to the commercial availability of a line of yellow, single-crystal industrial products that are being sold under the De Beers Monocrystal® trademark for industrial tools (figure 1).

Although these synthetic crystals are cost effective only in the range of 1–4 ct, the improved technology has made possible the experimental growth of a 34.80-ct yellow industrial-quality (i.e., it contains numerous metallic inclusions) synthetic diamond crystal—which is significantly larger than the 14.2-ct synthetic diamond crystal mentioned in the Winter 1990 Gem News section. According to De Beers, the growth of this large crystal required 600 hours in the synthesis cycle. Dr. Phaal credits research by the De Beers Diamond Research Laboratory in South Africa and a specialized production plant on the Isle of Man for making this technological feat possible.

. . . and De Beers CVD industrial synthetic diamond products. Dr. Phaal also discussed the De Beers line of CVD (carbon vapor deposition) synthetic diamond products. He feels that the low-pressure, polycrystalline synthetic diamond thin films complement the classic high-pressure, high-temperature single-crystal synthetics. The commercial De Beers CVD products fall into two main categories: (1) tool inserts and parts subject to wear, and (2) optical-quality films. These are marketed under the names CVDITE® and DIAFILM®, respectively. It should be noted that, although De Beers is the second company in the world (after Sumitomo) to offer high-quality synthetic diamond products for sale, industrial CVD synthetic diamond products are available from a number of companies, such as General Electric, Norton, and Crystallume.

“Flanders Brilliant” cut debuts in U.S. The internationally registered Flanders Brilliant cut (figure 2) was promoted for the first time in the United States at the June 3–5 Las Vegas Jewelry '93 Show. The most distinctive feature of the Flanders Brilliant, according to National Diamond Syndicate Inc. vice-president Garry Zimmerman, is that, when viewed from above, the star facets appear to be two perfect squares, stacked one on top of the other at a 45° alignment.

The Flanders Brilliant is currently available in sizes ranging from about 10 points up to about 3 ct and in col-



Figure 2. This "Flanders Brilliant"-cut diamond weighs 1.02 ct. Photo courtesy of National Diamond Syndicate Inc.

ors E to L on the GIA diamond color-grading scale. It is very similar to rounds in terms of weight retention, according to Mr. Zimmerman.

With the aid of computers and the Technical and Scientific Research Centre for Diamonds (the latter attached to the Diamond High Council in Antwerp), the cut was developed in 1988 in Antwerp by Jan Storms, Johan D'Haene, and Dirk Obbers. However, previous marketing efforts focused on Japan.

Sakha (Yakutia) building up diamond reserves. The republic of Sakha (formerly known as Yakutia), in the Russian Federation, Commonwealth of Independent States (C.I.S.), is building its own diamond reserves, independent of those in Moscow. In the future, Sakha might use locally fashioned diamonds from these reserves as collateral in obtaining loans from Western banks, according to a local government official interviewed by Reuters news service. It was also made clear, however, that Sakha had no intention of flooding the market with diamonds and would wait to sell the gems until the economic and political situations in Russia had stabilized.

Under an agreement made between the Russian Federation and Sakha, the latter now retains 20% of its diamond production. Sakha subsequently signed an agreement to sell 50% of this retained rough to De Beers. The remaining 50% held by Sakha goes into its independent reserves, from which some rough is sold to the local cutting industry. (*Mining Journal*, March 12, 1993, p. 182, and May 7, 1993, p. 326).

Venezuela diamond production up. Venezuela posted an almost 50% increase in diamond production in 1992 over the previous year, contributing to an overall jump in the value of the country's mining-related output. Total production of diamonds in 1992 was 478,000 ct, up from 337,000 ct in 1991. (*Mining Journal*, January 15, 1993, p. 47)

COLORED STONES

Blue cancrinite from Greenland. W. Aage Jensen, from the Department of Mineralogy, University of Copenhagen and Troels F. D. Nielsen, from the Geological Survey of Greenland, have provided the following report on the discovery of a deposit of gem-quality blue cancrinite (figure 3) in southeast Greenland.

The cancrinite occurs in one of several nepheline syenite dikes in an area located at the head of the Kagssortoq Fjord, just south of Skjoldungen Island, at 63°14'N, 42°00'W. No actual mining has taken place to date, but a few kilograms of rough material have been brought to Copenhagen for examination. Fourteen oval cabochons, 8.61 to 57.11 ct (the largest about 40 × 22 mm), have been fashioned from this material.

Cancrinite is a hexagonal carbonate containing sodium, calcium, aluminum, and silicon. It occurs intergrown with sodalite and albite, and also contains inclusions of calcite, hematite, mica, pyrite, and rutile. The sodalite and albite components are whitish gray; the cancrinite is light-to-medium blue. Mr. Jensen noted that cabochons cut from the material always show aventurescence.

Mr. Jensen recorded refractive indices of $\omega = 1.499$ and $\epsilon = 1.493$, with a birefringence of 0.006, on the fashioned specimens. He also determined a specific gravity of 2.43 ± 0.01 and a hardness between 5 and 6 on the Mohs scale. The material fluoresced dark red to purple to short-wave ultraviolet radiation, and dark violet to long-wave U.V. The spectroscope revealed absorption in the red from

Figure 3. Cancrinite from a new source in Greenland was fashioned into this 8.61-ct cabochon. Photograph © GIA and Tino Hammid.



650 nm up, and in the blue region from 440 nm down. Mr. Jensen also found that cancrinite effervesces when tested with hot dilute HCl acid, and the blue body color disappears when the material is crushed.

“Emerald matrix” from North Carolina. Big Crabtree Mountain in North Carolina is the only emerald-producing locality in the United States. In addition, the occurrence of the emerald is unusual—within a well-defined pegmatite in mica schist. Although the mine has been worked sporadically for almost a century, few regard this as a commercial source of emeralds because little facet-grade material has been produced.

Today, the area is being mined primarily to recover attractive “matrix” material: well-formed, although typically fractured, hexagonal prisms of emerald and small black tourmaline crystals in a bright white quartz-feldspar matrix (figure 4). At the February 1993 Tucson show, Emerald City Gem Shop was marketing both fashioned and rough specimens. The fashioned material, referred to as “emerald matrix,” was in the form of solid cabochons (again, see figure 4) or doublets, the latter consisting of a thin slice of the “matrix” with a colorless quartz cap.

This family-owned business is also involved in a partnership that operates the mine. They conduct annual field trips, in conjunction with the August Spruce Pine Mineral and Gem Festival, to allow rock hounds to do their own collecting. Visitors can also use facilities at the gem shop to wash and separate the ore.

Gemstone globe and maps. At Tucson this past February, Hong Kong-based Lucky Gems and Jewellery displayed a globe about 30 cm (1 ft.) in diameter that had been fashioned from slabs of gem materials (figure 5). The oceans were fabricated from lapis lazuli, while countries were constructed of gem materials such as abalone shell, aven-

Figure 4. This 31.98-ct (34.20 × 16.46 × 6.09 mm) “emerald matrix” cabochon was cut from material taken from the Big Crabtree mine in Mitchell County, North Carolina. Courtesy of Emerald City Gem Shop; photo by Maha DeMaggio.

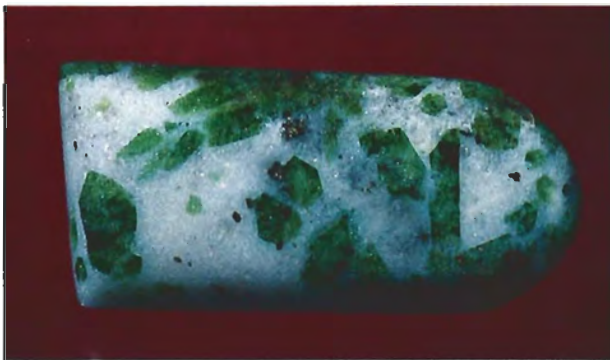


Figure 5. This globe, approximately 30 cm in diameter, uses gem materials to represent countries and oceans. Photo courtesy of Lucky Gems and Jewellery.

turine quartz, hematite, malachite, picture jasper, obsidian, and unakite. Where possible, the gem material used for a country was one found in that country. For example, turquoise was used for Iran and rhodonite for Canada. The firm also produces custom-made globes using materials specified by the client, and flat maps were available following the same general motif.

The first flat map was completed about four years ago, according to Horace Wong, marketing manager for the firm. The first globe, completed in 1990, took eight months to produce. Production of the globes and maps begins in a factory in Ping Wu, Shenzhen, China, with finishing done in the firm’s Hong Kong workshop. The globes are constructed of a spherical wood frame on which the gem materials are placed. All of the gem materials are cut and polished by hand.

Lapidary art. One of the lapidary delights at the Tucson Show this past February was created by Kevin Lane Smith of Tucson. Fashioned from a piece of optical-quali-

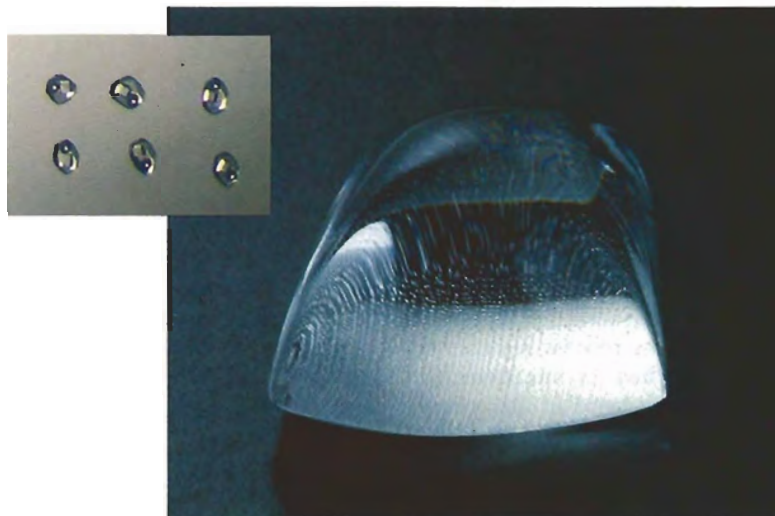


Figure 6. This 72-ct quartz cabochon, which resembles a melting ice cube filled with air bubbles, was designed to reflect a single plane of tiny inclusions. At 40× magnification (inset), one can see that each inclusion actually has three phases. Photo by Maha DeMaggio; photomicrograph by John I. Koivula.

ty quartz, this 72-ct free form contained a flat, uniform plane of tiny inclusions that Mr. Smith had positioned just above the surface of the base so the high-domed cabochon could act as a magnifier (figure 6). Examination of the stone with magnification revealed that these are classic three-phase inclusions (figure 6, inset), each containing a single cube of salt together with a vapor bubble, all in what must be a brine.

Banded iridescent obsidian. Obsidian, a natural volcanic glass, occurs in a number of forms, including snowflake (white cristobalite patches in a dark gray to black body color), banded (with curved or sinuous layers), and Apache tears (naturally occurring small gray-to-brown pebbles that may be transparent to translucent).

Another familiar type—commonly seen as small carvings fashioned in Mexico—is sheen obsidian, which has a black body color that exhibits a typically golden sheen at certain orientations. When such material exhibits a variety of iridescent colors, it is sometimes referred to as “rainbow” obsidian.

At Tucson this February, Kevin Lane Smith showed one of the editors some truly exceptional carved obsidian. The material, which he referred to as Mexican “Mayan” rainbow obsidian, displayed multi-hued iridescence in distinct, parallel bands (figure 7). Mr. Smith reported that the material came from a remote area in the Mexican state of Jalisco that is reached by an eight- to 10-hour drive northwest from the city of Magdalena. He estimated that approximately 30 tons of obsidian have been recov-

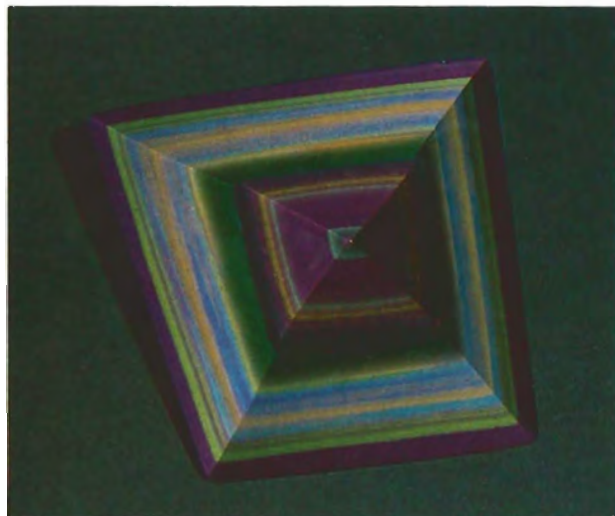


Figure 7. Fashioned from volcanic glass that has been promoted as Mexican “Mayan” rainbow obsidian, this carving (approximately 65 mm wide × 31 mm thick) displays striking iridescent colors. Courtesy of Kevin Lane Smith.

ered from the area, virtually all with some iridescence. Of the 12 tons of material he saw, roughly 10% displayed what he described as exceptional iridescent colors.

Gems from Orissa, India. The state of Orissa, in eastern India, is becoming a significant gem source. Since 1989, we have seen an increasing number of rhodolite garnets from Orissa; more recently, we have seen attractive aquamarine and ruby from this locality.

At the 1993 Tucson Show, Amar J. Jain showed one of the editors a 2.99-ct faceted alexandrite from Orissa, as well as a parcel of dark grayish blue tourmalines (see, e.g., figure 8). Subsequent gemological testing on the 1.74-ct emerald-cut tourmaline in figure 8 revealed properties consistent with those published for tourmaline from other localities, including refractive indices of 1.620 and 1.640, birefringence of 0.020, and specific gravity of 3.11.

Hessonite (grossular) garnet is being mined near the town of Kanta Bhaji, in the Kalahandi area. Anil B. and Ketan Dholakia had faceted samples that ranged from reddish orange to orange to orangish brown in medium to dark tones. However, many of these showed the “roiled” effect generally associated with Sri Lankan hessonites. This was so pronounced in some stones that they appeared translucent, resembling the sard variety of chalcidony. Gemological testing on the 2.19-ct orange stone in figure 8 revealed properties consistent with those of hessonite, including an R.I. of 1.748 and an S.G. of 3.65.

After Tucson, the editors received a letter from Shyamala Fernandes, a gemologist with the Gem Testing Laboratory of Jaipur, India, telling of a “new find”



Figure 8. Orissa is the source of this 1.74-ct tourmaline (left) and 2.19-ct hessonite garnet (right). Tourmaline courtesy of Amar J. Jain Fine Gems (NY); hessonite courtesy of Anil B. Dholakia, Adris Oriental Gem & Art Corp.; photo by Maha DeMaggio.

(December 1992) of chatoyant sillimanite in Orissa. The material was marketed as "moonstone cat's-eye" until local traders realized that it was not a feldspar.

The Gem Testing Laboratory in Jaipur identified the material as sillimanite. They reported the following gemological properties: R.I.—1.659 to 1.678 (flat facet), 1.66 (spot); S.G. (by hydrostatic weighing)—3.25; biaxial optic character; and Mohs hardness between 7 and 8. Microscopic examination revealed the parallel acicular inclusions that cause the chatoyancy. Also noted were two- and three-phase inclusions in "fingerprint" patterns, as well as black platelets of undetermined composition.

According to Mrs. Fernandes, the sillimanite ranges from transparent to translucent and from colorless to gray, pinkish brown, yellowish brown, yellow, green, and blue-green, all of which generally occur in lighter tones. Almost all of the cabochons fashioned to date exhibit well-defined cat's-eyes and a good, vitreous luster. Fashioned material generally ranges up to 20 ct. Although no firm production information was available, Mrs. Fernandes reports that the material has been in ready supply on the Indian market since its reported discovery.

Cultured freshwater pearls from Hanoi, Vietnam. In January 1993, Kenneth Scarratt, of the GIA Gem Trade Laboratory in New York, visited a freshwater pearl-culturing farm on a lake in Hanoi, Vietnam, with a group of other notable gemologists. The farm, named Ho Tay after the lake, is small and production is low (about 3,000 pearls in 1992, but up from 1,000 the previous year). However, local officials report that expansion is planned for the near future, with Ho Tay scheduled to be the largest of three such operations in the northern part of the country.

Ho Tay Lake also provides the mussels (*Cristaria plicata*) for the pearl-culturing operation. The use of wild mussels, rather than those cultivated from young mol-

lusk (spat), is one of the farm's unusual features. Another is the use of mother-of-pearl beads as nuclei, instead of the more common practice of cultivating freshwater pearls by a process of tissue grafting only (i.e., mantle-tissue nucleating), as is prevalent in China today.

The mother-of-pearl beads are hand-cut to imperfect spheres from the thicker portion of a shell harvested from rivers in the northern part of Vietnam. The culturing process starts with the insertion, in one side of the mollusk, of three or four mother-of-pearl beads. Squares of mantle tissue are then placed in contact with the beads and the process repeated on the other side of the mollusk. When the insertions have been completed, the mussels are placed in flat, circular cages that are then hung from a raft (figure 9). Growing periods reportedly vary up to two years. The cultured pearls produced range in color from mauve and pink to orange, white, and gray. The largest that Mr. Scarratt saw was approximately 11 mm in diameter and had an appearance reminiscent of some natural Scottish pearls, which have a somewhat low luster and very pale pink body color.



Figure 9. Nucleated mussels, held in plate-shaped cages, are hung from this raft at a pearl-culturing farm on Ho Tay Lake in Hanoi, Vietnam. The cultured pearls produced represent a range of color. Photo by Sriuraj Prijasilpa.

Peridot from Zabargad Island. One of the best-known sources of peridot—and, historically, the first—is the Red Sea island off Egypt's Ras Banas Peninsula that is known as Zabargad or Saint John's Island (see E. Gübelin, "Zabargad: The Ancient Peridot Island in the Red Sea," *Gems & Gemology*, Spring 1981, pp. 2–8). In the editors' experience, peridot from this locality is rarely seen in the trade. It was thus a pleasant surprise to find small quantities of uncut crystals (approximately 150 grams) and oval faceted stones (227 ct) being offered for sale at the February Tucson shows this year (see, e.g., figure 10).

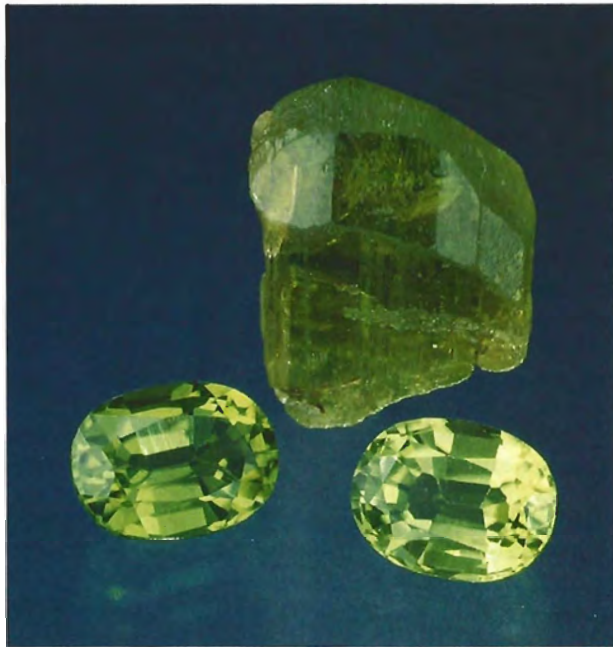


Figure 10. Zabargad is the source of these two faceted peridots (1.63 and 1.65 ct) and the uncut crystal (9.17 ct). Photo © GIA and Tino Hammid

According to Ron Romanella, Afco Far East, Bangkok, Thailand, the material was mined commercially for roughly 30 years in the early to middle part of this century by the privately owned Red Sea Mining Company. Mining activity ended with nationalization in 1958 under Egyptian President Gamal Abdel Nasser, although the then-government-owned firm continued to sell accumulated stocks of material. The stones being offered at Tucson this year were obtained in Egypt in 1985 from old stocks.

Ornamental porphyry from Canada. One of the newer ornamental stones seen at Tucson this February was a porphyry being marketed under the trade name "Flower Rock." (A porphyry is a fine-grained igneous rock that contains conspicuous crystals known as phenocrysts.) According to the firm offering this material, it consists of a gabbro-porphyry matrix containing grayish white phenocrysts of feldspar. The material is recovered from the approximately 1,000 km² (400 sq. mi.) volcanic Texada Island, just off the coast of British Columbia. It was being sold in a number of fashioned forms, including animal figurines, carved eggs, tablets, and cabochons. Gold and rose quartz are also reportedly abundant on the island.

We obtained the fashioned cabochon shown in figure 11 for characterization. It consists of a semitranslucent to opaque, fine-grained black groundmass surrounding grayish white phenocrysts. We determined, by hydrostatic weighing, a specific gravity of 2.89 for this specimen. The



Figure 11. Marketed as "Flower Rock," this ornamental material (37.90 ct, 25.01 × 34.44 × 6.15 mm) is a dark porphyry with light-colored feldspar phenocrysts. Courtesy of West Coast Semi-Precious Stone; photo by Maha DeMaggio.

material was inert to U.V. radiation and exhibited no distinct absorption features through a desk-model spectroscope. X-ray diffraction analysis performed on one phenocryst produced a pattern consistent with plagioclase feldspar. Similar analysis on one spot of the groundmass revealed the presence of an amphibole component, plus additional lines most likely attributable to a metallic-appearing mineral that can be seen under magnification with reflected illumination. On the basis of these features, the stone meets the criteria for a porphyry, although without petrographic analysis we could not determine if it is a gabbro-porphyry or a diorite-porphyry.

Natural resin from Colombia. This year at Tucson, in addition to amber from the Baltic region and the Dominican Republic, a few dealers offered a natural resin from Colombia. Interestingly, some promoted it as amber; others labeled it copal, a fossilized resin of more recent origin, or stated that they did not know which designation was appropriate.

Andrea Nisbet, of Colombian Amber Source of Crestone, Colorado, informed us that the material was being extracted from 11 mines in the Santander area of Colombia. Because the material comes from more than one mine, it is possible that some is amber and some is copal (Ms. Nisbet reported that investigations were being conducted in both the U.S. and Japan to characterize the material more accurately). What is perhaps most notable about this resin is the wealth of fascinating inclusions preserved therein (see, e.g., figure 12), including well-formed leaves, a scorpion, and a spectacular cricket.

It is interesting to note that polarized light revealed the presence of fine lint fibers "glued" to the surfaces of

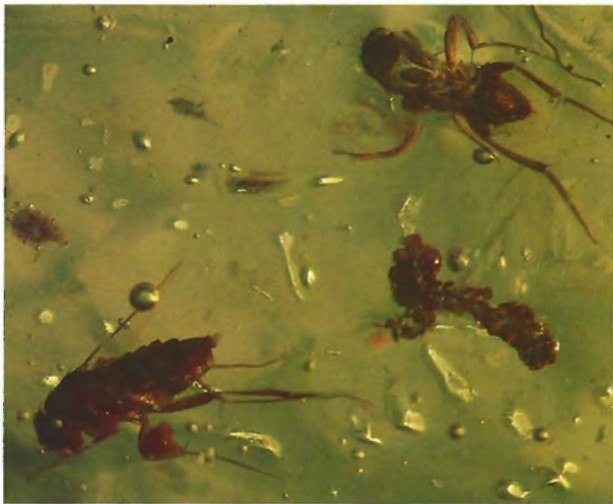


Figure 12. This natural resin from Colombia hosts a multitude of "inclusions," such as these two flies (Diptera) and a frond of liverwort. Photomicrograph by John I. Koivula; magnified 3 \times .

much of the material examined. According to two sources, this results from the use of one of two processes to produce a quick polish: dipping in acetone (which softens the surface, making it sticky) or coating the surface with varnish.

Figure 13. Miners wash gravel in their search for ruby and other gems at the Ruvu mine, near Mahenge, Tanzania. Photo by Keiko Chung.



Ruby Mining near Mahenge, Tanzania. In September 1992, Keiko Chung of Gemstones and Fine Jewelry Company in Los Angeles, California, visited the Ruvu mine near Mahenge, Tanzania, which is owned and operated by Kimon Mantheakis, director of Ruvu Gemstone Mining Company, which operates several mines in Tanzania. The trip to the mine required about nine hours driving south from Dar-es-Salaam, mostly over unpaved roads in a mountainous forested area. This high, cool region was a resort during the colonial period. The forests contain ebony, mahogany, and teak, and are home to a variety of wildlife. Most of the ruby mines are found in small valleys on the lower part of the Mahenge mountain range. They were discovered by hunters around 1984.

Mining claims are filed with the government and posted at each concession, which is typically 900 feet by 900 feet (300 m \times 300 m). About half of the various operations run by Europeans had been abandoned by the time of Ms. Chung's visit. Thai companies have brought in heavy equipment and are now actively producing and prospecting. The Ruvu mine, a smaller operation, is an alluvial deposit where the ruby-bearing gravels are recovered from the bottom of hand-dug pits 5–6 m deep, with various steps and levels.

The nearby mine village has a population of 200 to 400 people, mostly miners and their families. They are generally seasonal workers from local tribes. Two to four miners work the gravels in each pit, shoveling the gem-bearing alluvium into sacks. When they have filled two sacks, they carry them to a stream about 500 m away for washing and sorting (figure 13). This stream floods during the rainy seasons (from May to June and from about mid-October to mid-December), and mining comes to a virtual halt.

In general, one or two rubies are found per sack, and one to two stones that could be fashioned into a good-quality 3-ct cabochon are found per day in the whole Ruvu mine (see, e.g., figure 14). The stones found in one sack belong to Mantheakis (the leaseholder), and he has right of first refusal over any gems from the second sack, which belongs to the miner. Gray corundum, pink-to-red spinel, and amethyst are also found.

ENHANCEMENTS

Opticon follow-up. The Summer 1991 issue of *Gems & Gemology* contained an article on the fracture filling of emeralds, with emphasis on the use of the synthetic resin Opticon. In this article, the authors reported the measured refractive index of Opticon as 1.545. However, we now know that some treaters have tried to make the treatment more permanent by adding varying amounts of hardener to Opticon. Hughes Associates, the manufacturer of Opticon, has subsequently stated that the R.I. of their product, including any possible change caused by addition of hardener, can range from 1.545 to 1.560. It is



Figure 14. These rubies (largest, 14.57 ct) are from the Ruvu mine near Mahenge, Tanzania. Courtesy of Gemstones and Fine Jewelry Co.; photo by Shane F. McClure.

important to note that the visibility of a fracture filler depends on relative relief, i.e., how close the R.I. of the filler is to the host material. Therefore, the relative relief of Opticon-filled breaks can vary due to differences in the R.I. of both the host gem and the Opticon itself.

Turquoise treatment stability. The stability of any gem treatment is always a very real concern. Unfortunately, some enhancements reveal their instability only over a long period of time.

Gary Werner, a dealer who has done considerable research into turquoise treatments, told us about a process he calls "hydrating," which consists of treating turquoise with organic compounds, typically substances that have low melting points. These include mineral oil, oil-based polishes, waxes, waxy polishes, lacquers, and sealers. Paraffins and shellacs are used most commonly in commercial treatments. While all these treatment substances reportedly maintain their integrity longer than do less viscous ones, they typically degrade within a year or two.

Mr. Werner loaned the editors three small strands of tumbled turquoise beads (approximately 9 mm long × 6 mm wide) that illustrate both the dramatic effect one such treatment has on the appearance of turquoise and how transient that effect can be. The typical natural, untreated material is pale blue and somewhat chalky (figure 15, left). When such material has just been treated with mineral oil, it exhibits a much deeper, uniform saturated color (figure 15, center). After approximately five months, this same treated turquoise is paler, and some beads have taken on a mottled appearance. While some beads retain some of the treated color, there are also distinct, irregular areas of pale blue to nearly white (figure 15, right).

SYNTHETICS AND SIMULANTS

Synthetic corundum as a topaz simulant. One of the more clever imitations seen this past February at the Tucson gem shows was a saturated pinkish orange flame-fusion synthetic corundum that was being marketed as an Imperial topaz simulant. The resemblance to this topaz variety was enhanced by the cutting styles: elongated and slightly windowed pear shapes and marquises (figure 16).

Russian flux-grown synthetic emeralds. The Summer 1985 *Gems & Gemology* contained an article on flux-grown synthetic emeralds produced at the Geological Institute of Akademgorod in Novosibirsk, Russia. To our knowledge, little of this material was ever marketed in the United States, although at least two firms have actively promoted Russian hydrothermal synthetic emeralds (see, e.g., *Gem News*, Spring 1991, p. 54, and Spring 1992, p. 63).

Figure 15. These three strands of turquoise beads (about 9 mm × 6 mm) show the effect of oil treatment over time: (left) unenhanced; (center) recently treated; (right) material similar to that in the center five months after treatment. Courtesy of Gary Werner; photo by Maha DeMaggio.



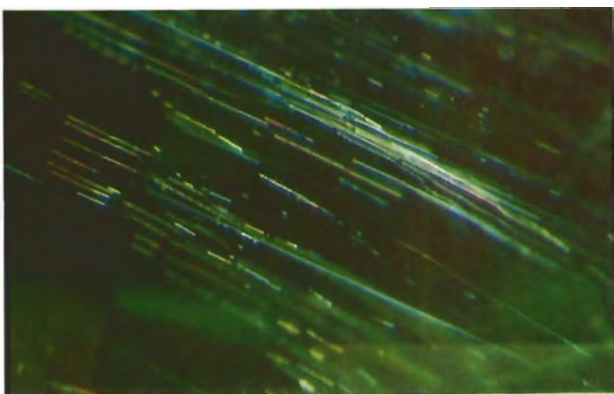


Figure 16. These flame-fusion synthetic corundums, 4.55–6.87 ct, have been fashioned for use as Imperial topaz simulants. Courtesy of L. P. Gems; photo by Maha DeMaggio.

Crystural Corp., a Russian-Thai joint venture with marketing and cutting facilities in Bangkok, debuted a Russian flux-grown product, "Crystural-Created Emerald," at the February 1993 Tucson show. The material is being sold in fashioned form in a number of shapes and standard millimeter sizes.

According to promotional material provided by the firm, the product was developed by a group led by Prof. Gennedy Bukin, who also developed the flux synthetic that was the subject of the above-referenced 1985 report. Gemological testing of two samples donated to GIA revealed properties consistent with those previously described in the literature. A third stone examined revealed numerous white, acicular inclusions (figure 17), as well as the "fingerprints" typical of a flux-grown synthetic; both types have previously been reported in Russian flux synthetic emeralds.

Figure 17. In addition to typical flux "fingerprints," this Russian flux-grown synthetic emerald contains numerous white, acicular inclusions. Courtesy of Judith Osmer, J. O. Crystal Co. Photograph by John I. Koivula; magnified 30 \times .



Novel opal simulants. Among the most novel items we came across last February at Tucson were two types of opal imitations that were being marketed by Manning International under the trade name "Spectaculite." One type consists of a holographic image on a dichromate gel that is wedged between two protective glass layers (figure 18, right), according to Gerry Manning. This type makes a rather convincing imitation of milky white opal.

The second type consists of an interference-imaged "polyprismaline" film embedded in the slightly recessed base of an acrylic cabochon. When no additional backing is used, the simulant is a good representation of crystal opal; a dark backing is applied to make an imitation of black opal (figure 18, left). The film, produced in three versions to simulate predominantly orange-and-red, blue-



Figure 18. The 8.67-ct opal simulant on the right employs glass and a holographic image to imitate play-of-color; the 1.68-ct piece on the left consists of an interference-imaged film and an acrylic cabochon. Courtesy of Manning International; photo by Maha DeMaggio.

and-green, and orange-and-green "play-of-color," produces optic effects somewhat reminiscent of those seen in "Slocum stone" glass imitation opal and in a plastic imitation described in the Summer 1991 Gem News section (pp. 124–125).

More on plastic imitation opal. The Spring 1988 Gem News section briefly mentioned a plastic imitation opal that had been previously described in the literature. Subsequently, however, the editors saw and heard little about this material.

At the February Tucson shows, however, one booth was dedicated exclusively to marketing this plastic imitation. Oval, marquise, round, pear, and heart-shaped cabochons in calibrated sizes up to 20 \times 15 mm were displayed by Universal Canal Jewellery, New York. All exhibited a white body color.



Figure 19. These two triplets, approximately 8 × 10 mm, have been fashioned with plastic imitation opal to provide the play-of-color. Photo © GIA and Tino Hammid.

A promotional flier contained information on the material's properties that were consistent with those previously reported. A sample 1.73-ct cabochon purchased for study revealed properties similar—if not identical—to this published information: spot R.I. of 1.50, S.G. of 1.17, and a strong bluish white fluorescence to long-wave U.V. radiation. However, some of this new material had a patchy mosaic play-of-color rather than the essentially pinpoint play-of-color typical of material we had examined in the past.

The promotional material also stated that it takes five to six months to produce material 2- to 3-mm thick with a surface area not exceeding 30-mm square and that it has been produced in sheets 0.4 mm or less in thickness for watch "faces."

The material was also being shown for the first time in two composite forms: as triplets using single slices of the opal simulant (figure 19), and in similar assemblages employing triangular fragments of the simulant. The latter resemble what are known as "mosaic opal triplets." Although these composites were not being sold at the show, the exhibitor said that they would soon be marketed.

"Synthetic opal" from Russia. The Winter 1991 Gem News column included information on synthetic opal from Russia (p. 256). Recently, we obtained a small amount of material described by the vendors as Russian "synthetic opal" (see, e.g., figure 20). Specimens with a black body color were provided by Dr. Solodova of the National Educational and Scientific Research

Gemmological Center in Moscow, while cabochons with a white body color were obtained from Dr. Alexandr A. Godovikov of the Fersman Mineralogical Museum. According to Dr. Godovikov, this material is produced in a number of places in Russia, including the Moscow area, St. Petersburg, and Novosibirsk.

Many of the white specimens we saw show evidence of mild to severe crazing, although Dr. Godovikov maintained that they had not shown any crazing prior to their arrival in Tucson. It is possible that the extremely dry atmosphere in this desert city is responsible for this effect.

Preliminary testing on three specimens of the white material revealed the following properties: diaphaneity, semitransparent to translucent; spot R.I., 1.44–1.45; long-wave U.V. fluorescence, strong bluish white to blue-white; short-wave U.V. fluorescence, weak to moderate greenish yellow to blue-white. The S.G. of this material, 1.75–1.78, is quite low as compared to both natural and other synthetic opal, perhaps a consequence of the high H₂O content. These cabochons exhibited play-of-color that could only result from an opal-like structure. Also noted was an unusual near-infrared absorption pattern which suggests that this material contains organic compounds, presumably to act as the "glue" between the silica spheres. Properties determined on a cabochon of the black material also revealed some unusual properties, including a 1.35 spot R.I. and a 1.65 S.G. The lower R.I. and S.G. values possibly result from the organic compound that was detected in the near-infrared absorption spectrum.

More on Paraíba tourmaline simulants. The most prevalent simulant for the bright greenish blue tourmaline from Paraíba, Brazil, is a very similar-appearing apatite from Madagascar (see, e.g., Gem News, Spring 1993, pp. 53–54). ICA Laboratory Alert No. 47, dated September 20, 1991, and coauthored by Dr. Hermann Bank and Dr.

Figure 20. These three specimens—0.56 to 3.04 ct—were described by the vendors as "synthetic opal" from Russia. Photo by Robert Weldon.





Figure 21. These beryl triplets (0.89 and 1.20 ct) are convincing imitations of the distinctive greenish blue tourmaline from Paraíba, Brazil. Photo by Maha DeMaggio.

Ulrich Henn, provides a good summary that lists this and other simulants of Paraíba tourmaline encountered in Idar-Oberstein, Germany. Among those mentioned are beryl triplets, a type of assembled stone most commonly encountered as an emerald simulant.

Recently, the editors examined two of these assembled-beryl imitators (figure 21). Both specimens exhibited a very convincing saturated, slightly greenish blue faceup color. Standard gemological testing confirmed that the crown and pavilion consist of essentially colorless natural beryl with the colored cement layer being responsible for the apparent body color. Gemological testing would

Figure 23. This 63.69-ct specimen (23.17 × 20.93 × 10.83 mm) is the first translucent synthetic quartz examined by the editors. Courtesy of Bob Lewis, *Gems Galore*; photo © GIA and Tino Hammid.

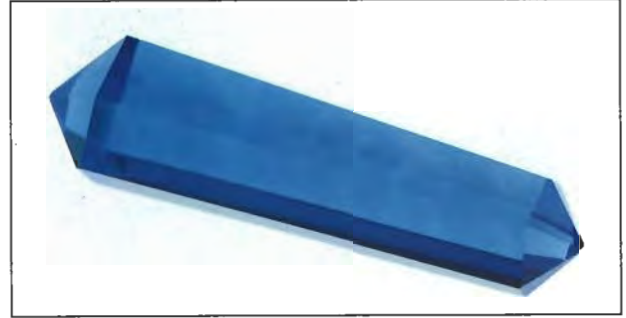


Figure 22. Color zoning is clearly visible in this 14.80-ct faceted "prism" of cobalt-doped synthetic quartz. Photo by Maha DeMaggio.

quickly separate these simulants, as it would any similarly colored natural or synthetic beryl, from Paraíba tourmaline.

Color-zoned synthetic blue quartz. In the Spring 1991 Gem News section (p. 55), we mentioned our first encounter with large quantities of a medium-dark "cobalt" blue synthetic quartz. Since then, we have seen this hydrothermal synthetic as faceted "prisms" and, increasingly, in the form of faceted gems (Gem News, Spring 1992, p. 65).

While looking through stocks of this material at a number of recent trade events, one of the editors noted that essentially all of the samples had eye-visible color zoning. One faceted "prism" was purchased and subsequently examined. A GIA GEM desk-model prism spectroscope revealed absorption features associated with

Figure 24. This 84.5-ct synthetic spinel boule was produced in the former German Democratic Republic to help satisfy internal demand for inexpensive gem materials. Photo by Maha DeMaggio.



cobalt, essentially identical to that documented for lighter blue cobalt-doped synthetic quartz. When the piece was examined between crossed polarizers, we were able to resolve a "bull's-eye" optic figure along the length of the "prism," as is typical for untwinned quartz. Observation with diffused transmitted light revealed roughly wedge-shaped zones of darker color alternating with very light blue zones—separated by poorly defined ("fuzzy") boundaries—throughout the specimen (figure 22). This feature was actually easier to observe without magnification.

Nontransparent synthetic quartz. Synthetic quartz is known to jewelers and gemologists primarily as a transparent material. In Tucson this year, we were shown sawn sections of translucent synthetic quartz, both white and blue. A 63.69-ct sample of the white material (figure 23) was subsequently loaned to the editors for testing.

The material appeared milky white in reflected light and—like white opals and so-called "opal" glass—yellowish orange in direct transmitted light. One surface has what Dr. Kurt Nassau describes in *Gems Made by Man* (Chilton Publishing, Radnor, PA, 1980) as the "pebbly" appearance associated with the rapid growth conditions of transparent synthetic quartz. We also recorded a spot R.I. of 1.55. When the specimen was examined between crossed polarizers, a doubly refractive reaction was noted. It was also possible to resolve a "bull's-eye" optical interference figure across the entire surface perpendicular to the optic axis. The material was inert to both long- and short-wave U.V. radiation, and no absorption features were visible through a desk-model spectroscope. Magnification revealed a faint columnar growth structure perpendicular to the "pebbly" surface; the material otherwise appeared internally homogeneous.

One unusual feature noted was a specific gravity of 2.37, well below the values reported in the gemological literature for quartz, both natural and synthetic. This would appear to be due to the porous nature of the material, which became apparent when the specimen absorbed water during the hydrostatic weighings.

EDXRF spectrometry suggested that the chemistry was typical of hydrothermal synthetic quartz, with silicon and traces of chlorine, potassium, calcium, and iron. Titanium was also detected.

At first, we considered a number of explanations for the reduced transparency, including the presence of TiO₂ inclusions or perhaps light scattering from submicroscopic fluid inclusions or voids (the latter would account for the porosity). However, an article in the November 1991 *Australian Gemmologist* ("Observations on hydrothermally synthesized massive agate-like crystals," by Masahiro Hosaka) sheds additional light on this material. This report describes the experimental growth of massive quartz in a near-horizontal autoclave, using α -cristobalite powder as the nutrient. The resulting product contained two zones of porous quartz with a specific gravity of 2.54. From this information and that gathered through the editors' investigation, it would appear that the Russian material is an aggregate of minute quartz crystals with parallel orientation.

Synthetic spinel from eastern Germany. One of the advantages of the opening of Eastern Europe and the former Soviet Union is that both natural gems and synthetic materials from these localities are becoming increasingly available in the West, marketed by joint ventures.

In addition to materials produced for export, we recently saw some inexpensive flame-fusion synthetics that had been produced in the former German Democratic Republic (GDR, East Germany) to help satisfy internal demand for gems. These consisted of synthetic spinel boules in various colors (see, e.g., figure 24). According to the vendor, they were grown at the Bitterfeld Plant near Leipzig, a facility that prior to the founding of the GDR was owned and operated by I.G. Farben.

ANNOUNCEMENTS

New Exhibit at the Royal Ontario Museum. Featuring a 1,625-ct peach-colored beryl, a 193-ct blue star sapphire, and a 3,000-ct natural blue topaz, the S. R. Perren Gem and Gold Room opened July 3 at the Royal Ontario Museum in Toronto, Canada. Seventy gold specimens and nearly 1,000 rough and cut gems are supplemented by interactive videos designed to teach visitors about gemstones. The exhibit is the first phase of the museum's plan to develop a complete Earth Sciences Gallery.

GEMOLOGICAL ABSTRACTS

C. W. FRYER, EDITOR

REVIEW BOARD

Jo Ellen Cole
GIA, Santa Monica

Emmanuel Fritsch
GIA, Santa Monica

Patricia A. S. Gray
Venice, California

Karin N. Hurwit
Gem Trade Lab, Inc., Santa Monica

Robert C. Kammerling
Gem Trade Lab, Inc., Santa Monica

Loretta B. Loeb
Visalia, California

Shane F. McClure
Gem Trade Lab, Inc., Santa Monica

Elise B. Misiorowski
GIA, Santa Monica

Gary A. Roskin
*European Gemological Laboratory, Inc.
Los Angeles, California*

Jana E. Miyahira
GIA, Santa Monica

Lisa E. Schoening
GIA, Santa Monica

James E. Shigley
GIA, Santa Monica

Christopher P. Smith
*Gübelin Gemmological Laboratory
Lucerne, Switzerland*

Karen B. Stark
GIA, Santa Monica

Carol M. Stockton
Los Angeles, California

Rose Tozer
GIA, Santa Monica

William R. Videto
GIA, Santa Monica

Robert Weldon
Los Angeles, California

COLORED STONES AND ORGANIC MATERIALS

The Australian sapphire industry. T. S. Coldham,
Australian Gemmologist, Vol. 18, No. 4, 1992, pp.
104–107.

This report, the text of a paper that was presented at the Gemmological Association of Australia Scientific Programme in Hong Kong in June 1992, begins by dispelling some misconceptions about Australian sapphires. Mr. Coldham attributes these misconceptions mainly to a lack of Australian involvement in anything other than the mining of the stones. He then discusses the role that Thai dealers play, including the importance of their fairly early knowledge of the heat-treatment process used to

improve the clarity of these often silky gems. Here he provides a most interesting theory, tracing this knowledge to Switzerland prior to World War II.

Mr. Coldham also offers some explanations as to why the term *Australian sapphire* is now used for any low-quality, dark-colored sapphire of volcanic origin. He traces this in large measure to Thai dealers, who favored low-profit, high-turnover marketing methods. The Thais' willingness to purchase and sell the poorest quality Australian rough led to the perception that Australian sapphire was inferior and encouraged the acceptance of increasingly lower standards in its fashioning. At the same time, the expansion of the middle class in the West contributed to the development of mass production of lower-value jewelry and created a demand for large quantities of poorer-quality stones. Low-quality sapphires from various volcanic sources were sold as Australian, while the better-quality Australian goods were misrepresented as coming from Pailin (Cambodia) or Thailand.

The roles played by one Australian miner and two Thai dealers—plus the impact of large quantities of rough from Nigeria, China, and the Bo Ploi fields of Thailand—are also discussed in this interesting and informative report. RCK

Behind the scenes 22. S. Bernstein, *Arts of Asia*, Vol. 23,
No. 2, 1993, pp. 136–140.

This illuminating article describes the priorities of an informed modern jade collector. Recent archaeological discoveries have helped rewrite previous accepted litera-

This section is designed to provide as complete a record as practical of the recent literature on gems and gemology. Articles are selected for abstracting solely at the discretion of the section editor and her reviewers, and space limitations may require that we include only those articles that we feel will be of greatest interest to our readership.

Inquiries for reprints of articles abstracted must be addressed to the author or publisher of the original material.

The reviewer of each article is identified by his or her initials at the end of each abstract. Guest reviewers are identified by their full names. Opinions expressed in an abstract belong to the abstracter and in no way reflect the position of Gems & Gemology or GIA.

© 1993 Gemological Institute of America

ture, and the jade collector of today has access to more factual information than ever before. Illustrated with stunning photography, this article is a veritable feast for eyes and mind alike.

The author, a jade lover since an early age, covers an evolution of taste in America and Europe, including such trends as the emphasis placed on spinach jade at the turn of the century and the popularity of translucent white nephrite carvings from the Ming dynasty during the 1950s. Dominant buyers from Taiwan, Hong Kong, Singapore, Japan, and Thailand are now concentrating on exceptional jadeite pieces, rather than those of lower-to-medium quality. In the 1980s, interest in (and prices of) brilliantly colored Burmese jadeite increased; recently, Asian collectors again have sought fine white nephrite jade.

The two principal techniques used in cultivating a quality collection of jade carvings are physical and stylistic inspection. Dating a particular jade helps determine the value of the piece. The author emphasizes that assigning a date to an individual item requires extensive knowledge and recognition of each dynasty in Chinese history, one reason why jade collecting is such an intellectual exercise.

The author obviously knows his subject and writes in a wonderfully clear and concise manner. This article is an excellent introduction to jade and jade collecting.

JEC

The care and study of fossiliferous amber. D. Grimaldi, *Curator*, Vol. 36, No. 1, 1993, pp. 31-49.

This article, written by an entomologist with the American Museum of Natural History in New York, discusses various practical techniques for the care and study of fossiliferous amber, including methods to observe and photograph fossil inclusions. Much of the article is devoted to the preparation of amber specimens—cutting, grinding, and polishing—to improve the visibility of fossil inclusions. The final section discusses methods used to store amber specimens—to protect them from strong light, heat, and air—and how specimens in collections should be cataloged. Situations where museum amber collections were not well maintained are cited, with practical suggestions made about trying to prevent such unfortunate losses in the future.

JES

Forme, structure et couleurs des perles de Polynésie (Shape, structure and color of Polynesian pearls). J.-P. Cuif, Y. Dauphin, C. Stoppa, and S. Beeck, *Revue de Gemmologie a.f.g.*, No. 114, 1993, pp. 3-6.

This article, the first in a series (all written in French), offers observations on the growth of nacre layers on cultured Polynesian pearls. In particular, it describes how

the emplacement of the piece of mantle tissue influences the final shape of the cultured pearl. Scanning electron micrographs graphically illustrate the various structures discussed in the text.

A comparison of the growth of nacre layers on the inside of the shell and on the surgically implanted nucleus shows some differences. On the inside of the shell, an organic layer develops and clumps of fibrous aragonite form, with their fibers oriented perpendicular to the shell. Then, a cyclic production of organic material perpendicular to the fiber starts, and fairly rapidly leads to the production of nacre (alternating layers of aragonite platelets and organic material). On the implanted nucleus, a thick, generally regular layer of organic material forms. The production of mineral layers occurs progressively, with a great variety of structures and patterns that are probably determined by the culturing conditions.

Two potential problems may arise during nacre production: First, the mantle tissue used for implanting is often selected for its dark color in order to produce a dark color pearl. Such tissue often comes from areas that tend to produce a prismatic structure like the outer part of the shell. However, the inherent thickness of the nacre layers on Polynesian cultured pearls and the culturing time involved usually allow for the transition from prismatic to nacre layers. Second, if the mantle grafts placed against the nucleus fold instead of lying flat, they may cause an abnormally thick organic layer in places. This may result in rings or other irregularities on the cultured pearls, with a corresponding change in the depth of color.

EF

The living museum: Forever in amber. D. Grimaldi, *Natural History*, Vol. 102, No. 6, June 1993, pp. 58-61.

Is there a dinosaur waiting to be cloned inside that insect in amber on your pinky ring? In Michael Crichton's best-selling novel *Jurassic Park* and the movie of the same name, scientists create a theme park full of Mesozoic monsters by cloning DNA from dinosaur blood, obtained from blood-sucking flies preserved in amber. Sound impossible? Think again.

Two teams of scientists, one of which included author D. Grimaldi, recently succeeded in amplifying and sequencing DNA from a 30-million-year-old termite preserved in an amber globule from the Dominican Republic. This is a considerable accomplishment, considering that scientists recently believed DNA could not remain unaltered for a million years. However, scientists are a long way from being able to reconstruct a full set of dinosaur chromosomes from DNA—a process that Mr. Grimaldi likens to reconstructing "Tolstoy's *War and Peace* from a gigantic vat of alphabet soup." Red blood cells contain very little DNA. Not to mention that you first would have to find undigested blood, no little feat. Then comes the biggest roadblock of all, the cost.

Consider that hundreds of researchers have spent billions of dollars trying to sequence a complete set of human chromosomes, even with fresh DNA readily available.

Besides detailing the reasons for, and results of, extracting DNA from the fossilized termite, the author compares other preservation mediums to amber, discusses amber formation, and mentions several deposits. After reading this article, it's hard to look at an insect "inclusion" in amber and not wonder whether that inclusion's last meal might have been a hadrosaur or *T. rex*.

Irv Dierdorff

Sapphires and rubies associated with volcanic provinces: Inclusions and surface features shed light on their origin. R. R. Coenraads, *Australian Gemmologist*, Vol. 18, No. 3, 1992, pp. 70–78, 90.

After briefly addressing corundum nomenclature and fashioning, the author reviews sources—both igneous and metamorphic—worldwide. The remainder of the article addresses corundum of alkalic volcanic origin, with the New England gem fields of New South Wales, Australia, as a case study.

Sapphires from this area occur predominantly as well-formed crystals or crystal fragments with slightly rounded edges and other evidence of chemical corrosion. Some crystals have pointed terminations; others occur as flat hexagonal prisms. Syngenetic minerals, which occur both as accessory minerals and as inclusions in the sapphires, include zircon, hercynite, gahnospinel, columbite, niobium-rutile, and ilmenite, among others.

Ion microprobe dating of syngenetic zircon inclusions in the sapphires showed that the minerals formed 34.9 ± 1.4 million years ago during Cenozoic alkali volcanism in the region. The author draws a number of conclusions based on further study of the inclusions, e.g., that the sapphires formed in a melt rich in iron, but deficient in silica and magnesium.

Next described are surface features typical of corundum from volcanic provinces. This is followed by an interesting description of the Australian sapphire mining industry, with subsections on its history, mining and processing, prospecting, sorting and grading, and enhancement practices.

The article, a useful addition to available literature, includes four tables and several color photos and photomicrographs.

RCK

Treasured in its own right, amber is a golden window on the long ago. J. F. Ross, *Smithsonian*, Vol. 23, No. 10, January 1993, pp. 31–41.

This beautifully illustrated article covers various aspects of the history, sources, and special qualities of amber. In particular, it details the history of the Amber Room, so

named for the jigsaw puzzle of 100,000 intricately carved pieces of amber that covered its walls. Originally a gift from Frederick William I of Prussia to Peter the Great of Russia in the early 18th century, the amber panels were stolen from the Catherine Palace near Leningrad by the Nazis during World War II. Although the search is still on, efforts are being made to recreate the room, using a paltry few surviving photographs and pieces of the original amber panels.

Russian amber mining near the town of Palmnicken is described. Marine deposits are recovered from a strip mine protected from the sea by a dike of sand and soil. The amber-rich glauconite is blasted with water cannons to form a slurry, which is then piped to a processing plant where the amber is separated by screens and suspension. Seven hundred tons of amber are recovered annually, about 13% of which is suitable for use in jewelry.

This article is accompanied by several photos of interesting inclusions in amber, among them the spectacular ant colony featured on the magazine cover and a bird's feather in Dominican amber.

Meredith Mercer

DIAMONDS

Clarity-enhanced diamonds being marketed in Australia. *Israel Diamonds*, No. 130, April 1993, pp. 54–55.

Adrian Zamel, director and chief diamond buyer for Zamel's Jewellers, a 31-store Australian chain, outlines his company's marketing plan for clarity-enhanced diamonds as part of a strategy to highlight lower-priced, low-quality goods during difficult economic times. The company sells clarity-enhanced stones, which it has dubbed "Genesis II Diamonds," obtained from the Koss diamond company of Ramat Gan.

Zamel's aggressive marketing tactics target the stones as low-cost alternatives to untreated high-quality diamonds, emphasizing the technology of the enhancement process. The company chose this strategy both to head off initial rumors that they were selling fake diamonds and to comply with Australia's strict consumer laws regarding disclosure of treatment.

Responding to criticism that such treated stones detract from the image of diamonds as precious because they are natural, Zamel and Koss assert that clarity-enhanced diamonds will not hurt the diamond market and are comparable to synthetic rubies and emeralds in this respect. They need only suitable marketing and disclosure of treatment to find their "proper place" in the diamond industry. Zamel and Koss would like to see a separate grading system developed for clarity-enhanced diamonds to help distinguish them from untreated stones.

Andrew Christie

The rarest gem. D. Kaye, *Europa Star*, Vol. 197-2, 1993.

This easy-to-read article reviews some key issues relative to colored diamonds. These "glorious freaks of

nature" are truly the gems of the elite, both because of their rarity and the prices they command. This is illustrated throughout the article by many examples of colored diamonds owned by the rich or famous. In fact, the two keys to pricing this gem are color and the customer. There is even an interesting discussion of the high prices brought by some exceptional colored diamonds because two customers competed to own them. Laboratory-treated colored diamonds are stated to be worth, conservatively, only one-fiftieth of their natural-color counterparts. The cause of different colors in diamonds is briefly discussed, although the very rare red color is incorrectly attributed to irradiation and heating of a diamond containing nitrogen, when it is actually due to plastic deformation. A fairly long, well-balanced discussion is devoted to the challenge of color grading colored diamonds.

EF

GEM LOCALITIES

Almandine garnet crystals from the Prydz Bay area, Antarctica. J. L. Keeling and R. B. Flint, *Australian Gemmologist*, Vol. 18, No. 3, 1992, pp. 85–88.

Red to brownish red almandine garnets are found both in gneisses and in pegmatites cutting across the foliation of the gneisses on Vikoy Island, in eastern Prydz Bay, Antarctica. This brief article reports on the microscopic examination of over 30 pegmatitic garnet crystals and SEM-EDS analyses of one of these.

All the specimens, which ranged from 8 to 20 mm in diameter, were euhedral but misshapen, with wide variation in the size and shape of the crystal faces. Dodecahedron, trapezohedron (the dominant form), or a combination of both crystal forms were found. Trapezohedral faces were distinctly striated, but even the trapezohedral crystals exhibited dodecahedral faces, usually as small terminal faces centered on twofold symmetry axes. Chemical analysis of the one sample confirmed that the garnets were essentially almandine in composition, with some substitution of ferrous iron by calcium, manganese, and magnesium (and perhaps some substitution of aluminum by ferric iron).

Based on the morphology, the authors make some suggestions as to the mode of formation of the garnets. Illustrations include maps and electron micrographs.

RCK

Desert fire. P. Selbert, *Lapidary Journal*, Vol. 47, No. 1, April 1993, pp. 109–112, 114, 118–119.

The author gives an overview of her recent expedition to the Opal Hill fire agate mine, located in California's Mojave Desert. According to the author, the area around Opal Hill offers such collectibles as dogtooth calcite, white barite, honeycomb-like red rhyolite (with nodules of common opal), "painted agate" resembling desert scenes, jasp-agate, knobby agate-filled geodes, blue

dumortierite, petrified wood, and metallic psilomelane. The Opal Hill mine, owned by Nancy Hill, is one of only four fire agate mines in the United States, and one of two mines open to the public.

Maha DeMaggio

Jaspers from Swierki near Nowa Ruda, Lower Silesia, Poland. W. Heflik, N. Pawlikowski, T. Sobczak, and N. Sobczak, *Journal of Gemmology*, Vol. 33, No. 6, 1993, pp. 356–359.

The authors report on the occurrence of jasper (chalcedony) in southwestern Poland, in beds as thick as 1.8 m. The material is described as "cherry-red, red-grey, brick-red, creamy-green and green" in color, with hematite streaks visible in hand specimens. Chemical analysis of representative samples revealed an SiO₂ content of more than 77 wt.%, with Fe₂O₃ content varying with the intensity of the red color component. Traces of copper were also found and appear to give rise to the green coloration. X-ray diffraction, thermal analysis, and infrared spectrometry contributed to the identification of included minerals such as opal, hematite, and dolomite.

CMS

The minerals of Greenland. O. V. Petersen and K. Secher, *Mineralogical Record*, Vol. 24, No. 2, 1993, pp. 1–65.

This entire issue of the *Mineralogical Record* is devoted to famous mineral localities in Greenland. Beautifully illustrated with photographs of both mineral specimens and views of the more important collecting localities, this issue represents one of the most detailed descriptions of the minerals from this region to date. Besides tugtupite, the most important gem material from the island, mention is made of the occurrences of ruby, corundum, sapphirine, and kornepurine, as well as numerous other minerals of interest to scientists. A location map of important collecting sites is included.

JES

Mong Hsu ruby update. U. T. Hlaing, *Australian Gemmologist*, Vol. 18, No. 5, 1993, pp. 157–160.

The Mong Hsu Gemstone Tract in Shan State, Myanmar (Burma), is one of that gem-rich country's newest ruby sources. It is located 250 km east of Mandalay, with the primary deposit occurring 16 km southeast of Mong Hsu town. The rubies are found *in situ* in marbles within a Precambrian-to-Silurian metamorphic sequence, in association with quartz, green tourmaline, red-brown garnet, staurolite, pyrite, and radiating acicular tremolite. Prospecting has indicated that the deposit may cover an area 27 × 19 km. Alluvial deposits have also been identified in terraces above the Nam Hsu River. When the author visited the locality in June 1992, about 2,000 miners were working the gem-bearing gravels.

Ruby crystals from the primary deposit are euhedral and of prismatic habit, displaying combinations of pyramid and rhombohedron; pyramid, rhombohedron, and basal pinacoid; and rhombohedron forms. Rhombohedral parting is common, with crystals often broken along parting planes. Occasionally crystals occur with plates of white mica and crystals of green tourmaline adhering to their surfaces. Characteristic internal features include black mineral inclusions oriented parallel to the c-axis, blue and purple "halos," angular banding, plates of brown mica, and liquid "feathers."

The author concludes that the mineralogical and gemological features of Mong Hsu rubies are distinctive from those of Mogok. RCK

Myanmar jade: An update. U. T. Hlaing, *Australian Gemmologist*, Vol. 18, No. 3, 1992, pp. 79–80.

Following a brief historical overview of the discovery and marketing of Myanmar jadeite, the author lists areas now being mined. These include 10 sites in Kamaing Township (six of which have only recently started production) and two in Hkamti Township. Forty-six plots have been earmarked for joint-venture exploitation; additional plots will be opened "as and when proposals are received."

Information on marketing includes a graph that plots jadeite sales at the Myanma Gem Emporiums from their 1964 inception through 1990. The author also states that Bangkok is emerging as a new jade trading center and that ownership of jade jewelry is expanding because of rising affluence in Hong Kong, Taiwan, Singapore, Korea, and other countries where this gem is highly prized. The report also includes information on the preparation of jadeite for sale and the display and bidding procedure at the Emporiums. RCK

Rhodochrosite from Argentina [sic]. J. A. Saadi and J. C. Grasso, *Australian Gemmologist*, Vol. 18, No. 4, 1992, pp. 125–132. Translated from the *Boletín del Instituto Gemológico Español* (No. 30) by D. McCrary.

Rhodochrosite occurs at a number of localities in Argentina, including commercial mines in the Province of Catamarca, 35 km due north of the city of Andalgalá at an elevation of 3,100–3,300 m on the east face of the Capillitas Mountain Range. Granite is the predominant rock type, with mineralization of the Capillitas Bed linked to a Miocene-Pliocene volcanic "chimney" that measures about 900 × 1,500 m. Here, rhodochrosite is found as the main gangue mineral in veins, the external portions of which are represented by sulfides and quartz. The rhodochrosite is also found in large pockets, occurring in direct contact with the surrounding rock.

The main active deposit is the Ortiz mine. Unlike

rhodochrosite from other areas of the bed, that from the Ortiz mine usually does not exhibit visible whitish banding; rather, it is formed from parallel arrays of long, thick, prismatic crystals of intense "violet-red" color. Material from both Ortiz and other nearby areas may be formed from euhedral, rhomb-shaped, or flattened star-shaped crystals that commonly cover the internal surfaces of vugs or the external surfaces of stalactites.

Chemical analysis shows that some of the Mn²⁺ is replaced by Fe²⁺, Ca²⁺, or Mg²⁺, with an increased Fe²⁺ content probably responsible for a purple tinge in the most desirable Ortiz material. X-ray analyses have also shown that the white veining in banded rhodochrosite consists of barite as well as carbonate material. Gemological properties for Ortiz rhodochrosite are: S.G.—3.665; hardness (Vickers scale)—263, (Mohs scale)—4^{1/2}; R.I.—1.594 to 1.805; U.V. fluorescence—weak dark "rose" (long wave), weak purplish red (short wave).

This well-illustrated report shows many of the forms in which rhodochrosite occurs at Capillitas. The authors report that rhodochrosite stalactites are found only in the Capillitas bed and in no other locality worldwide. RCK

INSTRUMENTS AND TECHNIQUES

A method for obtaining optic figures from inclusions. J. I. Koivula, *Journal of Gemmology*, Vol. 33, No. 6, 1993, pp. 323–325.

The identification of inclusions remains one of the most important tests to help determine the nature and provenance of the host gem. However, many of the tests that gemologists rely on to make these identifications cannot be performed on inclusions that are extremely small or completely surrounded by their host. In this brief article, Mr. Koivula describes a simple method that can be used in many cases to determine the optic character of an inclusion. The method is particularly valuable for inclusions that lack characteristic morphology. It involves the use of a conoscop placed in contact with the host gem directly above the inclusion, with a drop of methylene iodide to provide good optical contact. The author also describes a custom-made apparatus designed to facilitate photography of the optic figure. Among the limitations of the method are: (1) both the host gem and the inclusion must be transparent, (2) the surface of the sample containing the inclusion must be clean, (3) the inclusion must be no more than 2 mm from the surface, (4) the inclusion should be no smaller than 1 mm, and (5) the optic orientation of the inclusion must be different from that of the host. The author concludes with two warnings: use caution in interpreting partially resolved optic figures; and do not mistake an optic figure accidentally obtained from an inclusion with that of the host gem material being identified. CMS

JEWELRY HISTORY

Magical Malbork. D. Stripp, *Lapidary Journal*, Vol. 47, No. 1, April 1993, pp. 64–67 ff.

This entertaining article recounts the author's recent visit to the Castle of Malbork in northern Poland. Home, in turn, to German crusaders, monks, Polish royalty, and soldiers from various lands, the castle now houses an impressive collection of amber treasures.

In 1230, the Duke of Masovia brought the order of the Teutonic Knights from the crusades in Palestine to defend the Christian Poles against the pagan Prussians. The knights conquered the Prussians and established a kingdom administered chiefly from the castle at Malbork. The crusaders apparently were not above seeking earthly rewards for their victory—among the privileges they claimed was a monopoly of all amber found in the area. The edict was brutally enforced, and unauthorized persons caught collecting amber were hung from the nearest tree.

In 1961, the Polish Tourist Society founded the Castle Museum at Malbork. The collection includes weapons, artwork, books, and coins, but its focal point is an extensive array of amber treasures. A baroque-style amber cabinet, which contains a statue of the Virgin Mary and originally belonged to the last king of Poland, is considered to be the most important piece. The amber masterpieces also include a figure of Ares carved in 1600, a 1-m-high baroque-style altar, a necklace created in 1610 and worn by Princess Sybilla Dorata of Brest from Silesia, a double-handled cup of amber and silver, and a 17th-century carving of mythological scenes by Christoph Maucher.

The article is illustrated by color photographs and enlivened by anecdotes about the history of the castle and the museum collection.

Denise Heyl

Out of Africa: The superb artwork of ancient Nubia. D. Roberts, *Smithsonian*, Vol. 24, No. 3, June 1993, pp. 90–100.

This article is a study of, and tribute to, an enigmatic people whose cultural remnants still exist in the modern world, although their civilization does not. In addition to a number of permanent displays that recently opened, an exhibition that includes Nubian jewelry and other jeweled personal objects is now traveling to various museums around the U.S. Many of these items have helped archeologists and anthropologists uncover some of the secrets of this lost civilization. Confounded by wars and cultural assimilation between the Nubians and their northern Egyptian counterparts, items once thought to be of Egyptian origin are now attributed to the Nubian culture. There is lively debate as to this question of origin, and Egyptologists are enjoying renewed interest in their field because of the questions now posed by these artifacts. The article includes photos of some of the more

important artifacts, as well as a map for geographic orientation.

JEC

SYNTHETICS AND SIMULANTS

A new type of synthetic ruby on the market: Offered as hydrothermal rubies from Novosibirsk. H. A. Peretti and C. P. Smith, *Australian Gemmologist*, Vol. 18, No. 5, 1993, pp. 149–157.

This well-illustrated article describes the in-depth examination of three synthetic rubies that were reportedly produced by the hydrothermal process in Novosibirsk, Russia. Gemological properties were consistent with those of natural and synthetic rubies from various other sources. The color is described as a very highly saturated red of medium-to-dark tone, with the stones exhibiting a certain "sleepiness." Magnification revealed that this latter feature is due to a striated pattern of graining, like that seen in Russian hydrothermal synthetic emeralds. Other features noted with magnification include color zoning, solid inclusions of copper alloys, fingerprint inclusions, and a single needle-like inclusion.

Ultraviolet-visible and near-infrared spectroscopy revealed features similar to those of certain natural rubies with relatively high chromium and iron contents. EDXRF analysis revealed (in addition to aluminum) trace concentrations of chromium, iron, titanium, copper, and nickel, with minor traces of vanadium and gallium. Infrared spectroscopy detected sharp absorption peaks believed to be due to hydroxyl anions in the synthetic corundum's structure.

The authors review the patent literature on hydrothermal synthesis of ruby and provide possible explanations for the presence of the trace elements that were detected. They conclude that the strong, irregular graining is the most striking diagnostic feature, with the metallic inclusions also being distinctive. In the absence of conclusive internal features, advanced instrument testing will separate these synthetics from their natural counterparts.

RCK

Vietnamese ruby fakes: A problem requiring urgent resolution. G. Brown and R. Beattie, *Australian Gemmologist*, Vol. 18, No. 4, 1992, pp. 108–114.

Beginning with a brief overview of Vietnam's two ruby localities, the authors address the problem faced by gemologists in detecting synthetic corundums that have been "salted" into parcels of both rough and faceted stones. Proposed solutions include: (1) Vietnamese government intervention to guarantee the authenticity of stones, (2) legislation and penalties for selling such adulterated parcels, and (3) publication in the trade and gemological literature of all such deceptions, along with identifying criteria.

The authors then proceed to document different types of counterfeits found in parcels of Vietnamese

goods that had been purchased either in Vietnam or Bangkok, such as: heat-treated, tumbled Verneuil synthetic ruby (sometimes quench-crackled and treated with substances such as oil, wax, or blue dye); a heat-treated, tumbled Verneuil synthetic that was cored and filled with fused particles of blue sapphire; similar tumbled material with saw cuts filled with fused sapphire; and natural pink sapphire coated with red nail polish.

Identification of the different categories is then addressed. Faceted imposters were the easiest to detect, while tumbled imitations of rough were the most difficult, sometimes requiring such advanced testing techniques as EDXRF, petrological microscopy to detect Sandmeier-Plato twinning ("Plato lines"), and short-wave U.V. transparency.

This important, well-illustrated report includes a table of inclusions found in both Vietnamese and Burmese rubies as well as inclusions that the authors consider characteristic of Vietnamese stones. RCK

PRECIOUS METALS

Jamestown leaf gold and The Gold Bug mine (two separate articles). J. Burnett, *California Geology*, Vol. 46, No. 3, 1993, pp. 63–65, 68–73.

Most of this issue is devoted to gold, California's state mineral—with "Jamestown Leaf Gold" as the cover story, illustrated by striking photographs by the Van Pelts.

The December 26, 1992, Jamestown find at the Crystalline-Alabama claim in Tuolumne County netted "several dozen pieces," including one weighing over 73 troy pounds (27 kg), the fifth largest gold mass found in the state. Geology of the mine (the third largest in California) is described, as are the specimens, unusual because they crystallized in bright flattened ribbons called "leaf gold." Some were speckled with rare microscopic crystals of gersdorffite.

"The Gold Bug Mine" article details the geology, isometric layout, and history of an inactive hard-rock mine in Hangtown (now Placerville). Although geared to tourists and hobbyists, both the article and a public tour offer insights into living and mining conditions endured during the peak of the get-rich-quick scramble of the late 1800s. Irv Dierdorff

MISCELLANEOUS

Minerals of the Houston Museum of Natural Science. W. E. Wilson and J. A. Bartsch, *Mineralogical Record*, Vol. 23, No. 1, 1992, pp. 1–33.

Lavishly illustrated with beautiful color photographs by Harold and Erica Van Pelt, this independent supplement to the *Mineralogical Record* begins with a chronology of early private mineral collecting. It then documents how several museums have as their nucleus one or more col-

lections originally assembled by prominent private collectors.

The first recorded mineral collector was G. Bauer (aka G. Agricola), who published several important books on minerals and mining from 1530 to 1556. His friends and fellow collectors—J. Mathesius, J. Kentmann, C. Gesner, and B. Palissy—also amassed substantial collections throughout their lifetimes. Because no established institutional museums existed to preserve their collections after their deaths, the minerals were dispersed and lost before the end of the 16th century.

During the 17th, 18th, and 19th centuries, European royalty and noted scientists collected specimens that eventually became the basis for museum collections in Prague, Vienna, Oxford, and London, as well as the establishment of the French National Museum and the Freiberg Mining Academy.

In the 20th century, C. S. Bement assembled one of the greatest private collections in history; this was later purchased by J. P. Morgan and eventually donated to the American Museum of Natural History. W. A. Roebing, builder of the Brooklyn Bridge, and F. Canfield greatly enriched the holdings of the Smithsonian Institution with their extensive collections. A. Chapman assembled what is perhaps Australia's best collection, which was recently purchased by the Geology Museum of the New South Wales Department of Mines.

The second portion of text concentrates on the creation, physical attributes, development, and growth of the Houston Museum of Natural Science. Beginning in the late 1920s, this Texas museum acquired several collections that contained modest accumulations of mineral specimens. But the most important acquisition, the Sams' collection, came in the mid '80s.

In the mid-1970s, Perkins and Ann Sams, with the guidance of Paul Desautels, aggressively set out to assemble one of the world's finest mineral collections. An important part of their strategy was to acquire key existing collections. They eventually absorbed those of D. P. Wilber, M. and J. Zweibel, C. Key, and P. Obeniche, as well as certain specimens from E. Swoboda. By 1983, the Sams family had assembled one of the finest private mineral collections in the world. Soon thereafter, under the guidance of E. Cockerell and with the help of many local supporters, the collection was acquired by the Houston Museum of Natural Science.

Adding this collection to its already substantial holdings established the museum "as one of the world's major repositories for fine mineral specimens," according to authors Wilson and Bartsch. Five hundred and fifty mineral specimens are displayed, which is only half of the museum's collection. This guide describes and illustrates 60 of the most important pieces. The numerous galleries and halls in the museum also feature educational displays of a recreated gem pocket, structural geology, rock and mineral formation, and the development of mineralogy as a science. LBL